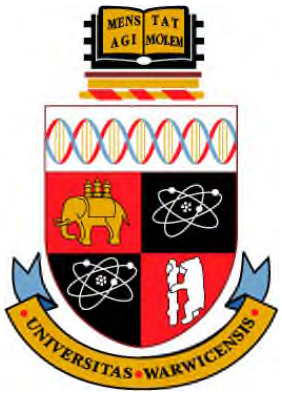

Underwater Optical Wireless Sensor Network

By

Zahir Uddin Ahmad

A thesis submitted in partial fulfilment of the requirements for the degree of

Doctor of Philosophy

School of Engineering

THE UNIVERSITY OF WARWICK

September 2013

For my father, Mobarak Ullah Dhali (In memoriam)

Table of Contents

List of figures

List of tables

List of abbreviations

ADC- Analogue to Digital Converter

APD- Avalanche Photodiode

AUV- Autonomous Underwater Vehicles

BER- Bit Error Rate

BPSK- Binary Phase Shift Keying

CDMA- Code Division Multiple Access

CSMA- Carrier Sense Multiple Access

CTS- Clear to Send

DSSS- Direct Sequence Spread Spectrum

FDMA- Frequency Division Multiple Access

FM- Frequency Modulation

FOV- Field of View

IrDA- Infrared Data Association

LED- Light Emitting Diodes

LOS- Line of Sight

LSB- Least Significant Bit

MAC- Medium Access Control

MSB- Most Significant Bit

NRZ- Non Return to Zero

OFDM- Orthogonal Frequency Division Multiplexing

OOK- On Off Keying

OW- Optical Wireless

PPM- Pulse Position Modulation

PSU- Practical Salinity Unit

QOS- Quality of Service

QPSK- Quadrature Phase Shift Keying

RF- Radio frequency

RISC- Reduced Instruction Set computing

ROV- Remotely Operated Vehicles

RZ- Return to Zero

RTS- Request to Send

SNR- Signal to Noise Ratio

SPI- Serial Peripheral Interface

TDMA- Time Division Multiple Access

TTL- Time to Live

USART- Universal Synchronous Asynchronous Serial Receiver and Transmitter

Acknowledgements

First of all, I thank God, for giving me knowledge and strength to complete this PhD thesis. The completion of the thesis would not be possible without the support and encouragement of many individuals. I thank all the people who have supported me throughout my PhD study.

I wish to express my sincere gratitude to my supervisor Professor Roger Green for his priceless support, guidance and suggestions throughout my study time here at Warwick. It was a great privilege to work under his supervision, and I was really fortunate to have him as my PhD supervisor. I would also like to thank Professor Evor Hines for being my second supervisor. I also thank all the staff of the University of Warwick, who has directly and indirectly contributed to this work. I also want to acknowledge the technical support facilities from the School of Engineering at University of Warwick.

I want to extend my appreciation to my colleagues in the Comsys Lab for their valuable suggestions and constructive discussions throughout. I would also like to thank all my friends from my childhood for their encouragement and sharing many

things together.

Above all, I can never express my gratefulness enough to my parents, wife, brothers, and other family members here in UK and in Bangladesh. My father (May God, grant him heaven) always encouraged me to go for the highest degree on earth. I do believe that, he is watching my success from the heaven. My mother and brothers always believed on my ability and supported right the way through. I am really grateful to them. All my family members in Bangladesh, USA and here in the UK supported me throughout my time here; I want to thank all of them for their valuable suggestions. My wife, Fatema Zannat had a very tough time and had to give up her career because of my PhD study. I thank her for her continuous support and endless love during all these years. Last but not least, I want to mention about my one year old son, Zarif Ahmad. He was my source of inspiration and enthusiasm during the writing period of this thesis.

Declaration

This thesis is submitted in partial fulfilment for the degree of Doctor of Philosophy under the regulations set out by the Graduate School at the University of Warwick. All work reported in the thesis has been carried out by Zahir Uddin Ahmad, except where stated otherwise, between the dates of November 2009 and September 2013. No part of this thesis has been previously submitted to the University of Warwick or any other academic institution for admission to a higher degree.

Zahir Uddin Ahmad
September 2013

Abstract

The thesis details the development of a short range, multi-hop underwater optical wireless sensor network. Multi-hop underwater optical wireless communication using a line of sight (LOS) link can provide a greater range compared to a single hop network, and provide physically secure connections for underwater sensor networks. This kind of system can be very power efficient, and supported data rate can be from tens of kbps up to a few hundred kbps. The aims were to build a cheap communication prototype using “off the shelf” components, such as a microcontroller, optoelectronics etc. for demonstration purpose. To support the built prototype, a directional MAC protocol has been developed which considers the directionality of light propagation. The multi-hop approach has not been considered for underwater optical wireless communication before, while most of the research focus is to develop long range and high powered communication links.

In this thesis, a custom built transceiver using blue and green LEDs has been developed, which supports a data rate up to 140kbps, when the NRZ-OOK modulation technique is used. For the transmitter part, a digital LED driver has been used, while on the receiver side, a transimpedance amplifier using a single transistor

has been developed. This configuration for optical wireless receiver system design has not been usual, but it works very well for the proposed prototype. A second stage voltage amplifier was also designed to boost the signal up to 5V for the microcontroller, which was also based on transistors.

To demonstrate the principle of multi-hop communication, a line-type network prototype using two sensor nodes and a gateway node has been designed, built and tested in the lab environment. Each node was equipped with two transceivers controlled by a microcontroller to make a full-duplex communication system. To minimize the cost, all components of a node were built on a single PCB board. To upload data from the sensor node to the gateway node, a green LED has been used, and to transmit the control signal from gateway node to sensor nodes, a blue LED was used. For the demonstration purpose the communication range was considered up to 1m, which can be increased significantly by using high powered LED, and external optics such as lenses, concentrators, etc.

A directional MAC protocol has been designed, considering the directionality of the network. The designed protocol is based on TDMA techniques, but modified for the proposed application. The gateway node controls all other nodes in the network and acts as a master node. Because of the directional full-duplex network, there is much less chance of a collision, when using a TDMA approach. Therefore, a random access protocol was not needed for the proposed architecture.

Finally, experimental results validate the fact that the multi-hop approach is a viable solution to increase the communication ranges for underwater optical wireless sensor networks. Different sets of experiments show that the proposed system can be implemented in the real environment, such as, oceans, canals and ponds.

Publications associated with this research work

The following papers have been published/ submitted as a result of the work contained within this thesis.

Journal Papers

Zahir Ahmad and Roger Green, “Development of a Visible Light Communication System for an Underwater Optical Wireless Sensor Network,” International Journal on Advances in Telecommunications (Revision submitted)

Conference Paper

Zahir Ahmad and Roger Green “Link Design for Multi-hop Underwater Optical Wireless Sensor Network” ICSNC 2012, pp.65-70, Portugal, Nov 2012 (Peer reviewed)

Chapter1 : Introduction

1.1 Overview

More than two thirds of the world's surface is covered by water, and this area is still mostly undiscovered by the human beings. Exploration of oceans is not restricted to fishing, transferring data from one part to another, or observing the different biological change underwater. It can provide a great deal of information regarding climate change, natural disasters, and also can provide significant data concerning the history of our planet. An efficient and reliable communication system is the first step towards the investigation of this huge underwater world.

Until now, most of the underwater communication has been based on either wired or acoustic methods. Wired technology has its limitation in terms of installation, maintenance and mobility. For short and medium range applications, wireless is a possible solution underwater, where the medium is very rough and harsh. So far, acoustic methods have been the dominant underwater communication system used for long range and low bandwidth links, because sound propagates very well underwater compare to other waves. However, the limitations of acoustic

communication are the lack of bandwidth to support high speed communication; for example, sound can propagate up to a few kilometres at a speed of 1500m/s, which is not enough for many applications. Time-varying multipath propagation and the low speed of sound underwater produces a very poor and high latency communication channel, which cannot support real time data transfer such as audio/video. Moreover, the cost of acoustic components can be very high, and the dimensions of components can be very large. All those limitations of acoustic communication have stimulated researchers to find a cheap alternative underwater communication system capable of allowing high bandwidth for real time applications.

1.2 Motivation

Motivation of this work has originated from the world-wide interest in exploring the underwater domain. At the moment, exploration of the oceans is not just because of curiosity, but necessary for the survival of human beings. During the last decade, source of the most natural disasters such as the tsunami, cyclones etc. originated from the deep ocean. Although, this kind of disaster cannot be controlled by humans, the volume of calamity can be minimized by taking precautions if they can be detected earlier. Moreover, exploring the colourful underwater world has attracted not only the marine scientists but also others, which has led to researchers studying the underwater world for a long time. Furthermore, there are also the commercial aspects of ocean exploration which involve exploring and maintaining the off-shore oil/gas industry, transporting water etc.

1.2.1 Ocean biology

Observing and monitoring underwater biological changes requires collecting specific data for longer period of time. The impact of human-generated pollutants, and how

global warming affects marine biology, can be determined only by monitoring those species underwater for an extensive period of their life cycle. For this purpose, a cheap communication system is required, which can operate for a longer period of time without human intervention.

1.2.2 Environmental research

Oceanographic research requires a vast amount of physical data such as temperature, current, pressure, and different dissolved components of water. An efficient system that can provide the above mentioned information continuously, can contribute greatly in developing an accurate model of the ocean, which can be used to detect any natural disasters like tsunamis, cyclones, etc.

1.2.3 Surveillance system

Monitoring harbours and borders is an overwhelming task because of the huge geographical coverage. Until now, mankind has been fully involved to accomplish this task by using boats, planes or radars. However, this task can be automated by deploying a sensor network underwater over a larger geographical area. An audio sensor can be used to detect some sort of engine noise to identify any vehicles. Through the triangulation process, the position of the boat can be calculated, and crews can be dispatched.

1.2.4 Seismic monitoring

Seismic monitoring underwater is very challenging compared to ground based monitoring. Seismic monitoring in the ocean involves a ship which equipped with an array of hydrophones as a sensor, and cannon as an actuator. This process is very costly and time consuming, which can be simplified by implementing a sensor network.

1.2.5 Ship hull and equipment monitoring

The hull of the ship is required to be monitored regularly for maintenance purposes. This task is accomplished by a diver, or by using a boat underwater, which is also time-consuming and very expensive. Other than ships, equipment monitoring also requires human involvement. Alternatively, this task can be performed by deploying visual image sensors underwater.

1.2.6 AUV/ROV operation

Groups of ROV/AUV operated underwater can be co-ordinated by deploying intercommunication ability between them. This is the case for on-land robot operations. On the other hand, because of the lack of a communication system, underwater robots operate autonomously. A suitable communication technology can make this operation more sophisticated.

1.2.7 Communicating with submarine/diver

Sharing thoughts and joys with others is the nature of a human being, even if it is for a short period of time. Because of the lack of the communication technology, a diver could not do this until recently. However this is no more the case; nowadays two divers can talk to each other by virtue of visible light communications underwater [1]. In the same way, communication between two submarines can be established using an efficient underwater communication technology.

1.3 Application scenario

As described in the previous section, most of the applications in underwater communication require long term deployment, either to collect environmental data to

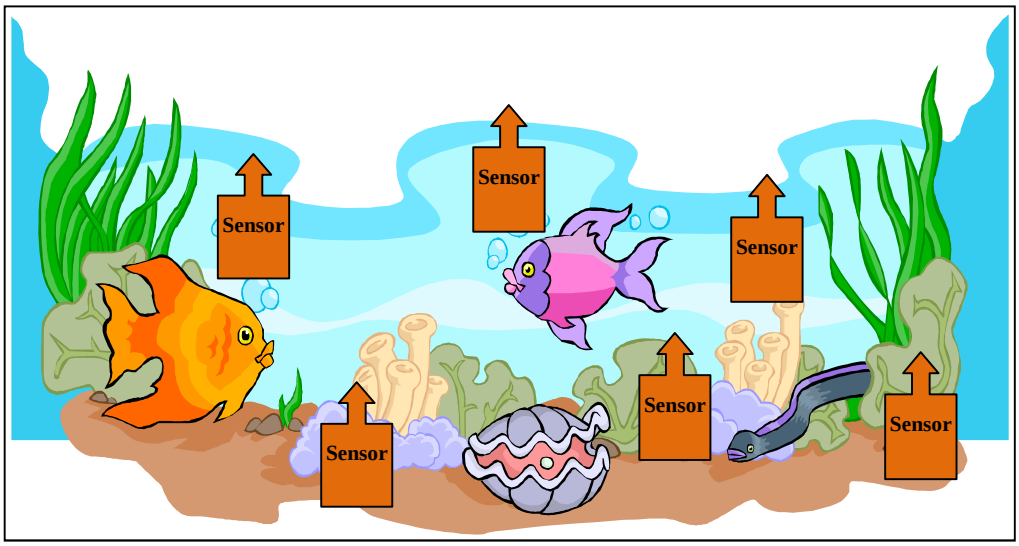

Figure 1-1 Application scenario

observe the environmental change, or to monitor a certain geographical area for a security purpose. Also some applications like communication between two AUVs, or communication between an AUV to sensor node, requires a short term, point-to - point, link. For collecting long term environmental data on land, widely used technology which are currently being deployed are sensor networks. In this process, sensor nodes are placed randomly in a geographical area and those nodes form a network autonomously by using radio communication and send the sensor information to a base station. In the same way, for collecting or observing a certain area, sensor nodes can be deployed underwater as seen in the figure 1-1. Technology used in free space communication cannot be used directly underwater, because radio signal do not propagate very well in water as they do in air, so, finding an alternative solution for underwater communication has stimulated the researchers to see the possibilities of other communication carriers like visible light.

1.4 Problem statement

To collect environmental data from water, an efficient communication system needs to be established, which does not require any human intervention. In fact, it is not possible for people to stay in the water for a long period of time, especially in the deep oceans and in very cold water. Alternatively, ROVs and AUVs are being used to do tasks underwater, from the middle of the last century, which is also very challenging and costly. An ROV/AUV has to return to the dock every time after collecting data from a sensor node, or after performing a specific task. Another option is placing those vehicles in the floor of the sea and communicating with them from the sea surface, where there should be a mechanism for it to charge itself for a longer lifetime. To communicate with the AUV/ROV, a competent and reliable communication system has to be established. Other than using the ROV/AUV, which themselves are very expensive and a time-consuming approach, a reliable network can be built which will be able to send sensor data to a neighbouring node and eventually to a station located on the sea surface.

Free space sensor technology which uses radio as a communication carrier cannot be used directly underwater because of the nature of the medium. Water, which is the medium for communication underwater, behaves totally differently compared to air. Moreover, different types of water have different characteristics, depending on their location, mainly because of the variations of particles in the water; for example, sea water has more salt elements than the canal water which will act differently as a medium when transmitting electromagnetic signals. So, traditional free space technologies are not applicable in underwater, and it is desired to have a customized solution depending on the applications and water types.

Until now, most of the underwater communication has been performed using acoustic waves, which propagate well compare to electromagnetic waves. However, limitations of this technology are: high cost, large size, and low data transfer rate [2]. Alternative approaches which have been recently investigated by researchers are either by using optical wireless, or radio frequencies which are frequently used in free space communications [3] [4]. Since water is very dense and conducting medium, so it is not so easy to propagate high frequency radio wave through water. One can use very low frequency radio waves, but again, the antenna size for this kind of communication system will be large, which is not acceptable.

Optical wireless can provide a large spectrum, starting from the mid infrared all the way to the visible, which can also offer a considerable bandwidth depending on the system design [5]. Free space optical wireless mostly prefers infrared because of the high bandwidth available using infrared transmitters and receivers. But, in case of underwater, infrared suffers greatly from attenuation. Thus, the best spectrum for optical wireless for underwater communications is in the visible range specifically blue and green region, which propagates well. Depending on the system design, data rates in the Mbps range can be achieved in the communication range up to tens of metres or more. Since commercial transceivers are not available for visible light communication, so, the first steps to achieve the goal are to design an efficient transceiver for the desired application.

A communication range in the region of few metres can be achieved with the available common design and architecture, but may not be feasible for most of the underwater applications mentioned above. Range cannot be increase dramatically because of the limited transmitted optical power by the source and also because of the eye safety regulation of optical wireless. So, an alternative approach has to be

taken to maximize the communication distance to support as many applications as possible.

Another problem in deploying a sensor network is to organize and manage the communication between each node. Medium access control (MAC) protocols have not been much studied for underwater optical wireless communication, as it is a relevantly new research topic. So, the need for investigating an efficient MAC protocol for an underwater optical wireless sensor network has also emerged. Different MAC protocols for underwater optical wireless sensor network have been studied, and a directional MAC protocol has been designed for the current application.

1.5 Approach

To increase the communication range and to cover more geographical area, a multi-hop system has been developed using a visible light communication carrier. Multi-hop communication is a well-known technique in free space communication for spatial reuse, which has also been proposed by many researchers for underwater optical wireless communication. In this process, intermediate nodes relay the sensor information to the gateway node, which ultimately stores and sends data to the base station when requested. To choose the optimum network architecture for multi-hop communication, several network architectures have been investigated, and the best one has been chosen.

For managing all nodes in the sensor network, a directional MAC protocol has been proposed for the designed network prototype. As the proposed network architecture is static, so directionality between the nodes has to be ensured for communication to happen.

The work began by selecting a photon source, and finished with the MAC layer implementation. At each step, attention was paid to minimize the cost of the system. The transmitter and receiver were designed for the specific scenario and performance analysis was done to choose the best one. A bi-directional communication system was adopted using blue and green coloured LEDs to make the system more realistic. To demonstrate the concept, a network prototype of three nodes was built inside the lab environment. Each node was equipped with two transceivers to communicate with the upper and lower nodes in the network. A microcontroller was used to control the medium access where the directional MAC concept has been implemented. Since this project adopted a line-of-sight communication link, so the chance of interference in the medium was very low. In the directional MAC approach, each node has to be aligned properly to other node, which is also mandatory for physical layer communication for the line-of-sight (LOS) network. So, implementing a directional MAC was easier in this sort of network.

1.6 Contributions

The contribution of the thesis can be summarized as follows:

- A novel approach in building a short-range, cost-effective, and high bandwidth bi-directional underwater optical wireless network based on visible light. Here, a green and blue LED is used to send and receive data from one node to another.
- A novel approach for underwater monitoring and data collection, which consists of sensor nodes, a gateway node, and a static multi-hop optical wireless network. To increase the communication range for an underwater communication system, a multi-hop approach has been proposed.

- The design and build of a unique underwater optical wireless transceiver capable of bi-directional communication. A simple receiver design was produced to minimize the cost of the system but still capable of supporting enough data rate and high sensitivity for an underwater sensor network.
- Design and build of a power-efficient underwater sensor node consisting of a temperature sensor to measure water temperature. This node is capable of storing, processing and sending data to the neighbour node using optical wireless transceivers.
- Design of an underwater Gateway station capable of communicating with sensor nodes using optical wireless link. It also has a PC interface using serial port to save and analyse the received data.
- Design of a TDMA-based directional MAC protocol which enables an all optical wireless communication underwater.
- Performance analysis of an all optical underwater wireless communication system using different types of water.

1.7 Application limit

The focus of this work has been to design and implement a network prototype to measure and collect different environmental parameters such as temperature, pressure, conductivity, turbidity etc. and investigate the performance of the network. Because of the simplicity of implementation, only a temperature sensor was considered in this thesis, but in a real application more than one sensor could be attached to the sensor node according to requirements.

The communication range was limited by the available water tank size inside the lab

environment. However, range can be increased by using external optics and using a high powered source. But the focus of this project was not to use expensive components rather to build a simple, cost-effective prototype just to demonstrate the concept of a multi-hop communication underwater for sensor network.

Finally, static network architecture has been considered for implementation purposes, although with a minimum modification, mobile network architecture could be adopted, and it would require slightly different network architecture which may use same physical layer design.

1.8 Outline of the thesis

The rest of the thesis is structured as follows:

- Chapter 2 describes the current underwater optical wireless advancement and also discusses different issues related to implementation.
- Chapter 3 introduces the transceiver for multi-hop underwater optical wireless sensor network. A transmitter and a receiver have been designed and implemented using green and blue LEDs. The performance of the designed transceiver has been discussed.
- Chapter 4 presents proposed multi-hop sensor network architecture. It also includes the discussion about sensor node design and gateway node design of for the proposed application.
- Chapter 5 discussed the different types of MAC protocol for underwater optical wireless sensor network. Also, a TDMA based directional MAC for the underwater optical wireless sensor network has been designed for the proposed application.
- Chapter 6 presents the experimental results of the proposed network

prototype.

- Finally, in chapter 7, conclusions and suggestions for future work have been mentioned.

Chapter2 : Background research and related work

2.1 Introduction

Underwater optical wireless communication has gained considerable attention during the last few years mostly because of the increasing demand for short range and high speed applications [5] [6] [7]. Compared to acoustic communication, which has been the mature communication technology until now for underwater, optical wireless can be more bandwidth-efficient and cost-effective for short range applications like sensor network [8] [9]. This is because of developments in low cost and high power optoelectronics such as LEDs, and photodiodes, during the last decade. Although acoustic communication will play its role for the long range underwater communication, and will be the primary communication technology, optical wireless can be a promising alternative for short range and high speed applications. So far, in short range free space optical communications, infrared has been considered to be the feasible solution, and also visible light is gaining interest recently. In the case of

water, the best spectrum range which propagates further is visible light, especially the green and blue part of the visible spectrum [10]. So most of the underwater optical wireless communication systems consider visible light for transmitting data from one point to another.

Several research groups are actively investigating different aspects of underwater optical wireless communication systems, starting from channel characterisation to system design [11] [12] [13]. The water medium itself is a complex medium, and light propagation varies in different types of water in different depths , so, it is not an easy option to find a generic solution for all types of water. Since underwater optical wireless is a relatively new research area, most of the work until now has focused on unidirectional single hop communications. At the same time, some groups have been investigating sensor applications using optical wireless communications [3] [15]. The rest of this chapter details the various aspects and implementation issues related to underwater visible light communication.

2.2 Communication requirements for underwater network

Underwater communication can be divided into two main categories. One of them is point-to-point communication for high volume of data transfer, and another one is sensor networks for monitoring a geographical area or collecting different environmental data from water. Point-to-point underwater communication can be used to communicate between two divers, loading information from an underwater sensor node to an AUV etc. Requirements of bandwidth and data rate are very high for this kind communication. In the case of a point-to-point communication link, the main focus is achieving greater communication range and high bandwidth, whereas in the case of sensor application the low powered, and low cost communication is

required for dense deployment of sensor nodes. Again, a targeted sensor network can be classified into two clusters depending on their applications [2]. The first one is non-time critical for long-term aquatic monitoring applications, such as collecting different oceanographic data, monitoring water pollutants, observing shore oil and gas fields, etc. The second category is a short-term time critical application, where an immediate response is required, for example, identifying a submarine, tsunami recovery etc. The communication requirement of each type of network is different, which is summarized in the following table 2-1 [2].

Table 2-1 Communication requirements for different underwater networks

Requirements	**Long-term non-time critical sensor network**	**Short term time-critical sensor network**	**Point-point network**
Transmission range	Short	Short	Long
Data rate	Low	Various	High
Deployment depth	Shallow or deep water	Shallow water	Shallow or deep water
Energy efficiency	Major concern	Minor concern	Minor concern
Real time delivery	Minor concern	Major concern	Depends on application

Long term non-time critical sensor network architecture can be either static or mobile, depending on the objective of the deployment. On the other hand, a short term time-critical application normally adopts mobile architecture because of the nature of application. The focus of this work is to build a non- time critical, long term, static underwater optical wireless sensor network.

2.3 Possible options for underwater communication carriers

In free space, the most common communication technology is either wired based on cooper and fibre optic cable, or wireless which is dominated by radio frequency communication. But in the ocean environment, none of them are appropriate for short or medium range applications. Fibre optic cables are installed very deep under the water to connect different continents, which are very expensive to install, and cost a lot of money to maintain. On the other hand, radio frequency communication suffers a significant amount of loss in water (conductivity 0.05mS/m) especially in sea water (conductivity 4mS/m), so may not be suitable for underwater communication. As mentioned earlier, acoustic communications also have their limitations in specific applications. In this section a detailed description of each of the technologies has been presented. The Pros and cons of each of the technologies are summarised in table 2-2 [16].

2.3.1 Research outcome of underwater radio communications

Because of the conducting nature of sea water, radio does not propagate very well underwater. Attenuation is higher in the high frequencies; therefore most of the commercial radio equipments, which operate in the MHz and GHz range, cannot be used underwater. Therefore, the choice is for using a very low frequency radio wave, which requires a very high power and a large antenna size.

During the mid of last century, radio communication underwater research was conducted extensively mostly for the military uses. The successful underwater electromagnetic communications using extremely low frequencies were developed by US navy and Russian navy for submarine communication. The US system used 76Hz and the Russian system operated at 82Hz to send few characters per minute

Table 2-2 Advantage and disadvantage of different communication carriers underwater

Technology	Advantage	Disadvantage
Acoustic	Mature technology. Range up to 20km. Energy efficient.	Limited bandwidth. High delay. Impact on marine life. Unpredictable propagation. Poor in shallow water. Doesn't transit in water/air. Not secured.
Electromagnetic	Transit through water/air. Immune to acoustic noise. No multipath affect. Unaffected by turbidity.	Limited range through water. Antenna size is very large. Require high power. Susceptible to electromagnetic interferences.
Optical	Ultra-high bandwidth. Low system cost. Very secured. System size is very small and power efficient.	Range is low. Need precise alignment. Susceptible to water turbidity

across the globe to call a specific submarine to come over the surface for radio communications. To develop a long distance radio based communication system, Wait proposed a model by which main propagation is established by using a Lateral EM wave, which travels on the sea surface [17]. To use this technique, a very low frequency needs to be used for communication to happen. Recently, Al-Shamma'a and Lucas presented theoretical analysis, simulation, and experimental results to confirm that radio frequencies in the range of 1-20MHz can propagate up to a

distance of 100m, at a cost of transmitting power of 100W, which can provide a data rate of 1Mbps [4] [18] [19]. In their research, they showed that the attenuation is very high in the first 10m of communication distance, but very low afterwards, which eventually makes communication possible up to the range of 100m. The reason is that seawater nearby the antenna acts as a high conductivity because of the intensity of the electromagnetic field formed by the transmitter antenna. When the distance increases, it starts to act more as a dielectric. Somaraju and Trumpf also suggested that large propagation distance is possible at MHz frequency spectrum. According to their model, conductivity of seawater decreases at small field strengths due to the hydrogen bonding of water molecules [20]. But, they also failed to prove experimentally how and why the conductivity of sea water decreases. The signal strength at a different distance can be found from figure 2-1 [17]. As seen, initially, signal strength decreases rapidly up to 10m, but eventually it becomes steady. It is also seen that the signal strength remains steady for a long distance even after 90m.

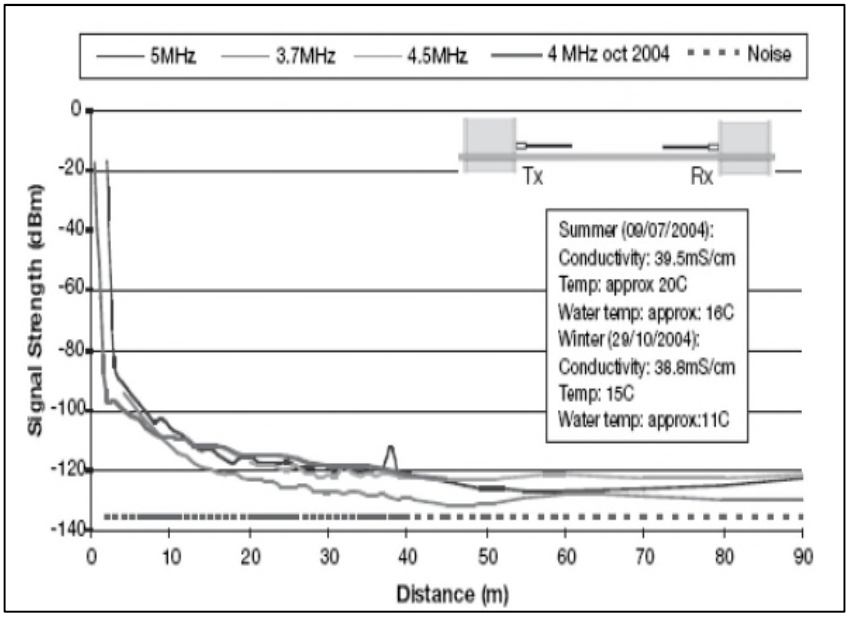

Figure 2-1 Signal strength as a function of transmitter antenna [17]

This is actually the noise strength, which has not been considered during the experiment.

The possibility of underwater radio frequency communication for different applications is presented in [16]. It has been reported that, the data rate can be up to 10Mbps for fresh water, but hardware implementation for this kind of scenario needs to be investigated. The design of an underwater sensor network based on 2.4GHz ISM frequency band has been reported in [21]. In this paper, different aspects of an underwater radio based sensor network have been discussed. The best modulation techniques which were observed in experiments are BPSK and QPSK for a communication distance of 17cm. A static, multi-hop wireless sensor network, implementing the AODV routing protocol has been reported in [22]. Wireless Fibre System launched a commercial underwater wireless modem capable of 1Mbps data transmission at a distance of 1m [23] . Because of the severe attenuation problem in water, implementing a radio-based communication system may not be a feasible solution for underwater sensor applications.

2.3.2 Acoustic communication

Acoustic wave is the primary carrier for communications underwater because of the possibility of longer communication range, due to low absorption of sound waves in water. Sound travels four times faster at the ocean surface than in air, and propagation speeds increase with increasing water temperature. The speed of sound increases 4m/s for an increase of 1 degree centigrade of temperature, and increases 1.4m/s for 1 practical salinity unit (PSU). It has also a relation to the depth of water; if the water depth increases to 1km, the speed of sound increase by 17m/s. The effect of sound speed with temperature in sea water is shown in figure 2-2, which is obtained from [2].

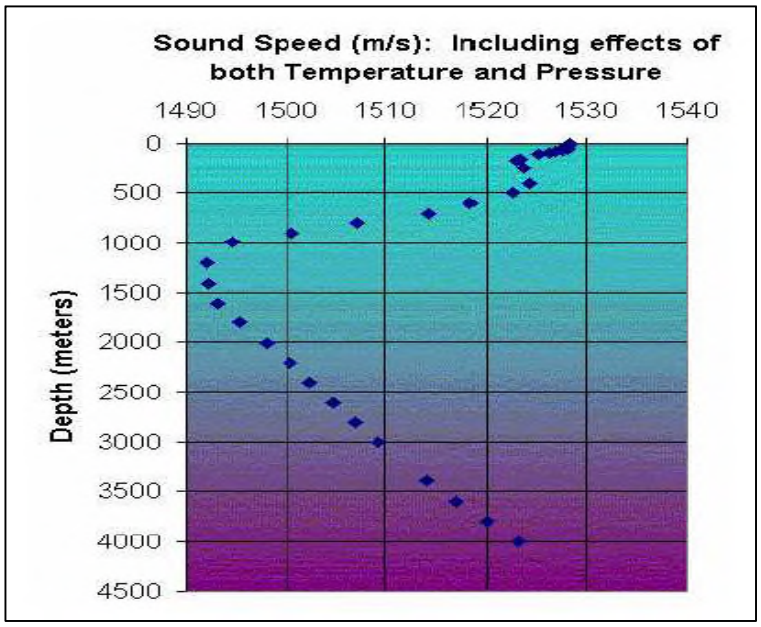

Figure 2-2 A vertical profile of sound speed as a function of depth [2]

The limitations and challenges of acoustic communications are presented in [24] [25] [26]. Most important factors which were discussed in those papers are:

- Bandwidth is very limited. The highest achievable bandwidth can be hundreds of kHz for a range of a few metres.
- Propagation delay (0.67s/km) is very high, which is in the order of five times larger compared to radio in free space.
- Sound travels in every direction. So it is easy to receive the signals anywhere even by the unauthorized receiver.
- High bit error rate due to multipath propagation caused by inter symbol interference.
- Doppler frequency spread requires a sophisticated receiver design to handle the inter symbol interferences.

Acoustic communication underwater has a long history, starting from the middle of the last century. A significant development was made during the World War II by a

group of scientists for military purposes. The research conducted at that time was mainly to understand ocean phenomena for sound propagation. The acoustic application underwater was not only limited to communication, it is also has been used for imaging, navigation, positioning etc. An early stage underwater communication system was reported by Norman in 1957 [27]. By using 8.087 kHz single sideband-suppressed carrier communication, distances up to 9000 yards were achieved. A short range (60m), high data rate (500kbps) communication system was reported by Kaya and Yauchi in 1989 [28]. The LinkQuest commercial acoustic modem can support data rates up to 15kbps, for the communication ranges in the region of few km. In recent years, researchers have been working diligently to minimize the limitations for better underwater communications using acoustic waves. For example, a high rate underwater acoustic link for transmitting video was reported in [29]. An efficient modulation technique and a sophisticated data compression technique were used to achieve a data rate of 64kbps. Another group has been trying to use an Orthogonal Frequency Division Multiplexing (OFDM) based solution to achieve a better link performance [30]. However, obtaining a high bandwidth using acoustic communication seems unlikely because of the characteristics of acoustic waves in water.

2.3.3 Underwater optical wireless communication

The limitations of acoustic and radio communications stimulated researchers to see the possibility of optical wireless especially visible light communication in underwater. Until now, the results which have been obtained look very promising. Some of the underwater optical wireless communication research is summarized in table 2-3.

Chancey designed and tested an FM optical wireless communication system for

underwater, which was capable of sending data at Mbps speeds [5]. In his thesis, he detailed the link budget for underwater optical wireless communication considering the scattering and absorption effects in sea water.

Table 2-3 Summary of different underwater optical wireless communications research

Groups	Network type	Topology	Achieved results	Comments
MIT	Sensor network and point-to - point communication	Unidirectional link	Range: 2.2m Data rate: 320kbps	Used expensive lenses and hardware to achieve results
Genova	Diffuse Sensor network	Star network topology	Range : 2m Bitrate:100 kbps	Used planner type transceiver and free space technology
North Carolina	Different fundamental things of U-OWC	Mainly point-to-point	Achieved significant results	Has done extensive research on UW-OW
Woods Hole Oceanographic Institution	Bi-directional Optical link	Point-to-point	Range: 200m Bitrate: 5Mbps	Very expensive hardware and setup
Ben-Gurion University of the Negev	Different types of ink for sensor and point-to-point	Point-to-point link	Communication up to 100m possible	Simulation based results

Later, his work was advanced further by Simpson ,Cox and Everett to investigate different issues such as forward error correction, modulation techniques, and communication link design for high data rates up to 1Mbps, which were reported in

[31] [32] [33]. Cox implemented a Reed-Solomon channel coding in the underwater optical wireless communication system, and found that the power requirement can be reduced by 8dB to achieve a bit-error- rate of 10^{-4} compared to OOK return-to-zero modulation techniques [34]. Later, Simpson implemented error correction coding for a 5Mbps link, and tested the system for up to 7.7m [12]. He also built a spatial diversity system to measure the optical fading in the underwater environment [35].

An unidirectional optical wireless link capable of sending data at 320kbps up to a distance of 2.2m for underwater sensor networks was presented in [3]. To achieve this communication distance, a high powered LED array was used, and the link was only used to upload the sensor data from sensor node to an AUV. The same group advanced their research to achieve a data rate of 1.2Mbps in the communication range of 30m [11]. Recently, they reported a bi-directional communication system to achieve a communication range of 50m [8]. In this paper, a software defined radio approach was adopted to perform different encoding and decoding techniques. They used 18, high power LEDs, in an array (each LED was driven at 600mA) at the transmitter side, and also used an avalanche photodiode at the receiver side to achieve the distance of 50m. A SNR of 5.1 was determined for a distance of 50m.

Anguita *et al* also presented a Physical and MAC layer architecture for an underwater optical wireless sensor network in [26] [15]. The main focus was to build a diffuse optical wireless communication system capable of interfacing with the current terrestrial wireless sensor network technologies. They achieved a data rate of 100kbps for a communication distance of 1.8m.

Farr and his group at Woods Hole Oceanographic Research Centre developed a modem for observing the seafloor, which was capable of sending data at a few Mbps rate up to 100m [6]. A different approach for aiming the transmitter and receiver has

been proposed by taking account of different link scenarios. This group later reported a high bandwidth communication link of 5Mbps over a distance of 200m in clean water using a diffuse optical communication link [36]. Depending on the turbidity of water, this can be as low as 40m. In their recent system named CORK optical telemetry system (CORK-OTS), they used both an optical and an acoustic modem for communications capable of operating up to 10Mbps [37]. They also used both green and blue light to make the system bidirectional, and used an acoustic modem to wake up the seafloor installation. Details of the CORK hardware and software were reported in [38].

Felix also reported a underwater communication system using an IrDA physical layer with 3W high power LEDs [39]. Hanson proposed a laser based communication link, which achieved data rate of 1Gbps over a distance of 2m using a water pipe in the laboratory, and predicted the distance which could be achieved up to 48m in clear water [9]. A cost-effective underwater optical modem was proposed by Feng to achieve a communication distance up to 10m [40].

Jaruwatanadilok modelled the underwater optical wireless channel using vector radiative transfer theory to investigate the multiple scattering and polarization of light [13]. He calculated the bit error rate for on-off-keying modulation and 4-level amplitude modulation with different fields of view (FOV). As concluded, the bit error rate increases according to the distance, and decreases when the FOV is decreased, because more FOV means more received optical power by the receiver. Arnon proposed three types of communication links, and analysed the performance of each type [41]. From his analysis it was shown that the communication performance decreased rapidly when water absorption increases, but obtaining a high data rate was still possible.

A basic comparison between different communication systems in underwater is given in the following table 2-4 [2] [4] [39] [42] .

Table 2-4 Comparison between acoustic, RF and optical medium underwater

Carrier/Features	**Acoustic**	**Radio**	**Optical wireless**
Speed (m/s)	1500	33,333,333	33,333,333
Input power	Tens of Watts	Watts to Mega-Watts	mWatt- Few Watts
Power loss	>0.1 dB/m/Hz	28dB/km/100MHz	Turbidity
Bandwidth	kHz	MHz	10-150MHz
Antenna size	0.1m	0.5m	0.1m
Range	Km	10m	10-100m

As seen from the table, optical wireless has huge potential compared to other two carriers in the short and medium communication range. The input power requirement for optical wireless communication is also lower compared to other two carriers, so it has been chosen as a communication carrier for the underwater sensor network.

2.4 Attenuation of optical wireless underwater

In spite of having high bandwidth and low power loss, optical wireless also suffers both from scattering and absorption, resulting in severe attenuation in water. Behaviour of light in water depends on the water components, so, before designing a system, one need to understand the propagation phenomena of light in water as it exhibits differently in different water types. Moreover, system design is affected by the optical properties of the water. Some of the attenuation factors for optical wireless have been summarized in figure 2-3 [5] .

The following equation describes the relation between attenuation and communication distance [15]

$$A = e^{-k(d_1 - d_2)(\frac{d_1}{d_2})^2} \quad \textbf{(2-1)}$$

Where the position of transmitter and the receiver are denoted by d1 and d2 respectively, and K is the attenuation coefficient defined by equation 2-2

$$k = \alpha(\lambda) + \beta(\lambda) \quad \textbf{(2-2)}$$

Where α is the absorption coefficient which depends on the light wavelength, and β is the scattering coefficient which mainly depends on wavelength as well as the turbidity of water.

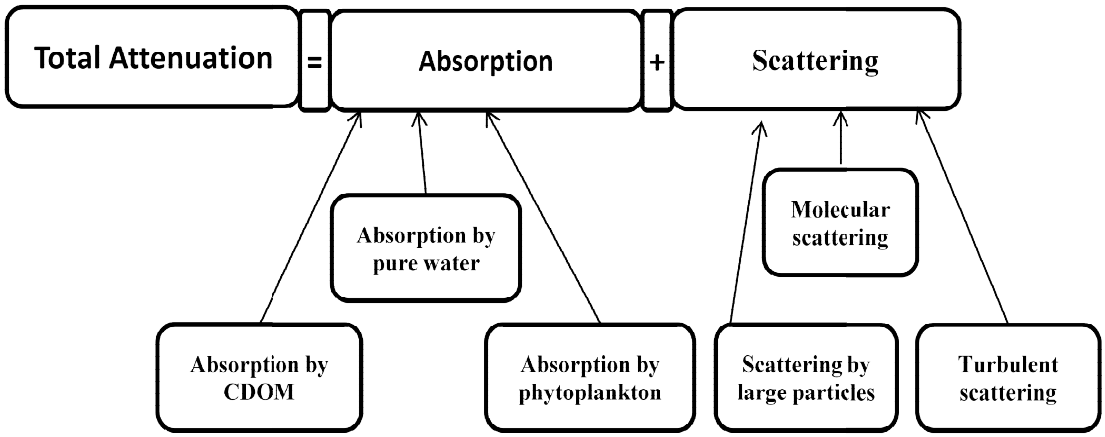

Figure 2-3 Functional block diagram of total attenuation [5]

2.4.1 Absorption modelling

Sea water is primarily composed of water (H_2O), but it also has different salts such as, $NaCl, MgCl_2, Na_2So_4, KCl$, which absorb light at specific wavelengths. Absorption also occurs due to organic materials like fulvic acid, chlorophyll and humic acid, as shown in figure 2-2. The total absorption coefficient $\alpha(\lambda)$ can be calculated from the

following equation [5]

$$a(\lambda)=a_w(\lambda)+a_d(\lambda)+a_f(\lambda)+a_h(\lambda) \quad \textbf{(2-3)}$$

Where $a_w(\lambda)$ is the absorption coefficient of pure water as a function of wavelength per metre, $a_{cl}(\lambda)$ is the absorption coefficient of chlorophyll, $a_f(\lambda)$ is the absorption coefficient of fulvic acid, and $a_h(\lambda)$ is the absorption coefficient of humic acid. Again, each of the absorption coefficients can be defined from [43] [44]. The absorption coefficient for sea water, $a_w(\lambda)$ can be defined from [44]which is given in equation 2-4

$$a_w(\lambda)=a_w^o(\lambda)[\frac{w_c}{w_c^o}]^{a_w^o} \quad \textbf{(2-4)}$$

Where $a_w^o(\lambda)$=0.0405λ , for a water concentration w_c^o = 1 mg/m^3 and $0 \le w_c \le 15$ mg/m^3

Chlorophyll concentration can be expressed as following [41]

$$a_{cl}(\lambda)=a_c^o(\lambda)[\frac{c_c}{c_c^0}]^{0.0602} \quad \textbf{(2-5)}$$

Where $a_c^o(\lambda)$ is the specific chlorophyll absorption coefficient as a function of wavelength, c_c is the total chlorophyll concentration in mg/m^3, and $c_c^0=1mg/m^3$. Similarly, absorption coefficient for humic acid and fulvic acid can be expressed by following equations [41]:-

$$a_h(\lambda)=a_h^o \times C_h \times e^{-k_h\lambda} \quad \textbf{(2-6)}$$

$$a_f(\lambda) = a_f^o \times C_f \times e^{-k_f \lambda} \quad \textbf{(2-7)}$$

Where k_h=0.01105/nm; q_h^o=18.828 m^2/mg is the specific absorption coefficient for humic acid, and k_f=0.0189/nm; q_f^o=35.959 m^2/mg is the specific absorption coefficient of fulvic acid. C_h and C_f are the concentration of humic acid and fulvic acid in mg/m^3. Now, total absorption can be re-written as follows,

$$a(\lambda) = a_w(\lambda) + a_c^0(\lambda)\left[\frac{C_c}{C_c^0}\right]^{0.0602} + [a_h^0 \times C_h \times e^{-k_h \lambda}] + [a_f^0 \times C_f \times e^{-k_f \lambda}] \quad \textbf{(2-8)}$$

By considering the attenuation effects mentioned above, it was found that the best wavelength which propagates in water is in the green-blue region of the visible spectrum (wavelength 400-550nm), as seen from the figure 2-4 [15]. So, this wavelength will be considered when designing a transceiver for underwater communication.

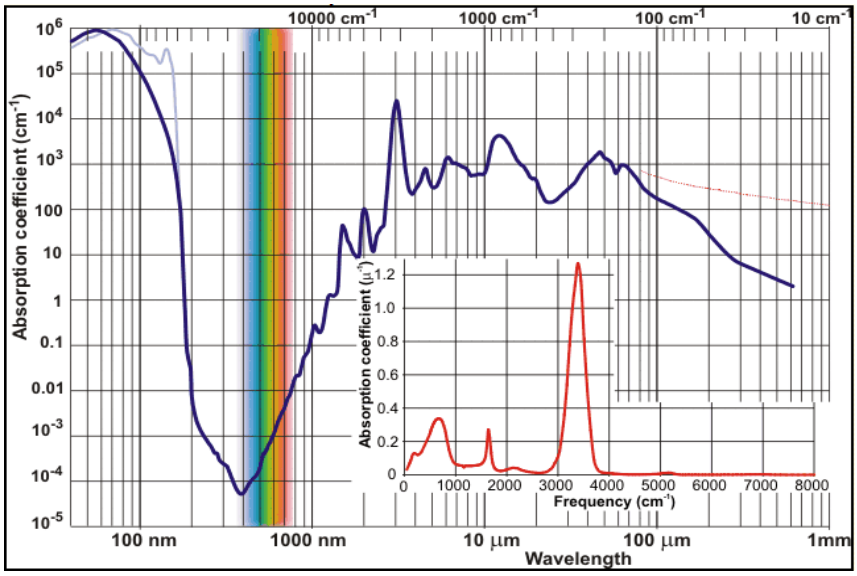

Figure 2-4 Light absorption in water [15]

2.4.2 Scattering modelling

The scattering coefficient $b(\lambda)$ is defined as the loss of flux due to the re-direction of photons, which is a combination of the scattering coefficient of pure water $b_w(\lambda)$, small particles $b_s^o(\lambda)$, and large particles $b_l^o(\lambda)$, as seen in figure 2-2. The total scattering coefficient can be calculated from the following equation [45],

$$b(\lambda) = b_w(\lambda) + b_s^o(\lambda)C_s + b_l^o C_l \quad \textbf{(2-9)}$$

Where C_s and C_l are the total concentration of small and large particles in gm/m^3. Again, to find each of the coefficients , the equation can be found from [5]

$$b_w(\lambda) = (\frac{0.005826}{m})(\frac{400}{\lambda})^{4.322} \quad \textbf{(2-10)}$$

$$b_s^o(\lambda) = 1.151302(\frac{m^2}{g})(\frac{400}{\lambda})^{1.7} \quad \textbf{(2-11)}$$

$$b_l^o(\lambda) = 0.3411(\frac{m^2}{g})(\frac{400}{\lambda})^{0.3} \quad \textbf{(2-12)}$$

Adding all three equations together gives the total scattering coefficient:-

$$b(\lambda) = (\frac{0.005826}{m})(\frac{400}{\lambda})^{4.322} + 1.151302(\frac{m^2}{g})(\frac{400}{\lambda})^{1.7}(C_s) + 0.3411(\frac{m^2}{g})(\frac{400}{\lambda})^{0.3}(C_l) \quad \textbf{(2-13)}$$

Figure 2-5 shows the light scattering behaviour of sea water. It is seen that the scattering coefficient is at its minimum in the green and blue part of the spectrum, around 400-600nm wavelengths [46].

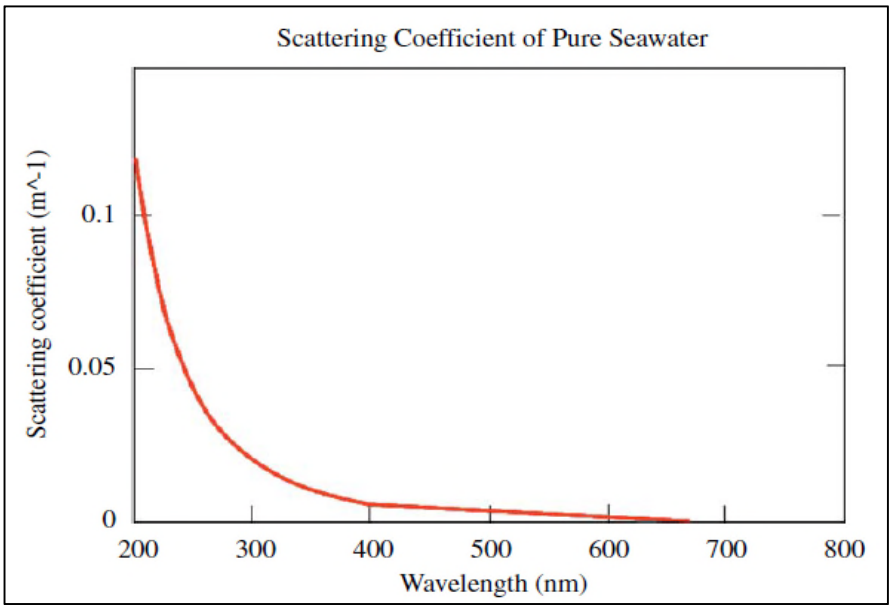

Figure 2-5 Light scattering coefficient of sea water [46]

Now, considering both the absorption and scattering coefficients, the relationship between received optical power with respect to transmission distance can be found from the equation 2-14 ,considering the attenuation [44].

$$P_R = P_T e^{-\alpha(\lambda) L_M} \qquad \textbf{(2-14)}$$

Where P_R is the received optical power, P_T is transmitted optical power, $\alpha(\lambda)$ is attenuation which is wavelength dependent, and L_M is the transmission distance. By keeping all other variables constant in equation 2-14, the relation between transmission distance and received optical power can be calculated for different wavelengths, which is shown in figure 2-6.

As absorption and scattering are in minimum level around the blue-green part of the spectrum, so these two wavelengths are selected for this communication system.

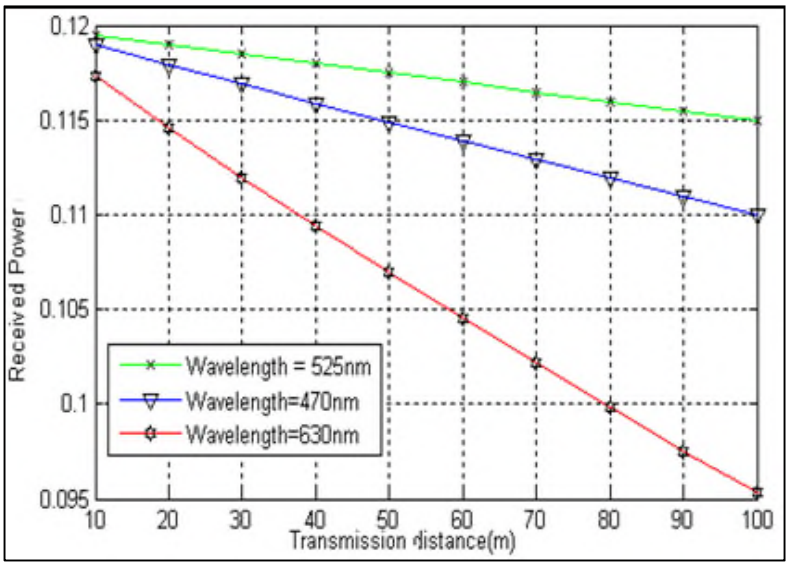

Figure 2-6 Received optical power vs. communication range

2.5 Issues related to system deign

In this section, some of the system level issues such as photon sources, photon detectors, and modulation techniques, related to underwater optical wireless communication will be discussed.

2.5.1 LED or Laser?

The first step to design an optical wireless transmitter starts with the photon source selection. A Laser, LED or incandescent light can be used as the source, but will depend on the switching speed, bandwidth, size constrains and power limitation of the required system. The most widely used photon sources for communications are LEDs and Lasers, which are compared in table 2-5 [47].

From the table, it is realized that the Laser has minimum divergence, and coherence compared to an LED, but it has a higher cost and medium life time. In terms of bandwidth, a laser can operate in the GHz range for high bandwidth applications compared to LED. On the other hand, an LED has high reliability, and also longer

life time.

Table 2-5 Comparison between Laser diode and LED

Characteristics	LED	Laser diode
Optical spectral width	25-100nm	0.1-5nm
Modulation bandwidth	<200MHz	>1GHz
Output beam divergence	Wide	Narrow
Cost	Low	High
Life time	Long	Medium
Reliability	High	Moderate
Range	Low	High

Besides all of these characteristics, one should consider the optical power versus current characteristic of a LED and a laser, which can be found from figure 2-7 [48].

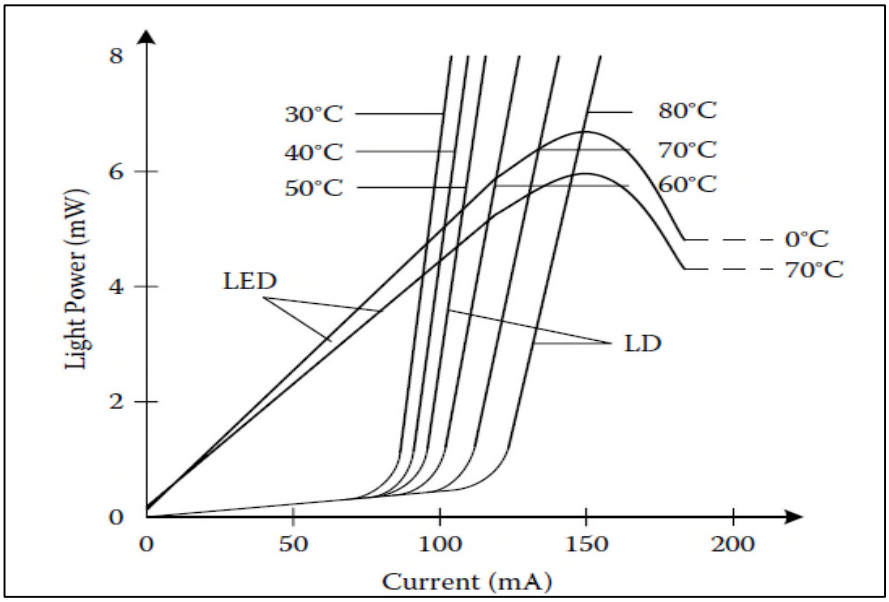

Figure 2-7 Light power versus current characteristics of Laser and LED [45]

As seen, an LED has the linear response near the origin, whereas a Laser is approximately linear above the threshold. Moreover, laser characteristics changes rapidly according to the temperature. Since the focus of this project is to build a cost-effective and reliable communication system for an underwater sensor network, so an LED was chosen as the photon source.

2.5.2 Photon detector selection

There are many types of optoelectronic device available as a photon detector. Ideally, a photon detector should receive all incident photons sent by the photon source without adding noise. The dominating noise source for an optical wireless communication system is ambient light, which is the summation of fluorescent light, sunlight, and incandescent light. The shot noise generated by the ambient light also degrades the communication performance. The SNR performance of the receiver is affected by background interference noise, which eventually leads to poor system performance. The power spectral density of different lights at different wavelength is shown in figure 2-8 [49].

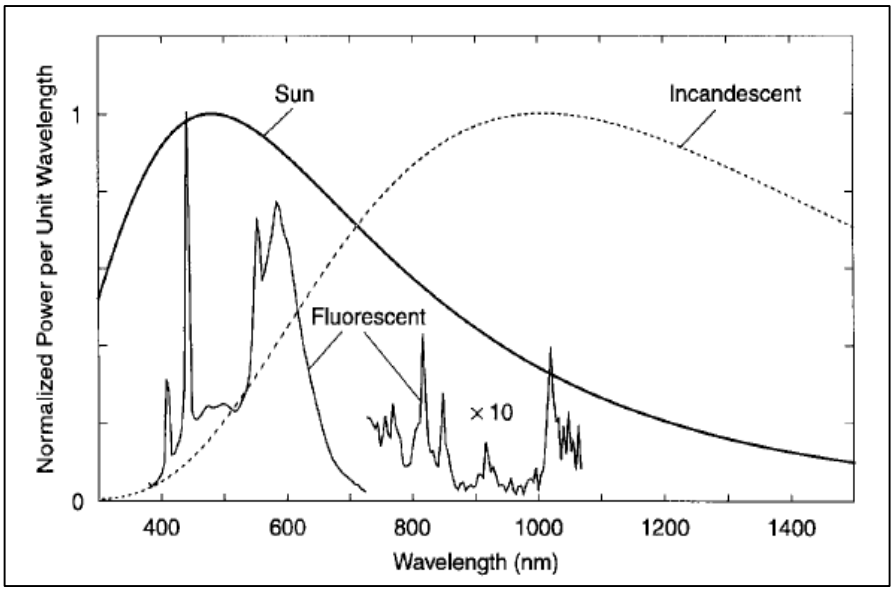

Figure 2-8 Optical power spectra of common ambient infrared sources [49]

As seen, the visible light spectrum is mostly affected by the background light as discussed above, so it is very important to choose the right photon detector for better performance. In addition to the noise performance, it has to be small, cheap, reliable, and power efficient. The most common photon detectors are compared in the table 2-6 [47].

Table 2-6 Comparison of photon detectors

Parameter	**Photo resistor**	**PIN photodiode**	**Avalanche Photodiode**
Speed	Slow <1Hz	Fast 10MHz To 10 GHz	Fast 100MHz To 10GHZ
Gain	Small	Unity	100-10,000
Noise performance	Good	Very good	Fair
Linearity	Small region	Excellent	Non linear
Size	Small	Small	Small

From the table it is understood that avalanche photodiodes (APDs) have higher gain, and also switch faster. However, in terms of noise performances and linearity, a PIN photodiode has a better performance. On the other hand, a photoresistor's gain and speed is very small compared to a PIN photodiode. Another very important factor which needs to be considered is the FOV. A large FOV is desirable to collect as many photons as possible, which ultimately ensures better gain. However, it may also degrade the quality of modulation signals depending on the turbidity of water, and the frequency of modulation.

In general, the selection of photon detector will depend on the application scenario and needs to consider the above mention factors. Since this project considers a short

range and cost effective system, so a PIN silicon photodiode was chosen for receiver design.

2.5.3 Modulation techniques

Modulation techniques play a vital role in all sorts of communion systems, including optical wireless. Three major characteristics of a modulation technique are transmission efficiency, power efficiency, and bandwidth efficiency, as mentioned in [50]. The modulation scheme should be able to deal with intersymbol interference, and also be able to maintain the BER at an acceptable label. A modulation technique with high bandwidth efficiency η_B ensures the overall system bit rate, so it is important to choose modulation techniques accordingly. The bandwidth efficiency can be expressed by the equation 2-15, where R_B is the achievable bit-rate, and B is the transceiver bandwidth [51],

$$\eta_B = \frac{R_B}{B} bit/s/Hz \qquad \textbf{(2-15)}$$

Finally, the power efficiency has to be considered to achieve a certain BER for a specific data rate. This is very important for the underwater environment for a higher life time for the system.

Different modulation techniques for optical wireless have been presented in [49] [52] ; among them the two most commonly used modulation techniques are OOK and PPM, which are briefly described here.

2.5.3.1 On-off keying

On off keying (OOK) is the simplest and most cost-effective form of modulation in terms of implementation. Here, the optical power is directly modulated by varying the source current, whereas, at the receiver side the detector produces a photocurrent

proportional to the number of received photons [26]. OOK can be either in the form of Non Return to Zero (NRZ) or Return to Zero (RZ). In this thesis, NRZ-OOK signalling is used because of its lower power requirement.

In both cases, to represent binary '0', no power is required, but to represent binary '1', in case of NRZ, this requires twice the power of the average, whereas in the case of RZ, it is four times of the average power, as shown in figure 2-9 which is adapted from [49].

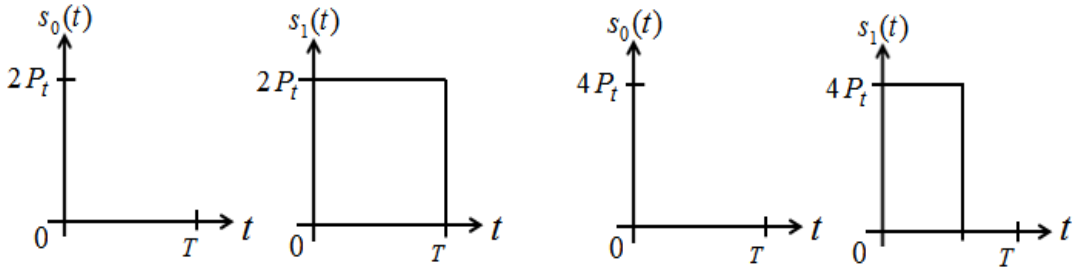

Figure 2-9 Comparison of (a) NRZ-OOK Pulse (b) RZ-OOK Pulse with duty cycle 0.5

The bandwidth required for an OOK system is the inverse of the pulse width which is $R_b = 1/T$, and bit rate of the system can be found from the following equation [52]:

$$BER_{OOK} = Q\left(\frac{P}{\sqrt{N_o R_b}}\right) \quad \textbf{(2-16)}$$

Where P the average is received optical power, N_0 is the power spectral density of the Gaussian noise, Q is the customary function of the digital communication, and R_b is the bandwidth of the system.

2.5.3.2 Pulse Position Modulation (PPM)

As named, the position of the pulse is changed in a clock cycle to represent a different bit in PPM modulation. In this method, the average power requirements are decreased compared to an OOK system by compensating the increase in bandwidth requirements. PPM can be either at two or multi-levels, depending on the requirements, represented by L-PPM. A 4-PPM pulse waveform is shown in the figure 2-10, which is adopted from [49], where all four pulses are transmitted during different clock cycles.

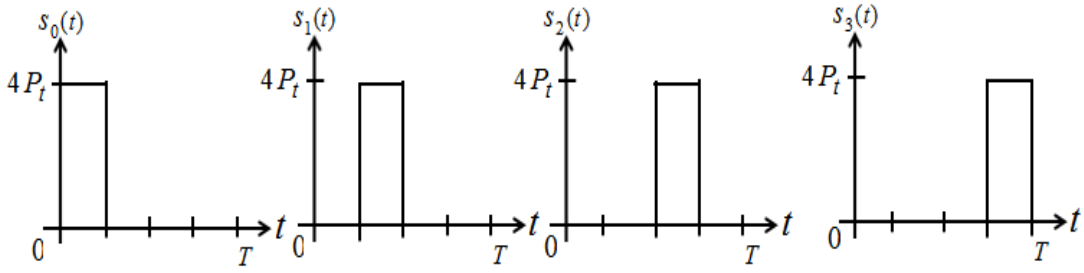

Figure 2-10 Transmitted waveform of 4-PPM

The bandwidth of an L-PPM system can be found from the equation 2-17, where L represents the number of levels and R_b is the bit-rate of the system [53].

$$B_{L-PPM} = \frac{R_b}{\log_2 L} B \qquad \textbf{(2-17)}$$

Other than OOK and PPM, there are various modulation techniques used in optical wireless communication system. Comparison between those modulation techniques has been mentioned in the table 2-7 [47].

From the table, it is seen that, in terms bandwidth requirements, OOK is the best solution, although it requires the same power compared to 2-PPM method. Implementation cost is also very low for OOK, which is why it is a widely-used

modulation technique in optical wireless communication systems.

Table 2-7 Comparison of various modulation techniques for optical wireless communication

Modulation scheme	Optical power requirement	Bandwidth requirement
OOK	$\sqrt{N_0 R_B} Q^{-1}(BER)$	R_B
2-PPM	$\sqrt{N_0 R_B} Q^{-1}(BER)$	$2R_B$
BPSK	$\sqrt{2N_0 R_B} Q^{-1}(BER)$	$2R_B$
L-PAM	$(L-1/\sqrt{L}-1/\sqrt{\log_2 L})\sqrt{N_0 R_B}$	$(R_B/\log_2 L)$
L-PPM	$(1/\sqrt{0.5L\log_2 L})\sqrt{N_0 R_B} Q^{-1}(BER)$	$(LR_B/\log_2 L)$

The performance of different modulation techniques in underwater environment was investigated in [54, 55]. Two most common and simple modulation techniques in free space optical communication are OOK and PPM, which are also suitable for underwater communications. In terms of BER performance it has been shown that

PSK is the best solution compared to the others, as shown in figure 2-11 [55].

As seen in the figure, for a communication distance up to 10m, most of the modulation techniques are well suited. So, considering the implementation complexity, the simplest modulation technique is OOK and this is adopted for this application.

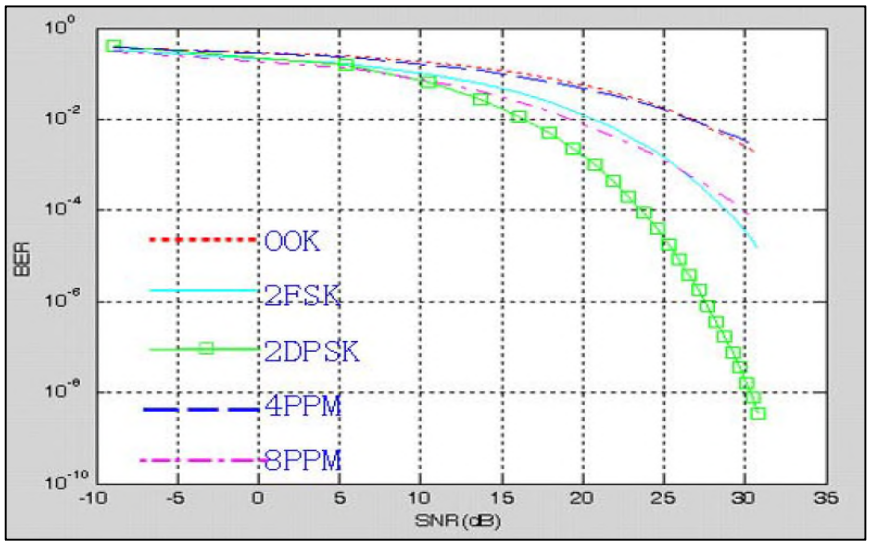

Figure 2-11 BER performance of different modulation techniques [55]

2.6 Different types of link for underwater optical wireless

An optical wireless communication link can be summarized in figure 2.12 which has been adapted from [56].

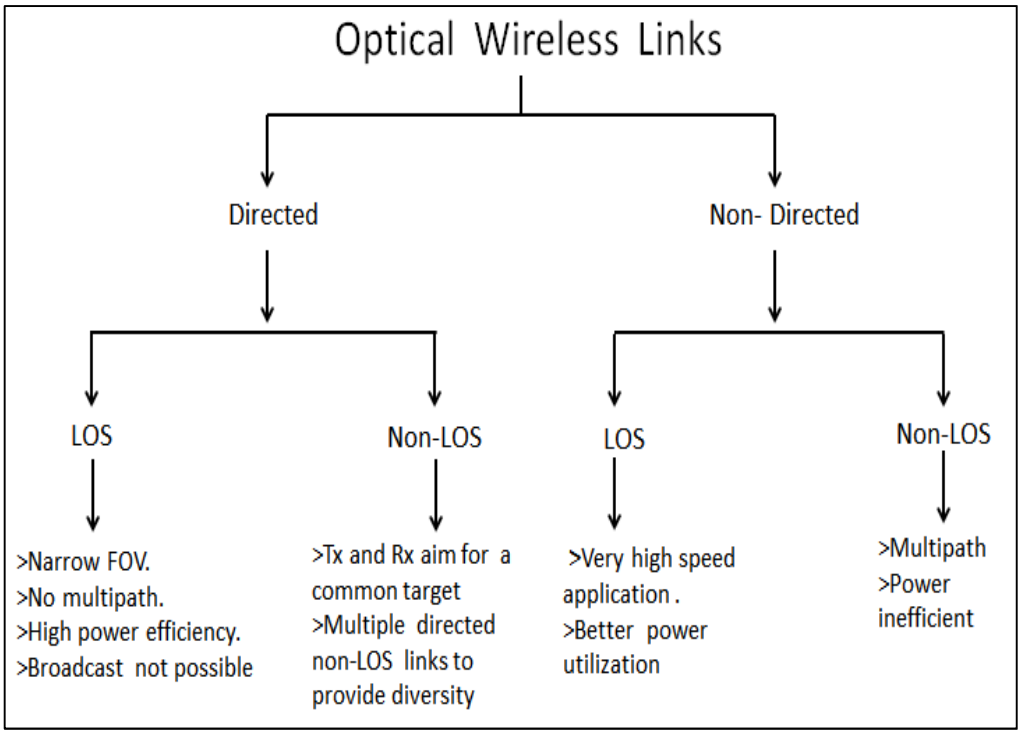

Figure 2-12 Links for optical wireless communication network

Depending on the positioning of the transmitter and receiver, the optical wireless communication link can be divided into either Line of Sight (LOS) or Non Line of Sight (N-LOS) which is also called as a diffuse communication link. Again, LOS can be divided into two categories depending on the direction. If the transmitter is directly aligned with the receiver, then it is called directed LOS communication. In directed LOS communication, the transmitter and receiver has to be aligned to get the maximum power and communication distance, whereas in Non Line of Sight (N-LOS) the transmitted signal is reflected back to the receiver from a surface or room ceiling to make the communication possible. So, the field of view (FOV) for LOS communication is very narrow and requires less power. In the case of a diffuse communication receiver the FOV needs to be larger to receive the maximum transmitted power. With the LOS link, less multipath distortion can be achieved but also the disadvantage is the precise alignment required between transmitter and receiver. On the other hand, with diffuse communication link, accurate alignment is not required and a signal can be achieved through the obstacles which improve the robustness of the system.

For an underwater communication system, the performance analysis and feasibility of different link types has been analysed by Arnon [7] [57] [41]. Arnon investigated three different types of underwater optical wireless communication links, as given below:-

1. Line of Sight (LOS) link
2. Modulating retro reflector link
3. Reflective link (Diffuse)

In case of a LOS link, the transmitter and receiver are aligned towards each other for the communication and until now, most of the underwater optical wireless

communication has adapted this type of link. On the other hand, a modulating retro reflector link can be implemented when one node has higher resources than the other communicating node, for example, in the ocean, a submarine has all the resource compare to divers. In this type of scenario, an interrogator can be put in one side (which has better access to resources) and a modulating optical retro reflector can be put on the another side (which has lees access to resources) of the link. Performance analysis of the two different types of communication links has been shown in the following figure [7].

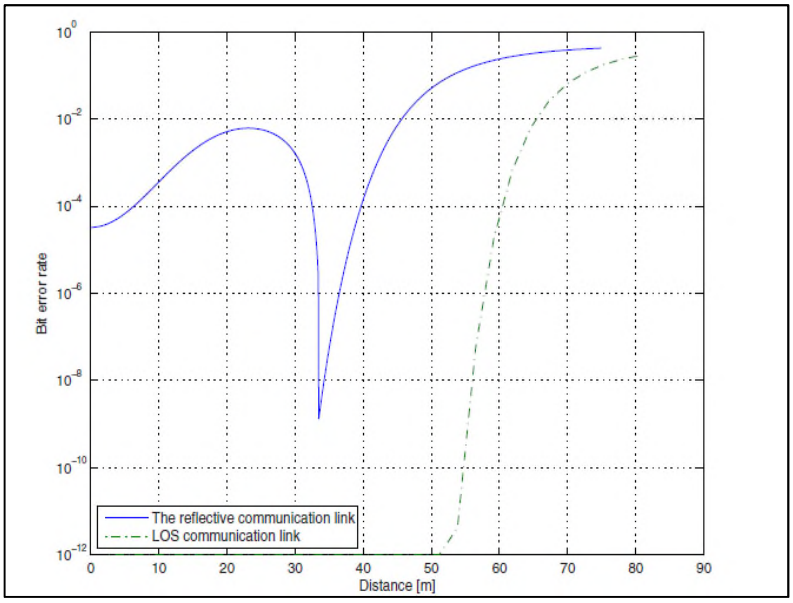

Figure 2-13 BER performance of two types of communication link underwater

Finally, the reflective or diffuse communication link can be used when broadcasting is needed. In this sort of scenario, the transmitter sends an optical signal upwards and this signal is reflected back to the receiver by the ocean surface, since the refractive index of air is lower than that of the water. This kind of scenario is shown in the figure 2-14 [41].

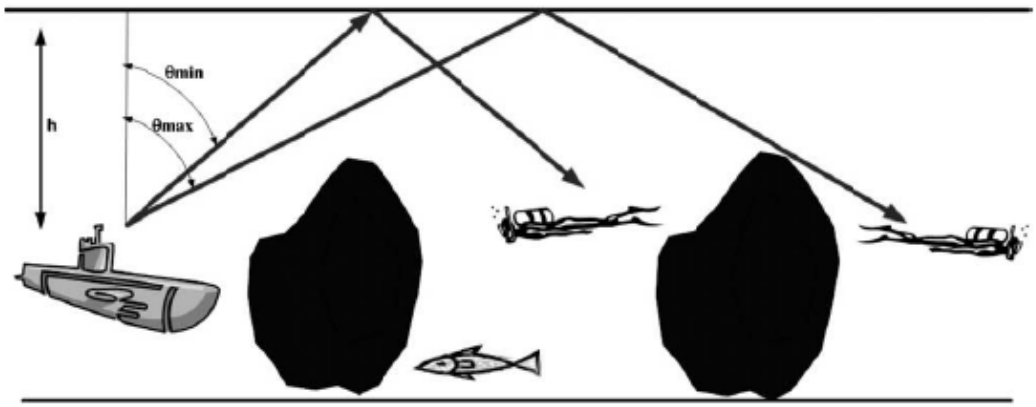

Figure 2-14 Reflection communication scenario

All three types of communication link can be used for underwater communication system, depending on their application. The bit error rate performance of the LOS and the reflective link are shown in the figure 2-13. As shown, the BER increases with the distance in both cases. In the range of few metres, both types of link can be used. Since this thesis focuses on building a multi-hop communication, so a directional LOS communication link has been chosen for this project.

2.7 Conclusion

In conclusion it can be said that optical wireless has a significant potential in the next generation underwater communications for oceanographic monitoring or collecting environmental data. There are still many open issues, which need to be resolved before it can be commercialized for real deployment. From the literature review it has been found that most of the previous work focused on increasing communication range and bandwidth of the system for long distance communication. Experimental and simulation results were reported that a range of tens of metres can be achieved. To increase communication range further, an alternative approach, such as multi-hop communication, has to be examined. However, none of these groups investigated the

possibility of multi-hop optical wireless communication underwater, which can solve the low range communication problem.

Chapter3 : Transceiver design and testing

3.1 Introduction

Most free space optical wireless communications are based on infrared which is not suitable for underwater communication. As discussed in the previous chapter, the best appropriate wavelengths for underwater communication are in the green or blue parts of the spectrum, so this chapter discusses the design of a transceiver based on green and blue LEDs. Since the goal of the project is to build a multi-hop bidirectional communication for an underwater sensor network, the transceiver is designed accordingly. The focus of this project is mainly to demonstrate the idea of multi-hop communication underwater using visible light, so achieving high bandwidth or maximum range is not the issue here, rather establishing a simple, cost-effective, and practical communication system within the lab environment is more important, although high bandwidth and more range can be achieved by designing complex circuit, increasing transmission power, and using expensive optics like a

lens, a concentrator etc.

In this application, a targeted communication range was set up to 1m for each link, which is limited by the water tank available inside the lab. Main focus here is not to use any external optics (Lens, Concentrator etc.), which is very expensive compared to the used optoelectronics. The required bandwidth for the sensor network is in the range of tens of kHz, so emphasis was given to achieve 100kHz, which would be a moderate bandwidth for sensor applications. Finally, each of the components was selected carefully considering the low power requirements, which is one of the main reasons for deployments of a sensor network, especially in underwater environments.

The rest of the chapter discusses the details of the transceiver design, selection of each components and performance of each block. The built transceiver was also implemented for a real application to send audio through the water.

3.2 Block diagram of the transceiver

Figure 3-1 demonstrates the block diagram of an underwater optical wireless transceiver, which is mostly similar to the free space optics except for the operational wavelength.

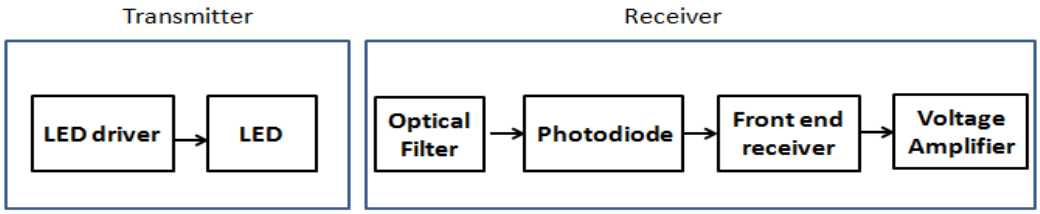

Figure 3-1 Block diagram of an underwater optical wireless transceiver

The transceiver consists of a transmitter and a receiver, which has been designed to meet the needs of a specific application. In this project, the transceiver was

connected to a microcontroller, so the received signal was converted to the 5V level.

First of all, in the transmitter part, a digital modulation circuit was designed to drive the LED in the form of OOK. In the receiver part, the first block represents the optical filter, which is used to separate the blue and green light and placed in front of the photodiode. The purpose of this filter is to reduce the ambient light, and also pass a specific light, which eventually increases the SNR significantly. The most important part of the receiver, as well as for whole system design, is the front end receiver circuit which determines the bandwidth and range of the system. As it is known, there is a trade-off between bandwidth and gain of the system, so much attention was given to this part to find the optimum solutions for required bandwidth and range. Different types of receiver were designed and tested with different types of photodiode to get the optimum range and bandwidth, as well to get the maximum SNR. The final block of the figure represents the amplifier to amplify the received signal into the 5V level, which is required for the microcontroller input.

3.3 Transmitter circuit design

The transmitter circuit can be either analogue or digital depending on the applications. There are different types of analogue transmitter circuit available, which can be used straightway.

Transmitter circuit mainly consist of a photon source and a driver circuit which can be called as a modulator circuit as well. One of the most commonly used On-off keying modulator circuit is illustrated in figure 3-2 [48]. In this circuit, the LED driving current is provided by the transistor's collector current, which is controlled by the resistor R3. So the value of R3 has to be determined accurately to ensure enough current passes through the LED. The DC base current is chosen by the bias

resistors R1 and R2, which forwards the bias current to the emitter base junction to turn ON the transistor. The resulting collector current is determined by R1, R2, R3 and the base-emitter voltage across Q1. The signal voltage V1 produces a time varying base current which adds to the DC base current.

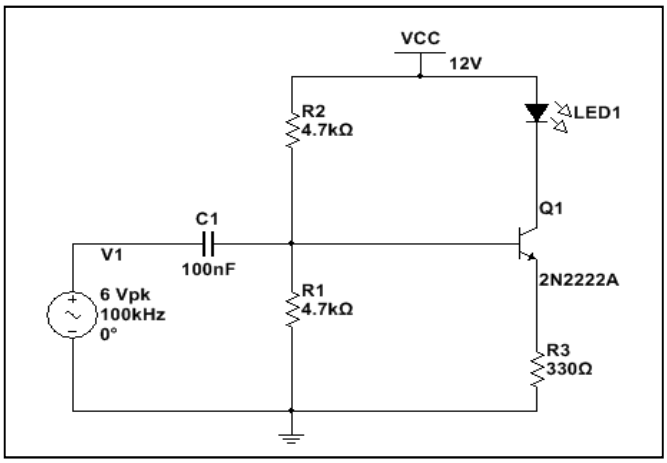

Figure 3-2 Basic optical wireless transmitter

Most of the visible-light LEDs are manufactured for lighting purposes rather than communication, so it is hard to find information regarding switching times or bandwidth supported by the LED in the data sheet. As a result, before designing a system it is essential to find the LED characteristics practically, especially the frequency response of the LED to estimate the supported bandwidth by the LED.

3.3.1 LED selection and Frequency response

After undertaking a careful research, Avago HLMP and Kingbright super flux green LEDs were primarily selected to see their frequency response and feasibility for the proposed system. Both of the LEDs are very cheap and power-efficient. The power dissipation for the first LED is about 116mW, and the Kingbright LED dissipates 120mW. Both of the LEDs have the peak wavelength at 525nm, and the DC forward current is about 30mA. The major difference between these two LEDs is their

viewing angle and intensity. The intensity of LED from Avago Technology is about 35000mcd, which is very high compared to Kingbright LED (5700mcd). The viewing angle of the Avago LED is also much less (15degree), compared to the Kingbright super flux (70 degree).

To find the frequency response of the two LEDs, an experimental setup, using a simple transmitter and a receiver, has been established. To drive the LED, the transmitter circuit shown in figure 3-2 is used. For photon detection, a simple optical wireless receiver front end, shown in figure 3-3 has been built.

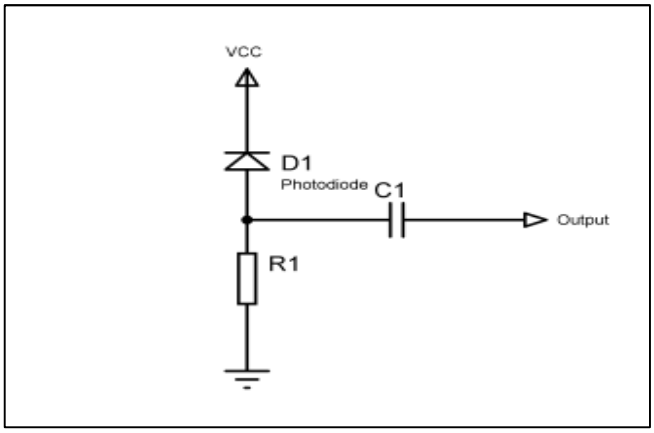

Figure 3-3 A simple optical wireless receiver

The frequency response of an LED cannot be measured if both transmitter and receiver do not support enough bandwidth. Now, the bandwidth of the receiver in figure 3-3 depends on the resistor value of R1 and also the photodiode's internal capacitance. The photodiode which is used for this experiment has an internal capacitance of 170pF for a 10V bias voltage, but is smaller in the reverse bias setup. So, a lower value of R1 is chosen for sufficient bandwidth of the receiver, which is expected to be higher than the LED frequency response. To find the frequency response of two LEDs, the same experimental setup was used. The measured

frequency response is plotted in figure 3-4.

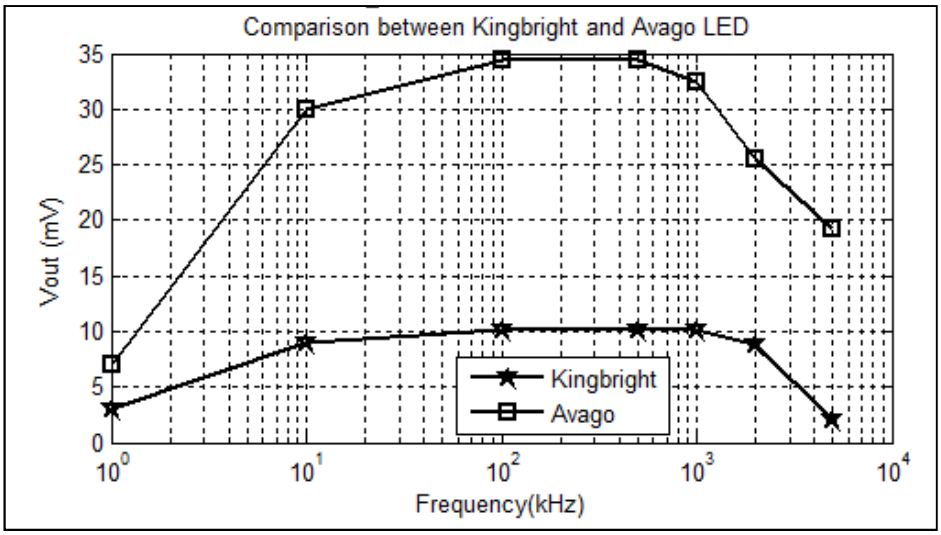

Figure 3-4 Frequency response of two LEDs

From the figure it is seen that the performance of Avago LED is much better than the Kingbright LED. Although the power dissipations for both LEDs are almost equal, because of higher beam divergence angle of Kingbright LED, the received voltage is much lower than the Avago one. Besides, the intensity of Avago LED is much higher compare to the Kingbright one, which is another reason for lower gain. Moreover the frequency response is also higher for Avago technologies' LED, which inspired the author to select this LED for the proposed application.

Same categories of Avago LEDs can be found at different colours, which is another advantage of choosing this LED. To implement two different channels, at least two different coloured LEDs would be required. The gain of red, blue and green were obtained experimentally in air to choose the best two colours. As seen from the figure 3-5, blue and green has better gain with similar frequency response in air. In fact underwater, green LEDs perform better than blue, so these two colours were chosen for this application.

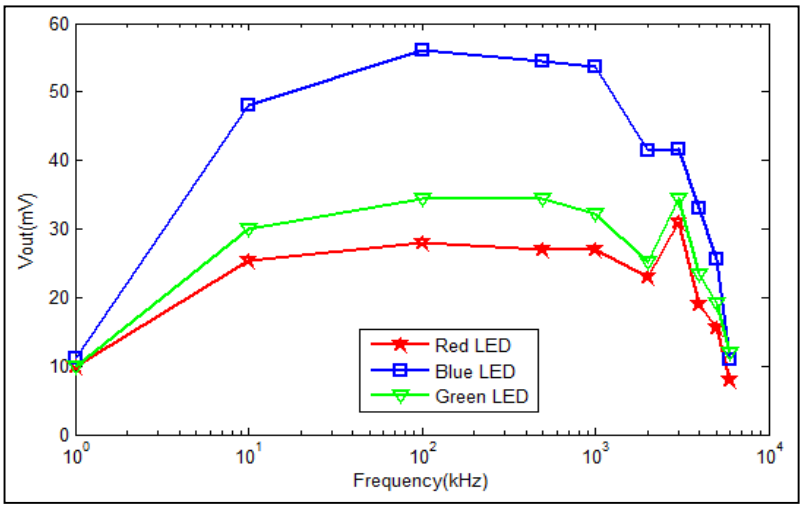

Figure 3-5 Frequency response of different coloured Avago LEDs

3.3.2 LED driver circuit

The purpose of the LED driver circuit is to turn the LED ON and OFF according to the input signal. The common way of accomplishing this is to use a transistor as an electrical switch to control the current flowing through the LED to make it ON and OFF, as shown in figure 3-6. For digital data, LED ON time will represent the binary '1', and the OFF time will represent binary '0', which is an actually on-off keying modulation technique. A digital optical wireless transmitter is shown in figure 3-6.

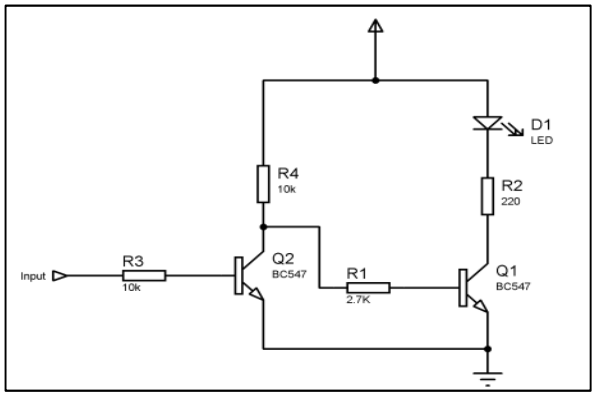

Figure 3-6 Digital optical wireless transmitter

In this configuration, transistor Q2 inverts the input signal so that at the receiving side, the original message is received rather than the inverted signal, which is inverted again after transistor Q1. The performance of the transmitter depends on the transistor characteristics, when the same LED is used. Also, R1 and R2 were chosen correctly for optimum performance.

3.4 Receiver design

The receiver front end design is the most complicated part in the optical wireless system design. The performance of the whole system relies on efficient and sophisticated receiver design. The target is to build a simple and cost effective receiver for the proposed application. Two of well-known optical wireless receiver configurations were built and optimized to find the optimal receiver for the proposed application.

3.4.1 Photodiode selection

The selection of a photodiode depends on the individual project aim. Of course, it is expected to have a higher depletion region, lower capacitance, and lower cost, which determine the performance of the system. For this application, a photodiode with peak response in the visible spectrum would be appropriate to detect the green or blue light. So, a first criterion was to find suitable photodiode operating in the visible range. The SILONEX SLD-70BG2 and OSRAM BP21 were selected initially to see the performance of each of them. Both of them have peak sensitivity in the green region and have BG filter to reject infrared wavelengths. The SILONEX photodiode has lower capacitance (180pF) compared to the OSRAM photodiode (580pF), and also the active area is (9.8 sq.mm) higher than for the second one (7.3 sq.mm). The OSRAM has a lower half angle (55degree) compared to SILONEX (60degree).

Again the problem is high device capacitance; both the devices have a very high capacitance, the effects of which need be reduced by an efficient front end design technique. The frequency response of the two photodiode is measured using the same setup described in section 3.4.1. The same transmitter and receiver were used to evaluate the performance of each photodiode by just changing the photodiode in the receiver circuit. The frequency response of the two photodiodes is compared in table 3-1. As seen, both the photodiodes support frequency up to 2MHz, but the SILONEX photodiode has a better performance in terms of gain, so for this project the SILONEX photodiode was chosen.

Table 3-1 Comparison between two Photodiodes

Frequency/	**Received output voltage(mV)**	
	OSRAM	SILONEX
1kHz	7	6
10kHz	24.4	26
100kHz	26.4	29
500kHz	25.6	29
1MHz	24.8	27
2MHz	22	22
3MHz	8	17

3.4.2 Receiver circuit configuration

Because of the limited transmitted optical power, the overall performance of an optical wireless communication system is determined mostly by the receiver performance [58]. Two main factors which are considered to measure the

performance of a receiver are bandwidth and sensitivity. The equation for finding the bandwidth is given in [48]:

$$f_{3db} = \frac{1}{2\pi RC} \quad \textbf{(3-1)}$$

Where R is load resistance, and C is the sum of photodiode capacitance C_d and input capacitance of the preamplifier circuitC_s. So it is clearly seen that, for a higher bandwidth, a lower resistor, and capacitor values are desired. On the other hand, a large area of photodiode ensures higher sensitivity by collecting the maximum transmitted optical power, but results in a high capacitance of the photodiode, C_d , eventually produce in a less bandwidth. The relationship between photodiode junction capacitance and area of the depletion region is shown in equation 3-2.

$$C_j = \frac{\varepsilon_0 \varepsilon_r A}{l_d} \quad \textbf{(3-2)}$$

Where C_j is the junction capacitance, A is depletion area of photodiode, ε_0 is the permittivity in vacuum and ε_r is the relative permittivity of the semiconductor, and l_d is the depletion region width.

From the above discussion, it is clear that the main objective of the receiver design is to minimize the effect of device capacitance, and increase the bias resistance, to achieve the maximum receiver performance. The common optical front end configurations are: Low impedance, High impedance, and Transimpedance amplifier. Besides the common techniques, there are several other approaches investigated by different research groups. Green first proposed the bootstrap transimpedance amplifier for bandwidth extension in 1989 [59]. Recently he also proposed a bootstrap amplifier with double peaking coil to enhance bandwidth of a high impedance receiver circuit up to 7.2 times compare to conventional high impedance

front end [60]. To improve the bandwidth of a transimpedance amplifier, a shunt bootstrapping technique was proposed by Hoyle and Peyton [61]. The performance analysis of the bootstrap transimpedance amplifier for large window optical wireless receiver was done by Idrus and her group [62]. The goal of all these technique is to reduce the capacitive effect of the photodetector to increase the system bandwidth and gain. In the next section, two new receiver designs are discussed for the underwater optical wireless sensor network, which are based on the bootstrap high impedance and transimpedance configurations.

3.4.3 Bootstrap front end

A bootstrap amplifier has almost unity gain with positive feedback. The relation between photocurrent with device capacitance and load resistance of a bootstrap techniques can be found in [60]. If I_P denotes the photocurrent and I_L is the load current then the amplifier voltage gain can be found from the relation,

$$I_L = \frac{I_P}{1 + j(1-A)\omega C_D R_L} \qquad \textbf{(3-3)}$$

Where if gain A gets close to 1, the effect of photodiode capacitance will become smaller, which results in a greater bandwidth. This technique is used when a higher bandwidth is the key issue for the communication system. In this project, the feasibility of this technique in underwater networks has been investigated. The circuit diagram from [60], was modified for the current application which is given in figure 3-7.

In this configuration, the photodiode is used in reverse biased mode to reduce the capacitance effect. The bandwidth of the system depends on the bias resistance and also the frequency response of the transistor. Hence, it is recommended to use a high

frequency transistor for this type of configuration. The limitation of these techniques is the lower bias resistance, because of the high base current requirement; one cannot increase the resistance very high, which results in the system being less sensitive.

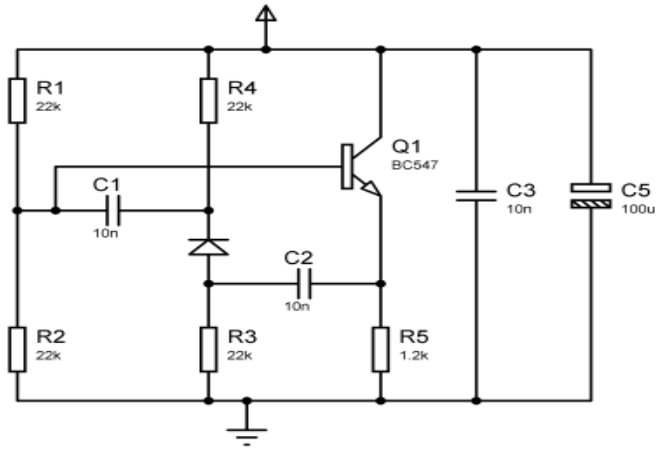

Figure 3-7 Bootstrap front end

Moreover, a high resistance means less bandwidth. Theoretically, the bandwidth of the system can be calculated from the equation 3-1, which is about 120kHz for the SILONEX photodiode. But practically, it is measured to be more than 600kHz because of the bootstrap effect, as seen in the figure 3-8.

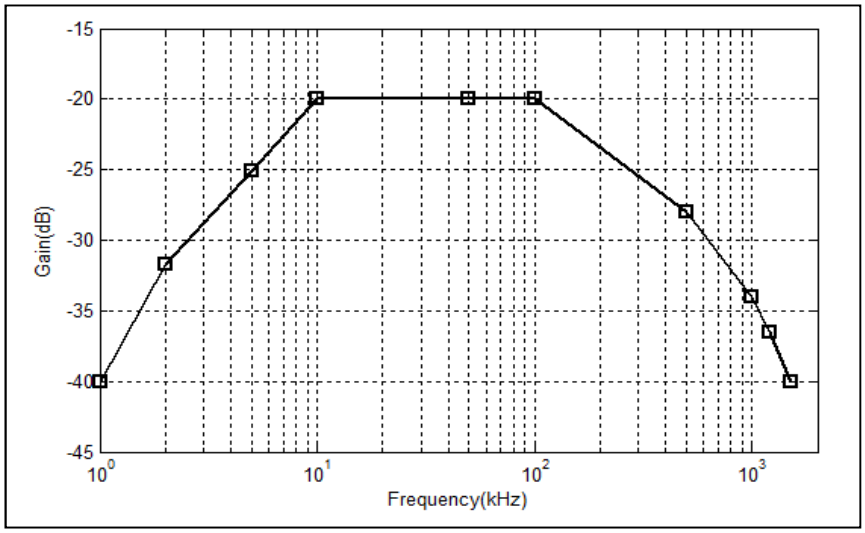

Figure 3-8 Frequency response of bootstrap amplifier

Although the overall bandwidth of this configuration is high for an underwater sensor network, the sensitivity of the receiver is very low; an optical signal cannot be detected after a few centimetres without using any external lenses. For this reason an alternative design was investigated for better gain.

3.4.4 Transimpedance front end

At present, the most commonly used front end receiver technique in optical wireless system is the transimpedance amplifier. In this technique, a high value of resistance can be used at low noise current without affecting the bandwidth of the system to increase the overall gain. This is because of the negative feedback configuration of the system. The basic configuration of a transimpedance front-end is illustrated in figure 3-9. The bandwidth of the system can be calculated using the following equation [59]:

$$f = \frac{1}{2\pi R(\frac{C_D}{A})} \quad \textbf{(3-4)}$$

Where R= load resistance, C_D = device capacitance and A = open loop amplifier gain.

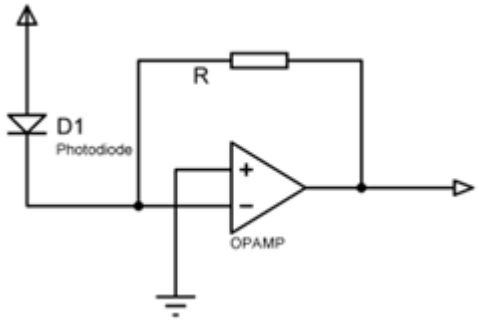

Figure 3-9 Basic transimpedance pre-amplifier

As seen, the device capacitance is reduced considerably as a result of the high gain at the amplifier. Meanwhile, this configuration can be simplified by using a transistor

rather using an operational amplifier. Thus, the single transistor transimpedance configuration is shown in the following figure 3-10.

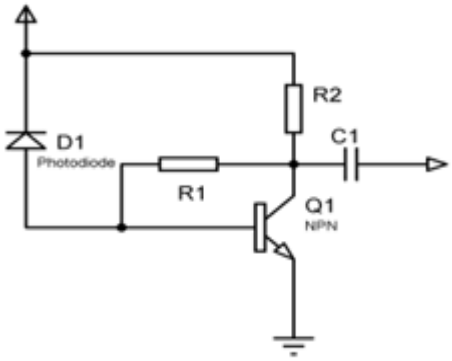

Figure 3-10 Single transistor transimpedance amplifier

In this kind of scenario, the bandwidth of the system can be calculated using the following equation 3-5, where C_{bc} is the transistor base emitter capacitance,

$$f = \frac{1}{2\pi R(\frac{C_D}{A} + C_{bc})} \quad \textbf{(3-5)}$$

Using a high frequency transistor with low capacitance is desired for this kind of application to achieve a better frequency response for the system.

As seen in the figure, in the transimpedance configuration, a resistor R1 as a shunt feedback is used across the base of the transistor, as negative feedback in the amplifier. Here the value of resistor can be high, because the negative feedback reduces the resistance by a factor of (1+A), which is seen by the photodiode, where A is the open loop voltage gain of the amplifier or transistor. The gain of a transimpedance amplifier can be approximated by equation [63],

$$A_z \approx \frac{V_{out}}{i_p} = \frac{-R_f}{1 + j\omega \frac{R_f (C_D + C_{in})}{A}} \quad \textbf{(3-6)}$$

Where A is open loop voltage gain, ω is angular frequency, R_f is the feedback resistance, C_D is the diode capacitance, and C_{in} is input capacitance of the amplifier. To find the gain of the amplifier accurately one should also consider capacitance C_f associated with the feedback resistor R_f. Then the equation can be re-written,

$$A_z \approx \frac{V_{out}}{i_p} = \frac{-R_f}{1 + j\omega \frac{R_f (C_D + C_{in})}{A} + C_f} \qquad \textbf{(3-7)}$$

To obtain a large bandwidth, either the value of R_f has to be reduced, or the value of A should be increased, which will result in less stability for the transistor/amplifier, and also reducing R_f mean higher thermal noise. Three different transistors were chosen to test the newly designed amplifier configuration. The characteristics of each transistor are summarized in the table 3-2.

Table 3-2 Comparison between three different NPN transistors

Characteristics	**2N2222A**	**BC548**	**ZTX320**
DC current gain	100	180	300
Current gain-Bandwidth product	250MHz	300MHz	600MHz
Output capacitance	8pF	1.7pF	1.7pF
Input capacitance	25pF	10pF	1.6pF

Frequency response and gain of the receiver were investigated using each of the transistors to find the best one as can be seen in figure 3-11. The ZTX320 transistor has lower capacitance compared to 2N2222A and BC548, so it has better gain and

frequency response, which is confirmed by the figure. For this project the ZTX320 transistor was selected.

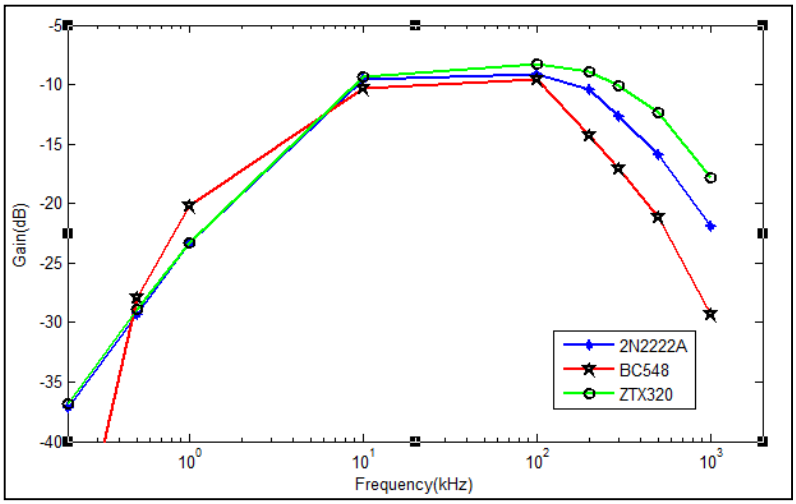

Figure 3-11 Gain of the TIA receiver using different transistor

As discussed previously, the feedback resistance has an effect on the gain and frequency response of the system, so it would be interesting to see how the output changes from higher load resistance to lower values. For a 5V Pk-Pk transmitted signal through the air, the received signal voltage is measured for different load resistances at a distance of 5cm. The values are plotted as shown in figure 3-12.

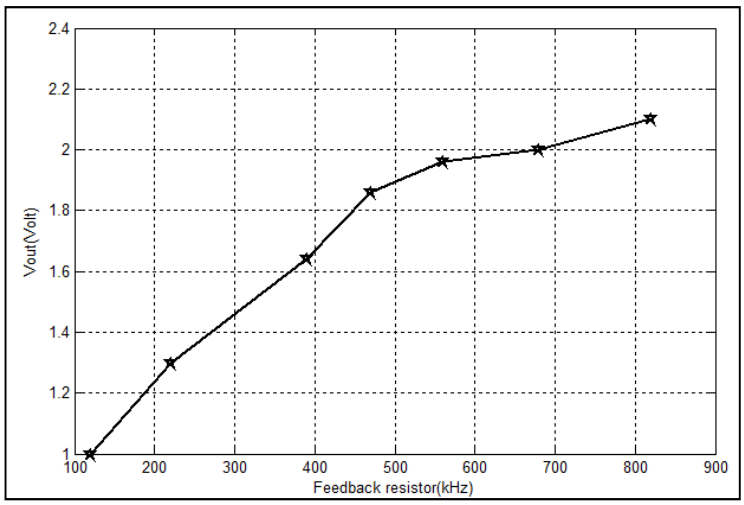

Figure 3-12 Feedback resistor vs. output volts

As seen in the figure, a higher load resistance means better gain which results in better sensitivity for the receiver. Contrarily, a higher resistance value decreases the bandwidth of the system. So, one should choose the optimal resistor value for a specific application considering the required communication range.

3.5 Amplifier circuit

The final block of the transceiver is the voltage amplifier, which boosts the small received signal to a TTL level, which then can be used as the input to the microcontroller. For this purpose an op-amp or transistor-based design can be used as an amplifier. In this system, a transistor-based amplifier was used to amplify a 30mV signal up to 5V. The circuit diagram of the designed voltage amplifier is shown in figure 3-13.

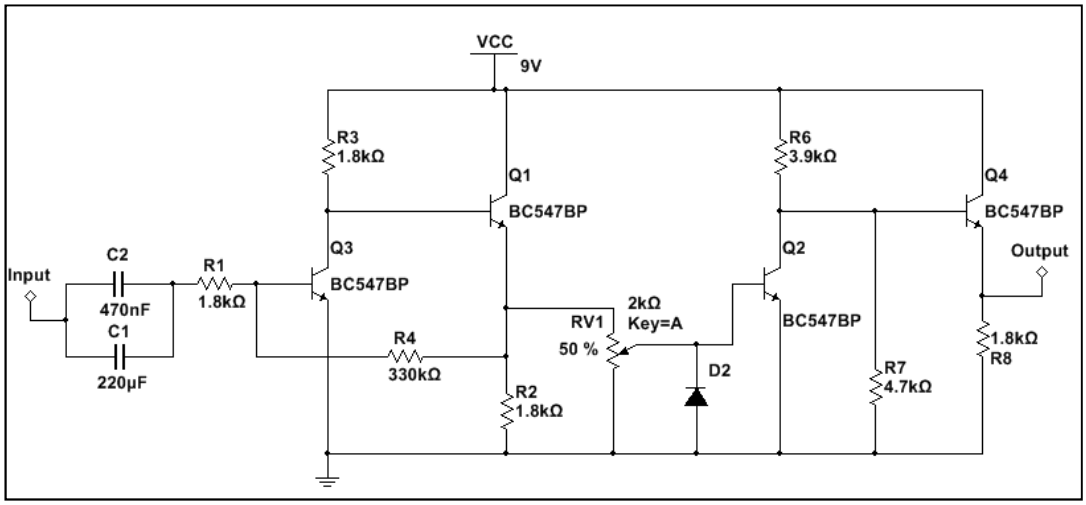

Figure 3-13 Voltage amplifier for optical wireless receiver

The amplification is done in two stages. Firstly, the received small signal is passed through the capacitors C1 and C2 to block any DC components of the signal and then amplified approximately 150 times by setting the value of R1 and R4 accordingly. Since the amplitude of the received signal is less than the 0.7V, which is the forward

base-emitter voltage for a silicon n-p-n transistor, so a feedback resistor R4 was used which determines the gain factor in the first stage. Once the voltage is above 0.7V, second stage amplification is done by using the Q2 transistor. Here, variable resistance R2 is used to obtain the optimum resistance value which will give best sensitivity for the receiver. General purpose diode D2 prevent transistor Q2 remains always ON as a result of any dc incoming voltage coming from the emitter of Q1. Finally, a voltage divider and a buffer were used to obtain the TTL output, which is fed to the microcontroller input for further processing or retransmission.

Figure 3-14 shows the built transceiver including the voltage amplifier which has been explained in the previous section.

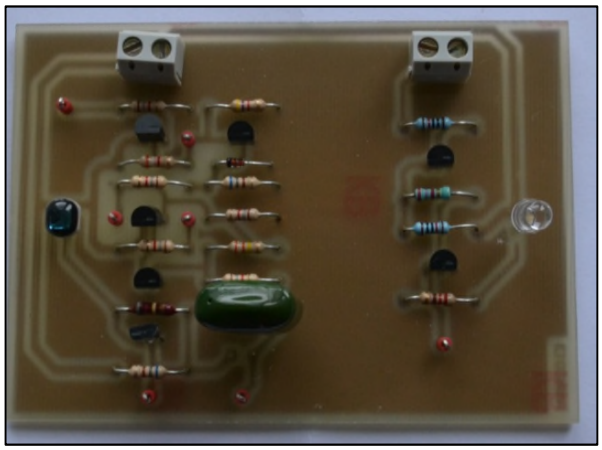

Figure 3-14 Image of the transceiver

3.6 Performance analysis of the designed transceiver

Performance analysis of the transceiver has been done in terms of link loss, bandwidth, and noise characteristics. To estimate the performance, all the experiments were carried first in air and then through water to compare them.

3.6.1 Loss of the link

First of all the loss of the system for different transmission ranges was measured, and is plotted in figure 3-15

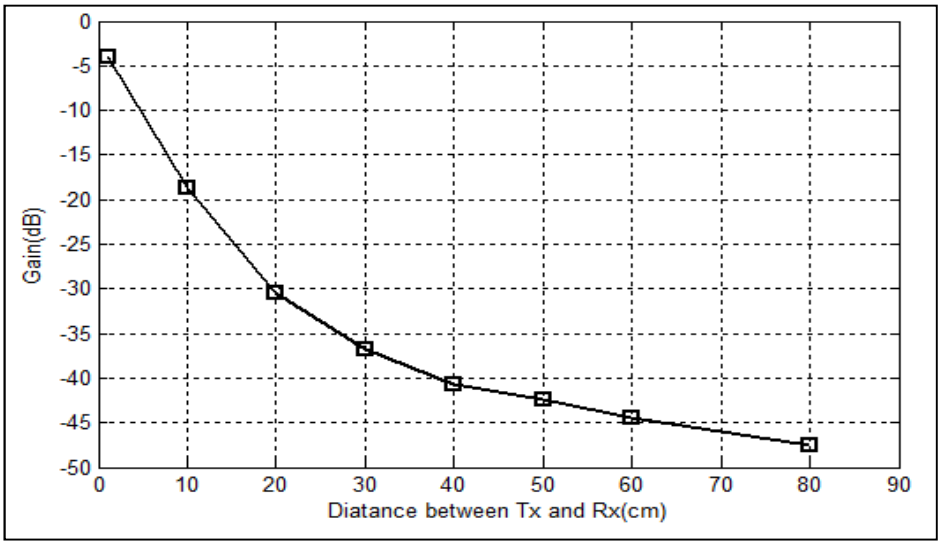

Figure 3-15 Link gain in different communication range

As seen in the figure, the gain decreases exponentially when the communication distance increases understandably because of the weak optical power received by the photodiode. Highest gain is achieved when transmitter and receiver is positioned very closely about 1cm, on the other hand side, when the distance between transmitter and receiver is about 80cm, loss is about 48dB. In this project the targeted communication range is about 60cm where the loss can be achieved about 45dB.

3.6.2 Bit-rate of the transceiver

The achievable bit rate of the designed transceiver has been estimated from the following figure. With the digital transmitter, finding the frequency response of the system is not a straightforward process, rather one can estimate the maximum supported bit rate of the system. So, for a communication range of 60cm, by varying the input frequency and keeping the input voltage fixed, the received output voltage was as plotted in the figure 3-16.

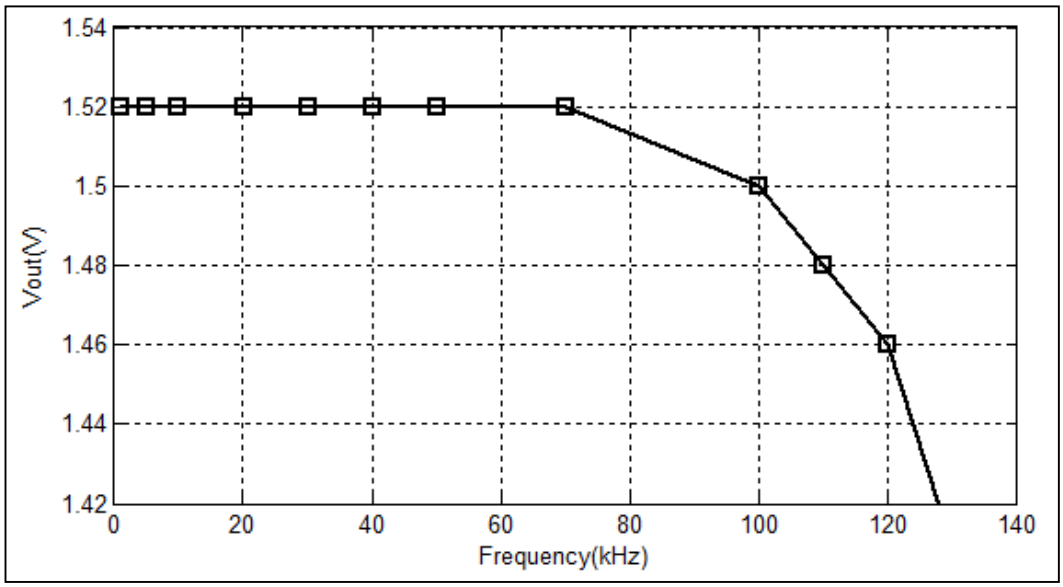

Figure 3-16 Maximum possible bit-rate of the transceiver

The above figure shows the received output voltage when input frequency is varied by keeping input voltage fixed. The bit-rate of the system is calculated from the figure which is around 70kHz. In general, sensor networks work in the kbps range, as data rate requirements are very low for this kind of application. So, the achieved bandwidth would be enough for the designed application.

3.6.3 Noise characteristic

In a communication system, noise is defined as the unwanted signal present with the transmitted signal which is received by the receiver. A noise source can be either external or internal in the system, which degrades the signal quality and puts a lower limit to the sensitivity of the system. For a visible light communication system, external noise can be daylight, florescent light, main power line etc. On the other hand, internal noise includes noise generated by the electronics itself. To find the noise characteristics it is very important to understand the different sources of noise in an optical wireless communication system.

The received optical signal is always highly attenuated because of the loss of optical power, so it is highly expected to have minimum noise for successful recovery of the original signal. But this is not always the case, as there are different sources of noise present which limit the performance of the system. The most common sources of noise in the photodetection process are shown in figure 3-17.

The detailed analysis of noise source in an optical wireless communication system can be found in [64]. The major noise sources which affect the system sensitivity are shot noise, dark noise, and thermal noise. Shot noise is the main source of noise in a photodetector which is due to the dark current, photocurrent or any other current flow through the junction.

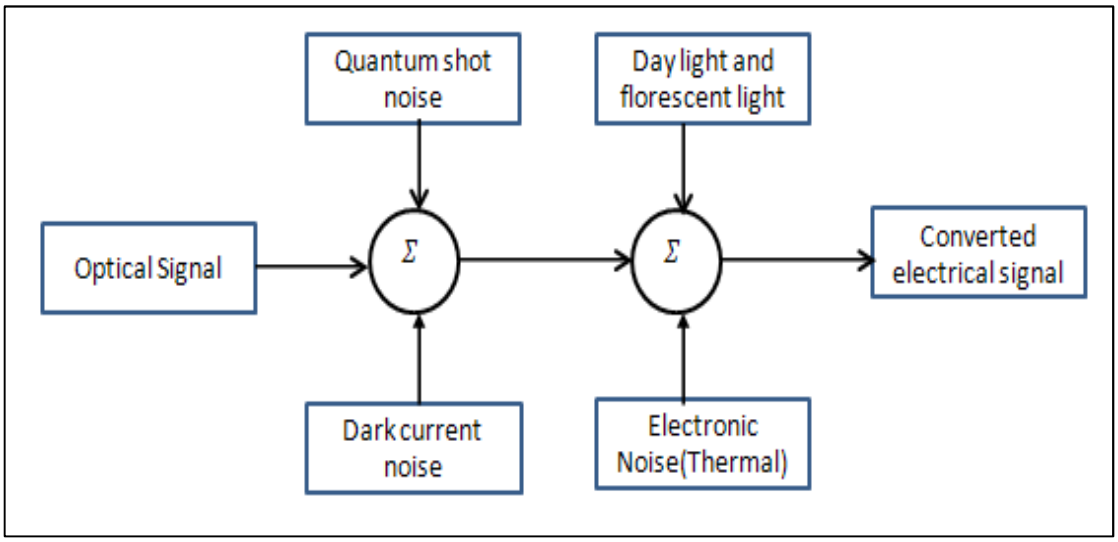

Figure 3-17 Noise source in photon detection system

It can be expressed either by as a voltage source or a current source. The mean square value of shot noise current can be found from the following equation,

$$\langle i_{sh}^2 \rangle = 2q \times (Ip + Id) \times B \times (A^2) \qquad \textbf{(3-8)}$$

Where q is the charge of electron, Ip is the photo-generated current, Id is the dark

current, and B is the noise bandwidth.

Thermal noise, which is also known as Johnson noise is produced because of the random fluctuation of a charge carrier in a resistance. The shunt resistance and load resistance are linked to this noise. The mean square value of the thermal current is given by equation 3-9.

$$<i_{th}^2>=4kTB/RA^2 \quad \textbf{(3-9)}$$

Where k is the Boltzmann's constant, T is the temperature in Kelvin, R is the resistance, and B is the noise measurement bandwidth.

The total noise current generated by a photodetector is shown in equation 3-10.

$$<i_n^2>=B(2q(Ip+Id)+(4kT/R)\times A^2 \quad \textbf{(3-10)}$$

The signal to noise ratio is the one of the main performance analysis indicator considered for the receiver. Finding the signal to noise ratio experimentally in an optical wireless system is challenging, due to the effects of ambient light in respect of shot noise in the detector, thermal noise in the input resistances (especially the load resistor), and the masking effect of the ambient light itself. To find the signal to noise ratio, the average peak-peak value of the signal and noise was measured, and signal to noise ratio was calculated from the following equation:

$$SNR = 20\log\frac{(S+N)_{Pk-Pk}}{N_{Pk-PK}} \quad \textbf{(3-11)}$$

Using the same equation, noise analysis of the system has been estimated in three different sceneries: first of all, signal to noise ratio is measured in the ideal situation where no ambient light and day light is present. The same measurement was done in the presence of ambient light, and in the night environment without any light sources,

to find the noise characteristics.

Figure 3-18 displays the output waveform at the receiver with and without ambient light during the day time. As seen, the ambient light has a strong effect on the communication system. The average ambient noise Pk-Pk value was measured about 16mV. A signal to noise ratio of 14dB was calculated without the ambient light and 10dB with the ambient light.

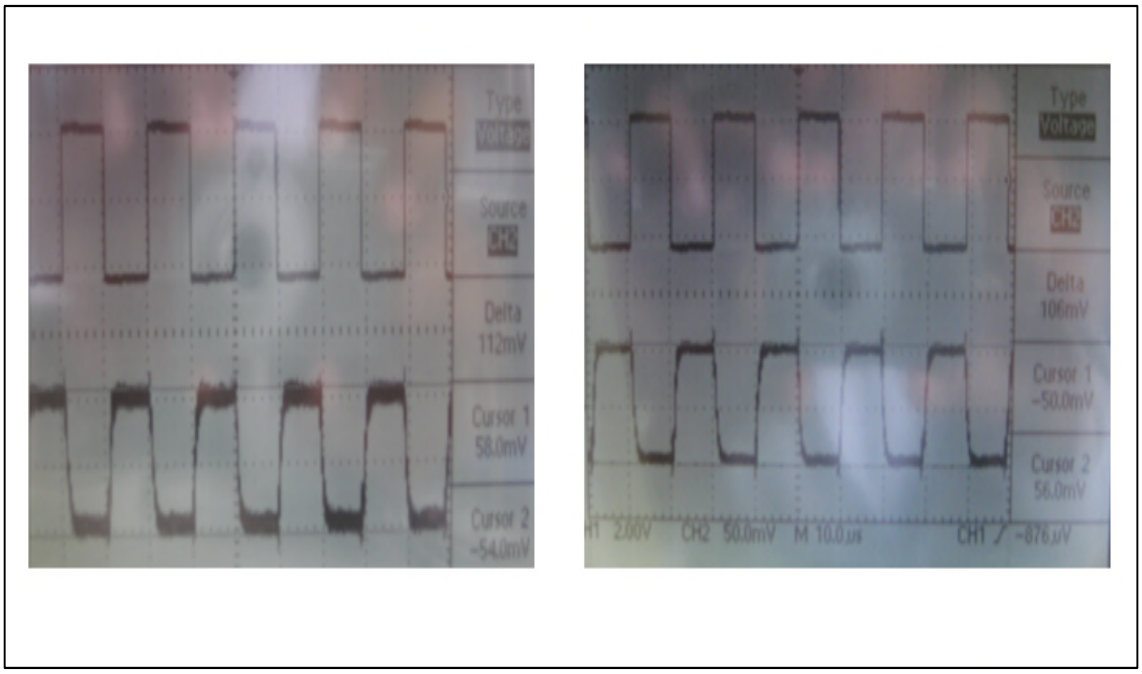

Figure 3-18 Signal output at the receiver with and without ambient light

3.6.4 Comparison of air test with water testing

All of the above mentioned analysis was done in free space, which may not be same for an underwater communication system. So, to see the performance of the designed transceiver in water, an experimental set up was established. A picture of the initial water test setup is shown in figure 3-19.

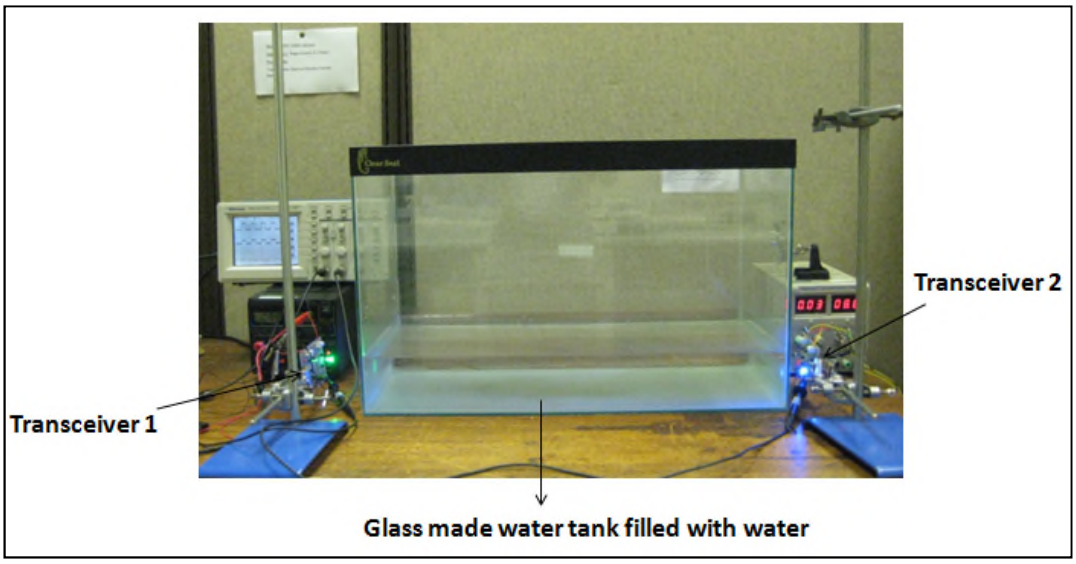

Figure 3-19 Water test setup

Here, a transmitter and receiver were placed on either side of the tank and pointed to each other to measure the gain of the receiver. The tank was made of glass, and its dimensions were 60cm x 30cm x 45cm. The tank was filled with 20 litres of distilled water and placed inside the laboratory.

To validate the air testing, the loss of the link has been measured for air and through water, for the same distance. The output waveform at the receiver can be found in figure 3-20.

As seen, the received output signal voltage was about 40mV for air, and about 60mV for water testing, for the same distance of 65cm and same frequency of 60kHz. Because of the glass water tank, some light was reflected back from the glass while propagating to the receiver, which made for a lower loss during water testing. The detailed explanation for this will be given in the experimental evaluation chapter. In reality, the loss in water must be higher than in air for visible light spectrum, as water is an optically denser medium than air in this range of spectrum.

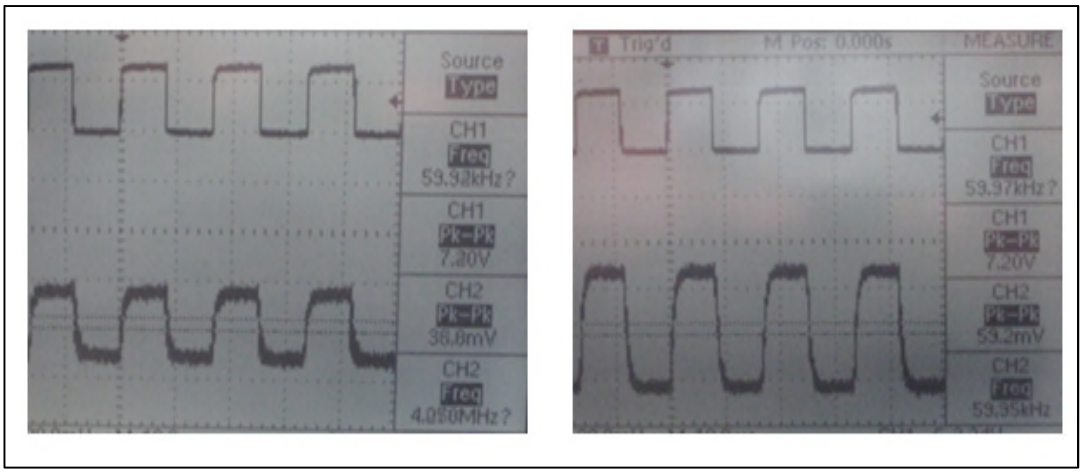

Figure 3-20 Comparison between output voltage at receiver (Left side through air and Right side through water tank

3.7 Testing the built transceiver

To verify the performance of the designed optical wireless transceiver a unidirectional underwater digital optical wireless system was built and used to transmit audio, as mentioned in the previous sections. The aim of this work was to understand the behaviour of an optical wireless system in water and also to gain knowledge of realistic system design by transmitting music from an audio source via a green LED and receiving it successfully on the other side. Audio transmission in underwater using optical wireless is not something new, as Nakagawa's lab [1] in Japan has already explored and commercializing a diver's communication system using visible light. Here the built network was just for demonstration purposes and to achieve the required skills for complex system design which will be required for developing the targeted system implementation. To transmit the audio, a digital modulation technique was used in the format of pulse width modulation, and at the receiver side signal was demodulated accordingly.

The block diagram of the test system for audio transmission which uses pulse width modulation technique is shown in the figure 3-21.

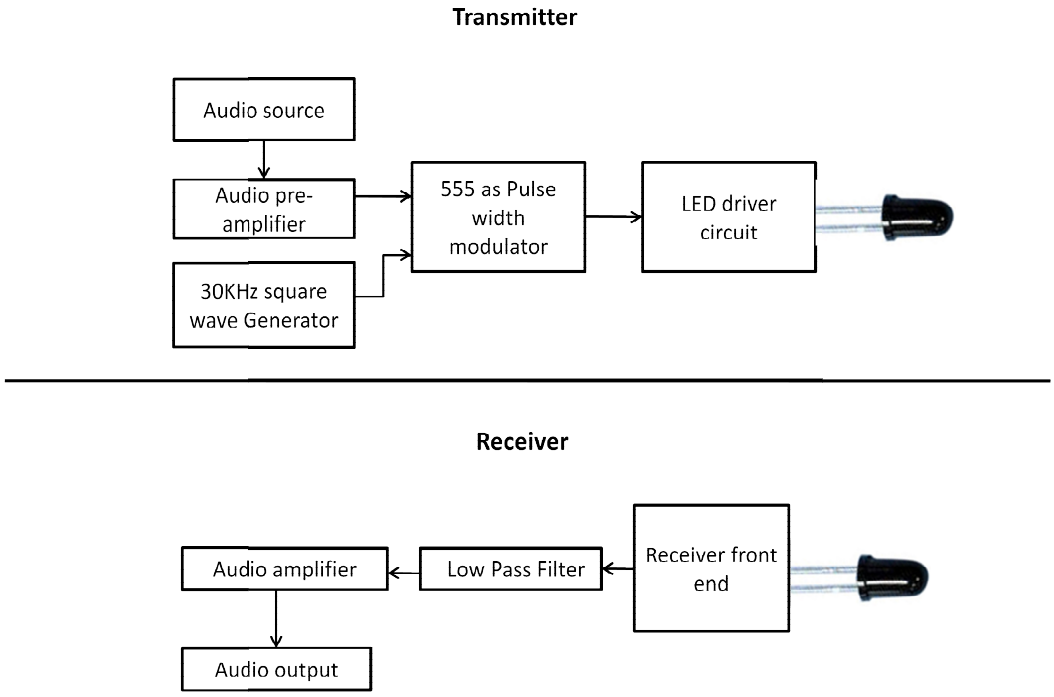

Figure 3-21 Block diagram of an underwater optical wireless audio transmission system

In the transmitter part, an audio signal generated from any audio source was amplified by using an audio amplifier and then modulated using a pulse width modulator before passing the signal through the optical wireless transmitter. Finally, the signal was transmitted using a green LED. In the receiver side, a photodiode received photons which were converted into current and passed to the receiver front end. This current was converted into voltage and amplified, and then it went through a low pass filter to remove the unwanted signals. The filtered signal was then forwarded to the audio amplifier to amplify the signals, and then was finally connected to the loud speaker.

Details of the each block are described in the following sections.

3.7.1 Audio source

The audio source can be either a human voice or anything from audio players. A 5mm audio socket was connected to the transmitter whereby any audio source for example an mp3 player, mobile, or any other device could be attached.

3.7.2 Audio preamplifier

An LM 386 low voltage audio power amplifier was chosen to amplify the input audio signal. This IC works for an input voltage of 4V-12V, and the output gain can be obtained from 20 to 200. For this specific system, the IC was configured for 20 times gain as shown in the following figure:-

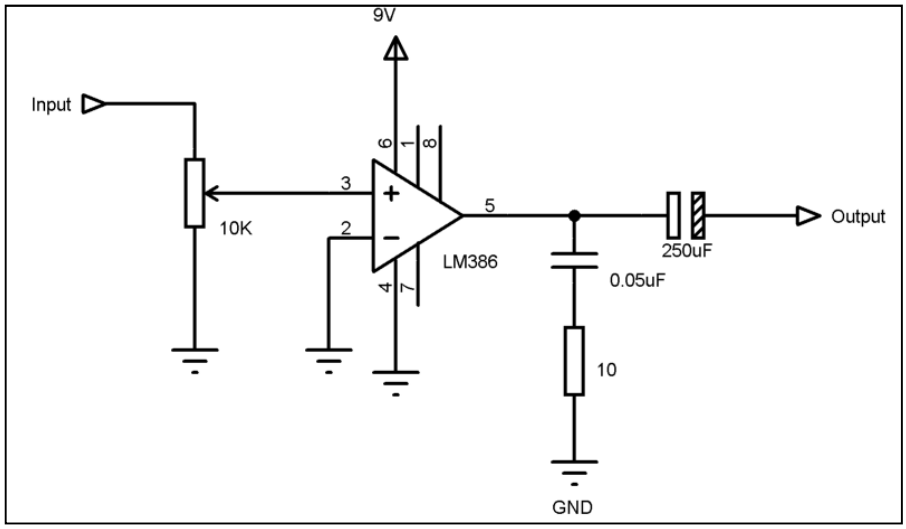

Figure 3-22 Audio pre-amplifier

3.7.3 Oscillator

Again, an LM386 IC was used as an oscillator to produce a 32 kHz square wave which was used to trigger the LM 555 IC. The circuit of the square wave oscillator can be found from the data sheet of the LM 386 as shown in figure 3-23.

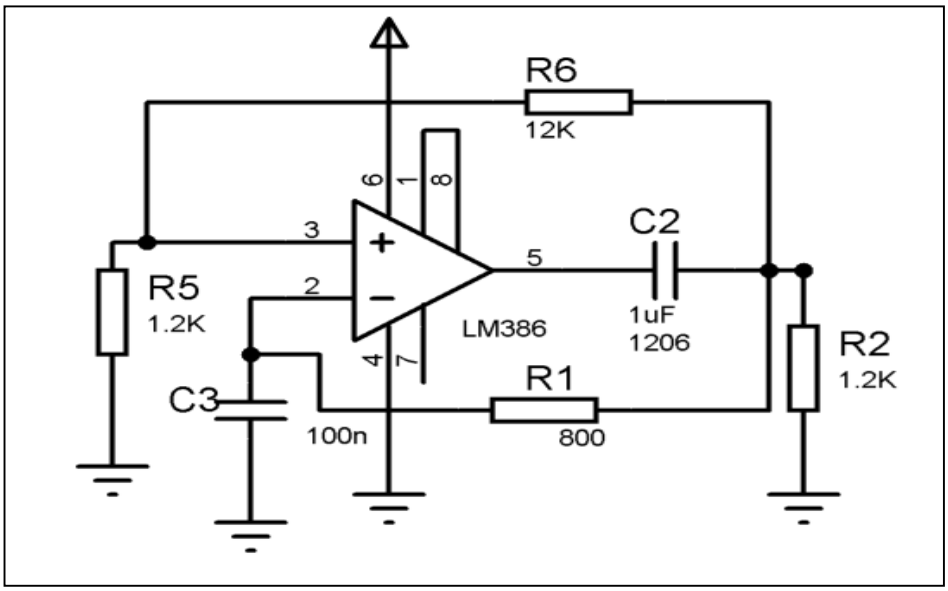

Figure 3-23 LM 386 as an oscillator

3.7.4 Pulse width modulator

LM 555 IC can be configured as a pulse width modulator, as shown in figure 3-24. To obtain the required performance, all the components have to be chosen correctly.

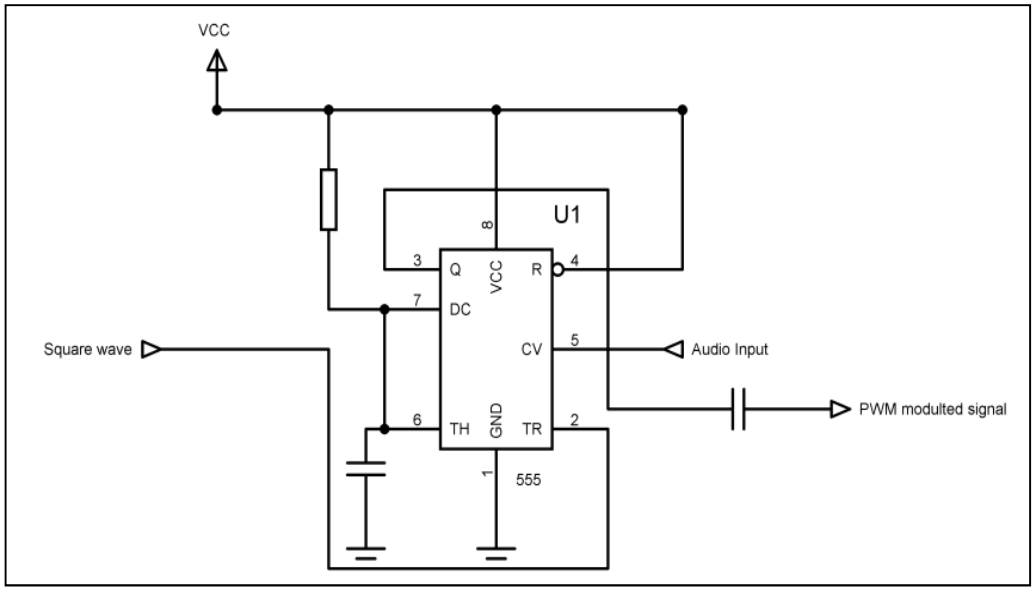

Figure 3-24 555IC as a Pulse width modulator

3.7.5 LED driver circuit

The LED driver circuit shown in figure 3-2 was used to build the underwater audio system. As this circuit supports a bandwidth in the MHz range depending on the component values, so sending a pulse width modulated signal in the kHz range was easily achieved. An Avago HLMP Green LED from Avago Technology was also selected, as it performs better than other tested LEDs.

3.7.6 Receiver circuit

In the receiver part, a bootstrap based amplifier was used as a front end circuit, as it supports a bandwidth up to 600kHz. An RC low pass filter was designed to block the carrier signal and to pass the audio signal, which was then amplified using the same audio amplifier as mentioned in section 3.7.2. Here the amplifier was configured to give a gain up to 200 times. Finally, the audio signal was sent to a loudspeaker. The designed receiver circuit diagram is shown in the following figure:-

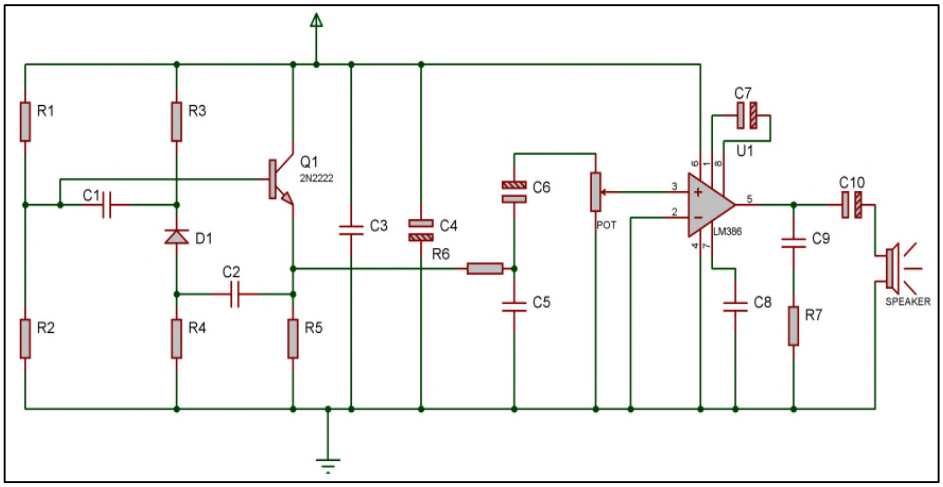

Figure 3-25 Receiver circuit for an underwater audio transmission system

3.7.7 Test results

Just to check how the designed system worked in water, a glass fish tank was filled with tap water. A transmitter with an audio source was placed in one side of the tank

and the receiver was placed on the other side. Music from a MP3 player was transmitted through the water up to few metres. The received sound quality was still very good. Since bootstrap receiver's sensitivity was very low, so, high quality lenses were used to send audio up to a few meters. Figure 3-26 presents the built transmitter and receiver for underwater optical wireless system for audio transmission.

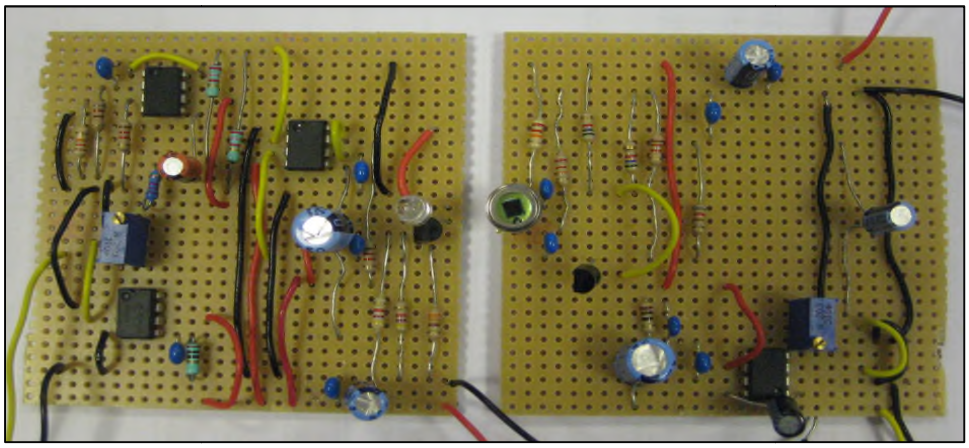

Figure 3-26 Built transceiver for transmitting audio signal underwater

3.8 Conclusion

This chapter discussed the details procedure of the transceiver design. Two types of receivers were investigated for the proposed application, and single transistor based transimpedance amplifier was chosen. The experimental results showed that transimpedance based application are suitable for the long range application if external optics is not considered. For sensor applications, low cost and low powered system is desired, which stimulated author to choose this configuration. Afterwards a transistor based voltage amplifier was designed to amplify the received signal in to TTL level. An audio system to transmit and receive audio through water had been demonstrated to prove the functionality of the designed transceiver.

Chapter4 : Multi-hop network design and implementation

4.1 Introduction

This chapter presents the multi-hop underwater optical wireless sensor network architecture, the design of different types of nodes and the implementation of the network prototype. A cost effective and realistic sensor network architecture for underwater environment using visible light has been proposed, and a network prototype using three nodes has been built to demonstrate the deployment scenario underwater. The proposed network architecture is based on a static configuration, and is specifically application oriented, where oceanographic data like water temperature, turbidity, pressure etc. for a certain area, will be collected. One of the main limitations of underwater optical wireless communications, which is the 'communication range', has been solved using the multi-hop approach. According to the author's knowledge, this approach has not been considered by any other group to date. The proposed network consists mainly of two types of node, which are the

sensor node and the gateway node. As an illustration of a deployment scenario, the sensor node has been equipped with a temperature sensor to measure the water temperature. Both sensor node and gateway node were developed using an ATmega1284P microcontroller, which encoded and decoded the data and controlled signals, and also controlled the communication in the network. The microcontroller also converted the analogue sensor data into digital format for sending to the gateway node through the optical wireless transceiver. The gateway node provides flexibility to the administrator, either to collect data locally by connecting a PC or exporting the data to the base station, using the GPRS module. The rest of the chapter discusses the details of the proposed network architecture, sensor node and gateway node design procedure, and the development of a multi-hop underwater optical wireless communication system for sensor applications.

4.2 Sensor network performance objective

To meet the requirements of certain applications, an underwater sensor network must have several unique features which are similar to the free space optical wireless sensor network. When considering the network architecture or designing a sensor node, these features need to be kept in mind to meet the overall expectation. Here some of the important features are discussed, which are adopted from [65], and detailed explanation has been given, explaining how those criteria are met for proposed underwater optical wireless sensor network.

4.2.1 Low power consumption

In the underwater environment, the power consumption needs to be kept at a minimum level, because the device needs to be in water for a long period of time to monitor certain things, and it would not be possible for nodes to harvest energy from

water. As one of the objectives of an underwater sensor network is to keep minimum human involvement, it is crucial to design a power efficient system. To make the battery life longer, which would be the only power source underwater, low power devices need to be designed. When nodes do not communicate, they need to be turned off to save power. The designed transceiver which has been discussed in the previous chapter consumes very low current. A same way an energy efficient sensor node has been designed. For this reason, besides the power efficient hardware, an efficient communication protocol is also proposed, which is discussed in the following chapter.

4.2.2 Low cost

Sensor nodes are deployed densely underwater in a certain geographical area, so a node's cost needs to be kept as low as possible. The cost of the custom designed optical wireless transceivers was kept very low by not using any external optics like lenses or filters, which are very expensive compared to common electronics and optoelectronics. In the same way, sensor node and gateway node need to be designed for low cost. Another aspect of cost is the maintenance cost of the deployed system. As the proposed network will be implemented underwater, the maintenance cost can be much higher compared to any land-based sensor network. For this reason, the network has to be made autonomous, which would not require much human intervention after deployment.

4.2.3 Network topology

The most common network topology which was previously being considered for free space sensor networks is the star topology. The problem of using this kind of topology is the physical coverage by a single network. Now a day's, either mesh or

tree based topology is the realistic solution to cover a larger geographical network. As the communication range is a big issue for the underwater environment, so, multi-hop network architecture is considered for the proposed application. Details of the network topology are discussed in section 4-3.

4.2.4 Security

Security is a very important factor for underwater communication, as it could be mostly used for military applications, where types of data are very sensitive. To make the network secure, a visible light has been chosen as a communication carrier and line of sight communication links are deployed. In this process, data travel only in one direction, so no-one can receive the transmitted information from other directions. Security is ensured in the physical layer; also, higher layer encryption will be required for a more secured system.

4.2.5 Data throughput

Data throughput requirements for sensor networks are not crucial compared to other communication systems. Here data throughput means real data which are being sent. For communication to happen, other kinds of signal, such as channel allocation signals, MAC layer frames etc. also need to be used, which consumes bandwidth. But real data can be temperature, pressure, turbidity information, which is only a few bits long. Although optical wireless communication can ensure a very high data rate, it is not the focus of this work to make a high speed system. Rather, the approach is to extend the communication distance, using multi-hop network architecture. The proposed network supports data rate of 38.4kbps, which would be sufficient to support the proposed application.

4.2.6 Message latency

In general, a wireless sensor network has a very low requirement of real time data transfer. In most cases, sensor networks do not send video or audio information which requires a certain level of Quality of Service (QOS). Therefore, the message latency requirement for a sensor network is very low, and this is also true for the underwater case.

4.2.7 Alignment between nodes

Like any other LOS optical wireless system, alignment has to be maintained accurately to get the maximum possible performance in the underwater optical wireless sensor network. Water as a medium is very harsh, and because of the water wave's continuous movement, nodes may slightly drift to the other directions, which would cause communication failure. Thus, when sensor nodes are anchored in water, one has to ensure that they remain in the same direction all the time.

4.3 Underwater sensor network architecture

Different architectures for underwater sensor networks have been discussed extensively in the literature [66] [67] [68] [24] [69],where most of them use acoustic waves as a communication carrier. Heidemann described a general network architecture where four types of nodes are deployed for sensing and data collection, as shown in figure 4.1 [66].

On the sea floor, a large number of sensor nodes are deployed, which sense data and communicate with other nodes using an acoustic modem. At the top layer, one or more control nodes are deployed with internet connection, which can be placed off-shore or on-shore, depending on the deployments need. The third kind of node is called a Super node, which has high speed internet connection capability for relaying data to the base station very quickly. This kind of nodes is deployed if the network

size is very large. Finally, robotic submersibles are used to communicate with sensor nodes acoustically for node maintenance purpose. The discussed architecture is a 2D architecture, where data are collected from the bottom of the sea only.

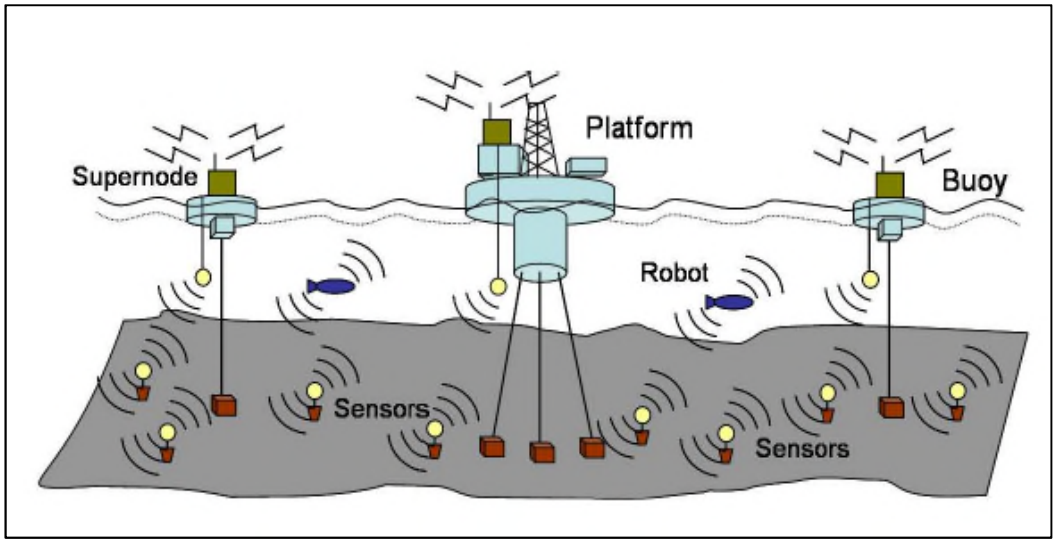

Figure 4-1 General underwater acoustic network architecture [66]

Akyildiz presents both a 2D and a 3D network architecture, which are capable of monitoring ocean columns at different depths [24]. The problem of this kind of network is to install nodes in different depths and to ensure that their position remains fixed throughout. In a 3D network architecture nodes must be able to relay data to the sink node, which eventually increases the coverage of the network.

On the other hand, most of the free space sensor networks are based on a radio technology, where nodes are deployed densely and form a network on an ad-hoc basis. Because of the long communication range of radio, a large geographical area can easily be monitored. Most of the time after deployment, a sensor network operates without human intervention, autonomously.

The underwater optical wireless sensor network architecture can utilize the concept of an acoustic sensor network or a free space sensor network, but the physical layer

and MAC layer protocol implementation would be substantially different. If an LOS communication link is used, then the overall network architecture would be different, because communication would be directional rather than Omni-directional, which is the case for the acoustic or radio network.

Thus, research on underwater optical wireless sensor network architecture has just considered the star based topology [70] [71], which supports 2D applications, as shown in figure 4-2.

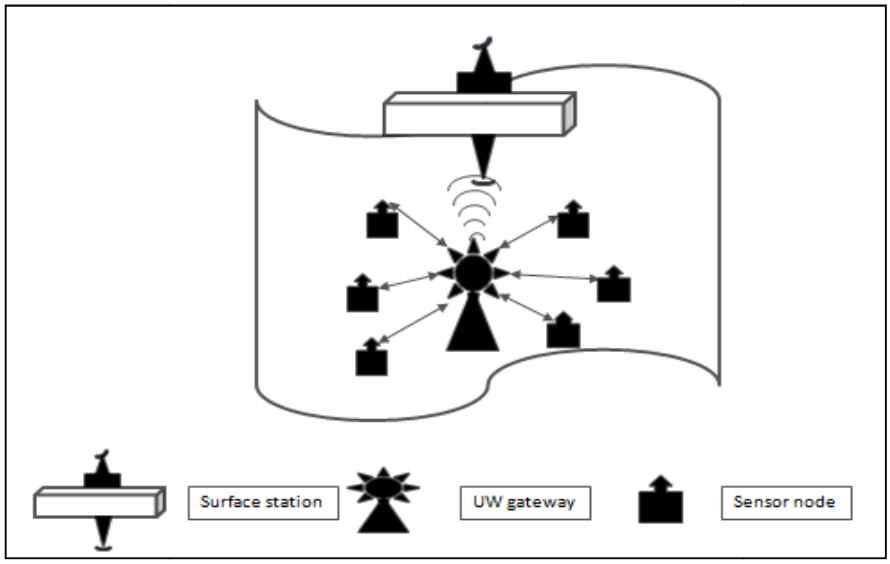

Figure 4-2 Star topology based network architecture

In a two-dimensional application, sensor nodes are anchored to the bottom of the ocean, and send sensor information to the gateway node using an optical wireless link. Here, the gateway node sends data to the surface station using either radio or any other medium.

Another possible architecture, based on a tree topology, is presented in figure 4-3, where each node relay the information to the next node and surface station receives all nodes information by its nearest sensor nodes. This is basically a 3D architecture

which can be implemented either horizontally, vertically, or in both cases, depending on the application scenerio.

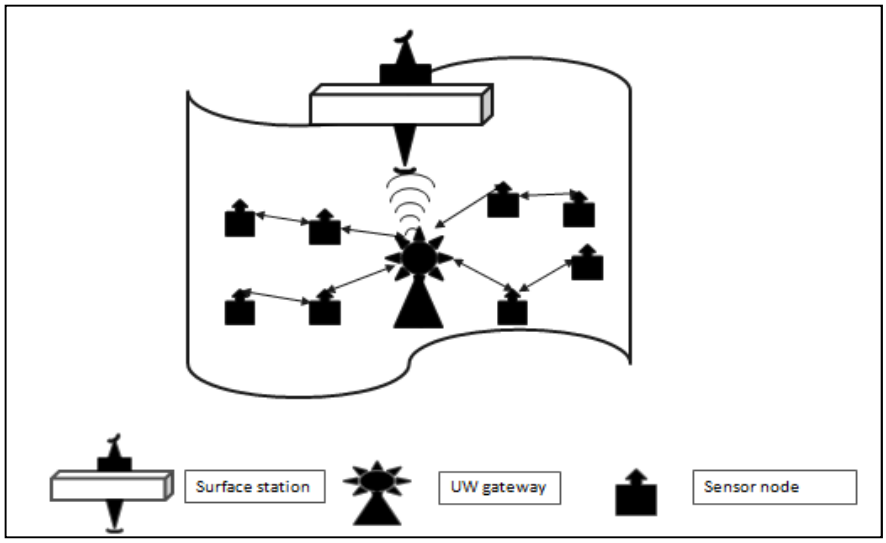

Figure 4-3 Possible multi-hop network architecture

Both the architectures have some advantages and limitaions; for example, in the first case protocol development will be easier, since the total communication system is based on one hop communication and it will require less power consumtion, because after passing the data to the gateway node,each node can go to the sleep state.This type of architecture has limitaions in terms of the covered distance. As it is single hop, so the design has to be implemented to ensure the maximum communciaiton range for covering large geographical area. On the other hand, the tree based multi-hop arcitecture has the advantage of covering a large geographcial area. In general multi-hop comunication needs a complex MAC and routing protocol, since each node needs to know its neighbour to forward information, especially in the mobile environment. The intermediate node needs to be ON when the end node sends or receives data from the gateway node. Another limitation is that, if the intermediate node fails, then data cannot be sent to the base station until it is put right.

Comparing both the architectures, and, taking advantage of larger geographical coverage which resolves the issue of communication range underwater using visible light, the tree-based, multi-hop topology has been selected for the proposed application. The network architecture is simplified by placing the gateway node on the water surface, so that it can have internet access, or data can be accessed locally by a human being. Adopted architecture consists of two types of nodes, which make it simple to implement, and also reduces overall system cost, still capable of supporting the full functionality of sensor network. The proposed network architecture is presented in figure 4-4.

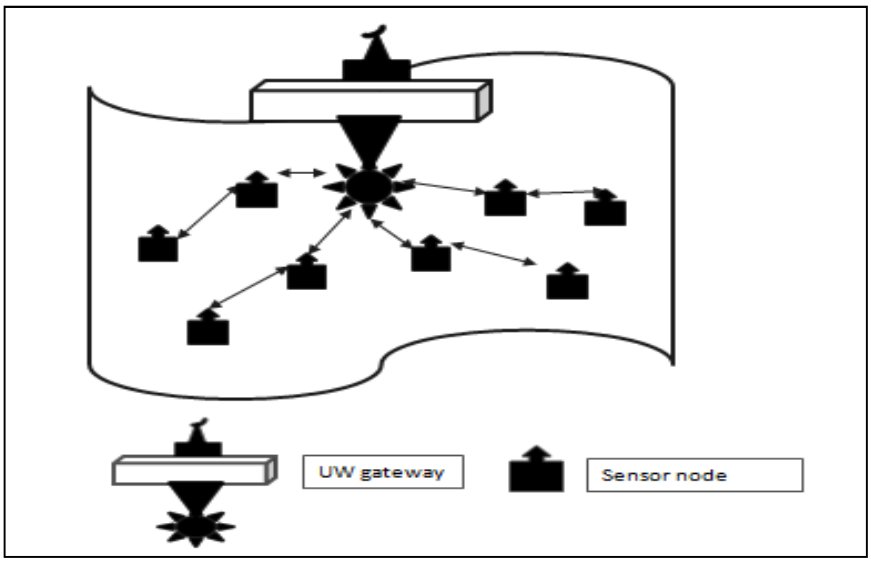

Figure 4-4 Adopted network architecture for multi-hop underwater optical wireless sensor network

Here, each sensor node in the network is equipped with two bi-directional optical wireless transceivers. The uplink and down link are designed using green and blue LEDs respectively. Each intermediate node decodes data and forwards it to the next node. The initial focus is to build 2 hops, which will be increased at a later stage.

4.3.1 Physical layer development

Physically, the link can be implemented in many ways. The possible physical layer architectures of the network are shown in figure 4-5. First of all, simplex communication is possible as shown in fig 4-5(a), where each sensor node simply forwards sensor information through an optical wireless link to the gateway station. In this case, the gateway node gives a command to the sensor node by using another medium for example, the acoustic medium underwater. Thus this is not fully optical communication, but rather, a hybrid communication mode. Having both optical and acoustic hardware increases the overall system cost, especially when the price of acoustic modem is taken into account.

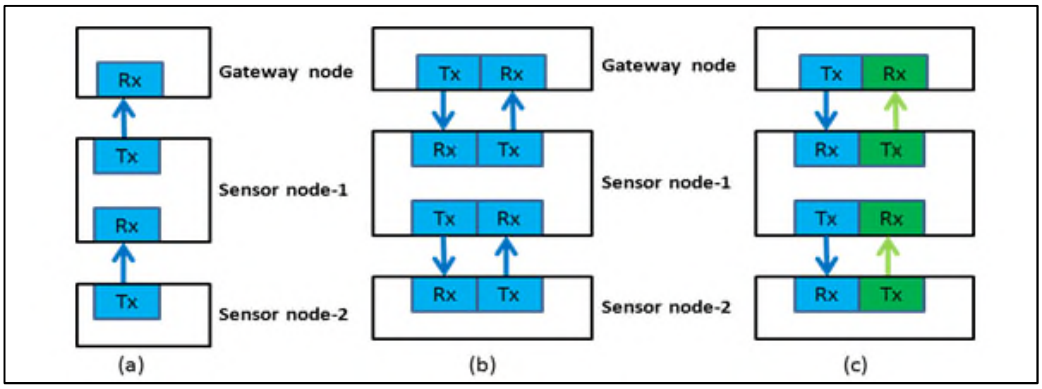

Figure 4-5 Physical layer structure of the multi-hop underwater optical wireless sensor network a) Simplex, b) Half-duplex, and c) Full duplex

Another approach is presented in figure 4-5 (b), where both the uplink and downlink are designed using the same coloured LED. In this system, interference will be high, and it will be hard to distinguish the uplink and down link, which may cause some confusion in the physical layer.

This project utilizes a bi-directional communication system using two different coloured LEDs. Compared to the half-duplex system, it has much higher bandwidth

efficiency with the cost of almost same complexity. A blue and green filter can be used in front of the photodiode to filter out the unwanted signal. By using two different coloured LEDs, two channels can be separated in the physical layer, which is the great advantage of implementing this kind of system. The pairing of blue and green coloured LEDs has to be ensured to achieve successful communication.

4.3.2 Pairing green and blue transceiver

For bi-directional communication, different coloured LEDs are used to implement the downlink and uplink. Blue LEDs are used for the downlink to transmit a control signal from gateway node to other nodes, and on the other hand, to upload data from the sensor node to the gateway node, a green LED is used. The main reason for using two different kinds of LEDs are to implement two physical channels, to make a full duplex communication system, which will therefore increase the overall system performance. Each sensor node will have two types of transceivers (one blue and one green), so that pairing them correctly is very important for error-free communications. Miss configuration can result in communication being impossible. Figure 4-6 demonstrates this kind of scenario, where two nodes are configured correctly with correct directions.

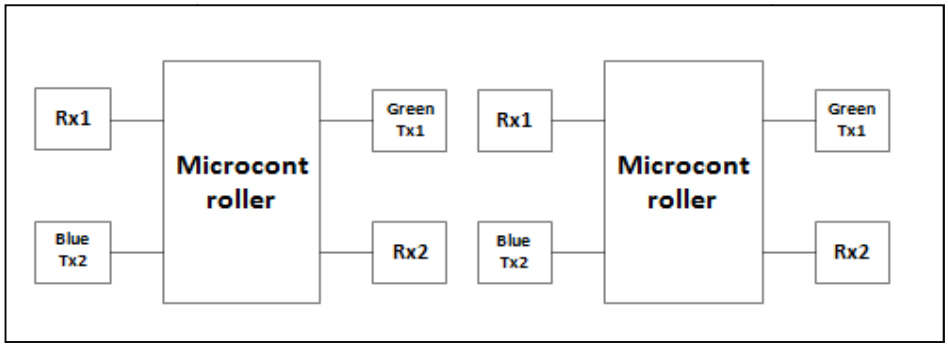

Figure 4-6 Pairing two different types of transceivers

4.4 Sensor node architecture

The architecture of the designed sensor node is shown in figure 4-7. As seen, each sensor node contains two optical wireless transceivers to communicate with neighbouring nodes, which were discussed in details in chapter 3. Of course, at the heart of a sensor node is a microcontroller, which controls the physical layer and MAC layer issues. To measure the temperature of the water, an analogue sensor is connected, and also other forms of analogue/digital sensors can be connected at a later stage. To convert the analogue sensor data into digital format, either an external ADC, or the built-in ADC of the microcontroller, can be used. Modern microcontrollers support an analogue to digital converter, and data conversion is accurate enough to regain the original data.

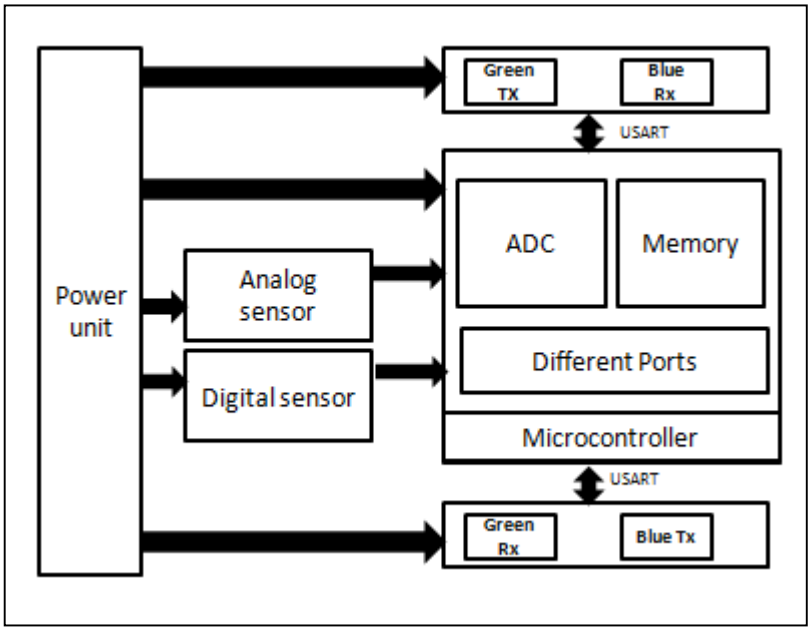

Figure 4-7 Sensor node architecture block

More precise conversion can be ensured by using an external ADC. For simplicity and cost effectiveness, this project utilizes the microcontroller built-in ADC for

converting the analogue sensor data into a digital format. The power unit is also designed to serve all the components connected to the sensor nodes. For example, the transceivers require a 9V supply, and the microcontroller works with a 5V supply. In the following sections, each of the components will be discussed in detail.

4.4.1 Microcontroller selection

After undertaking a careful investigation, Atmel Corporation's ATMega1284P, 8-bit low power and high performance microcontroller was selected for this project. The CMOS microcontroller is based on AVR core, 8-bit RISC microprocessor architecture. In the active mode, the microcontroller consumes 0.4mA current, whereas, in the power down mode it consumes 0.1uA. This microcontroller operates at 20MHz, and has 32 programmable I/O pin for different purposes. It has several other ports for interfacing and to download programs into the microcontroller. It can be programmed using the C programming language, and instructions can be downloaded either using the JTAG or ISP interface. An STK 600 development board has been used for downloading programs using the JTAG interface, which is the primary developing board for Atmel microcontrollers. For programming the microcontroller, AVR studio5 software was used, which uses C language to program the microcontroller. To reduce the complexity, the same microcontroller was used to build the sensor node and gateway node and it fulfilled all the requirements.

For bi-directional communication, at least two transceivers are needed for each node. Each of the transceivers is connected using a USART (Universal Synchronous Asynchronous serial Receiver and Transmitter) port for transmission and receive data. For this project, at least two USART ports are needed to connect two transceivers, and this microcontroller has two USARTs, which is the most important reason for selecting this microcontroller.

To connect a number of analogue sensors, the microcontroller should support an adequate number of analogue to digital conversion units to reduce the additional system cost, since most of the sensor data are in analogue form. The ATmega1284P microcontroller has 8-channels, 10 bit ADC (Analogue to digital converter), which is appropriate for the proposed application. Another important requirement is to have enough memory to store instructions and sensor data, so that no additional memory is required. It has 128kbyte of in-system self-programmable flash memory, 4kbytes of EEPROM, and 16kbyte of SRAM, which was sufficient for the application. All the features mentioned above encouraged the author to select this microcontroller.

4.4.2 Communication unit and interface selection

As discussed before, each of the sensor nodes was equipped with two optical wireless transceivers. The details of the transceiver design procedure were discussed in chapter 3. The built transceiver can support a bandwidth up to 70 kHz, for a communication range up to 100cm in air, without using any external lenses. The range can be increased further, using a concentrator, but the system cost will increase, as lenses can be expensive. To connect a transceiver with the microcontroller, at least two ports are needed for the transmitter and receiver. There are few options available to interface with microcontroller. One is using the Serial Peripheral Interface (SPI), which is a three-wire, synchronous, data transfer unit. This interface can be set up in master or slave mode, and can be used in full duplex mode. There are also byte -oriented two-wire serial interfaces, which can be used for a communication interface. These are a better option for wired communication where two microcontrollers are connected to each other. The third choice, which has been chosen for this project, is using a programmable USART port. Each of the USART ports can be configured for a synchronous or asynchronous mode of operation, and,

for this project, both of the USARTs were configured in the asynchronous mode. By using a USART, one frame, which consists of 8 data bits, 1 start bit, and 1 stop bit, can be transferred sequentially, starting from the LSB to the MSB. The parity bit can be configured for error detection at the receiver side. The USART data transmission rate can be configured in the initialization part, according to the system requirements. For the current project, the data rate was 38.4kbps, which was setup in the USART initialization process.

4.4.3 Sensors and sensor interface design

An LM35, precision centigrade sensor is used to measure the water temperature. The output voltage of the LM35 is linearly proportional to the Celsius temperature, and does not require any external calibration. The source voltage can be anything from 4V to 20 V when configured as a basic centigrade temperature sensor, and the output voltage was in an analogue form, where each degree centigrade corresponded to a 10mV change. This output needed to be converted into digital format, and, as discussed, the microcontroller's built-in ADC was used to convert this. Figure 4-8 shows the LM 35 interface with the ATmega 1284P microcontroller, where output of the sensor was connected directly to the ADC0 input of the microcontroller. As is known, the resolution for the ATmega 1284P microcontroller is 10bit, and the reference voltage used was 5V, which gave a voltage resolution of 5mV, approximately, which is half of the actual change of 10mV/centigrade. As a result, to obtain the temperature in degree Celsius, the ADC output value needed to be divided by two. Following the same procedure, the ADC value was calculated at least 10 times for each reading, and then averaged to get more accurate results.

As the built prototype was not to be submerged into water, so the temperature sensor was not populated on the same board as the sensor node. Rather, it was built on

another board which was cased in a waterproof bag and placed in water.

The output of the LM35 was then connected to the ADC, and temperature was calculated accordingly. In the same way, seven more analogue sensors could be connected to the microcontroller's ADC1-ADC7. At the same time, digital sensors could be connected using any of the I/O ports, or using two-wire serial ports.

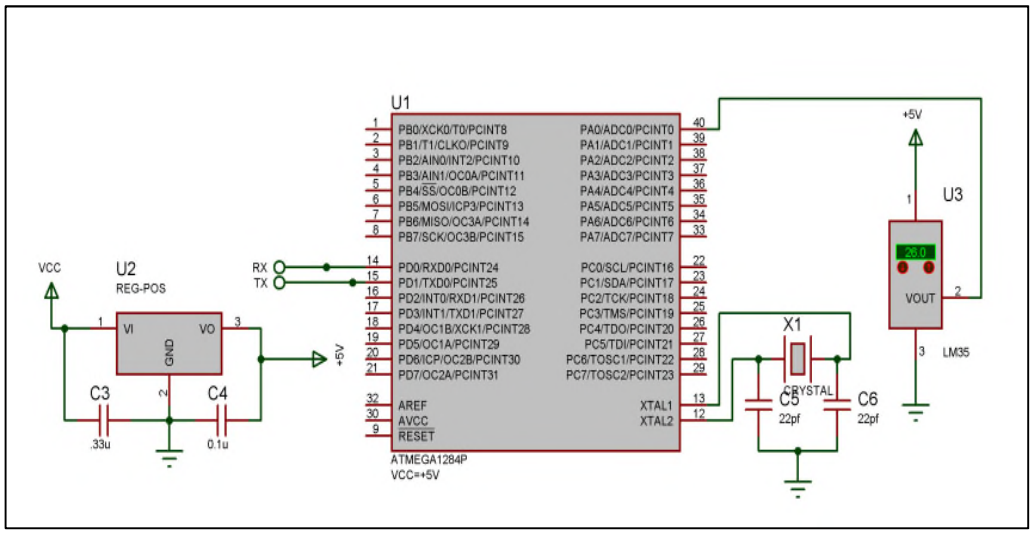

Figure 4-8 LM35 interface with ATmega 1284

4.4.4 Power source module design

The power supply module was designed to supply power to each of the modules, including the microcontroller, transceivers and temperature sensors. The node was powered by a lithium 9V battery, which lasts five times more than an alkaline battery. As all modules in the node shared the same power source, so an LM7805CT voltage regulator was used to produce 5V output from 9V input. The LM 78005CT has three terminals, where input is connected to 9V, another terminal is connected to ground and 5V output is produced by third terminal. The Microcontroller and temperature sensor worked with a 5V supply, so these two modules were connected to the 5V point. In the demonstration prototype, a heat sink was used in each node to

prevent the voltage regulator becoming overheated.

4.4.5 Hardware implementation of the sensor node

In order to develop a functioning multi-hop underwater sensor network, two sensor nodes were built and tested. The schematic and PCB layout of the sensor nodes were drawn using Altium designer software. The PCB boards were developed using the local facilities. The final schematic of a sensor node is shown in figure 4-9.

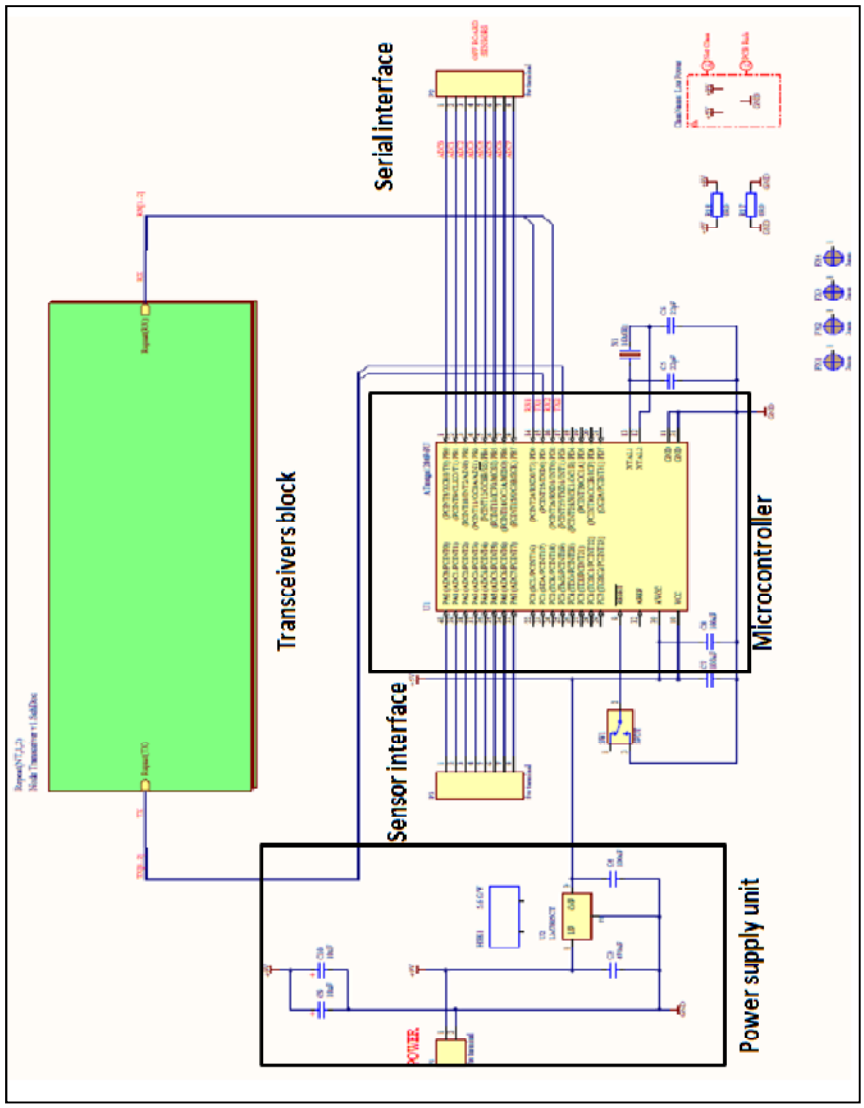

Figure 4-9 Schematic layout of the sensor node

The built sensor node is shown in figure 4-10 and in figure 4-11. In figure 4-10, a top

view of the built sensor node is presented. As seen, a single PCB board was designed to accommodate two transceivers, a microcontroller and other peripherals. It should be noted that the sensor was not connected in the board, as it was connected to the ADC pin of microcontroller using an external connection, as discussed before.

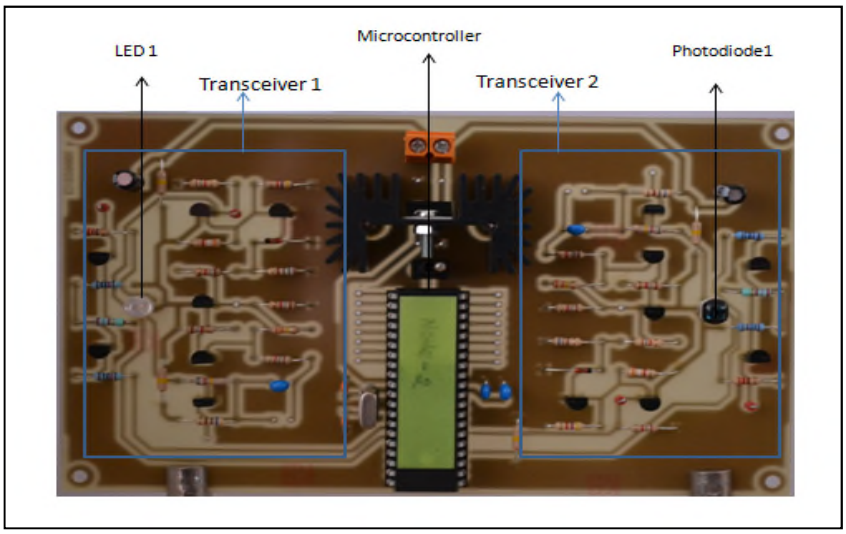

Figure 4-10 Picture of the top view of built sensor node

In figure 4-11, a lateral view of the node is shown. It can be seen clearly that two LEDs and photodiodes are place in opposite directions to transmit and receive data.

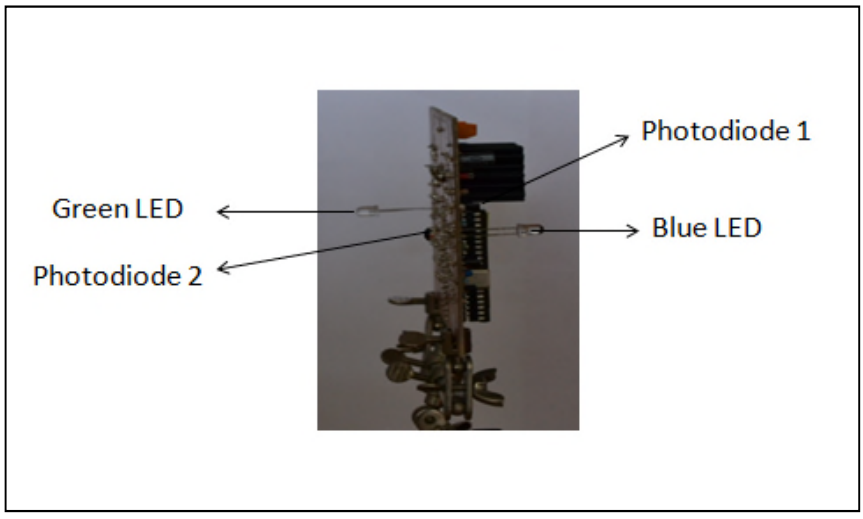

Figure 4-11 Side view of the built sensor node

The distance from an LED to a photodiode was kept nominally identical for each node, which helped to align the nodes during experiments. An identical PCB board was used for the gateway node where the components for one transceiver were populated.

4.5 Software design for the sensor node

The node software can be divided into two parts. One is the communication protocol software and another one is application software. The communication protocol software will be discussed in detail in the following chapter, and the application software is discussed here. The main task of a sensor node is data acquisition, using the connected physical sensors, processing the data, and sending it to the gateway node in an appropriate situation. The designed sensor sends data to the gateway node in two situations. The first situation is if a request is received by the sensor node from the gateway node, and the second one is if any abnormal condition is detected by the sensor node, for example, the measured temperature value is unexpectedly high or low. Other than this, the sensor node is responsible for communicating with the neighbouring node to establish a connection.

A flowchart is shown in figure 4-12, describing the sensor node's main application. After completing the initializing process and setting up timers, the sensor node communicates with gateway node to obtain a MAC address and afterwards, it goes into a sleep mode. The sensor node senses the temperature of the medium periodically, and stores the data in memory, unless it finds any abnormal condition such as an unexpected high or low value of the temperature. In this kind of situation, the sensor node sends this information to the gateway node. Otherwise, it waits for the gateway node's request to send information. After sending data to the gateway

node, the sensor node goes back to an idle state.

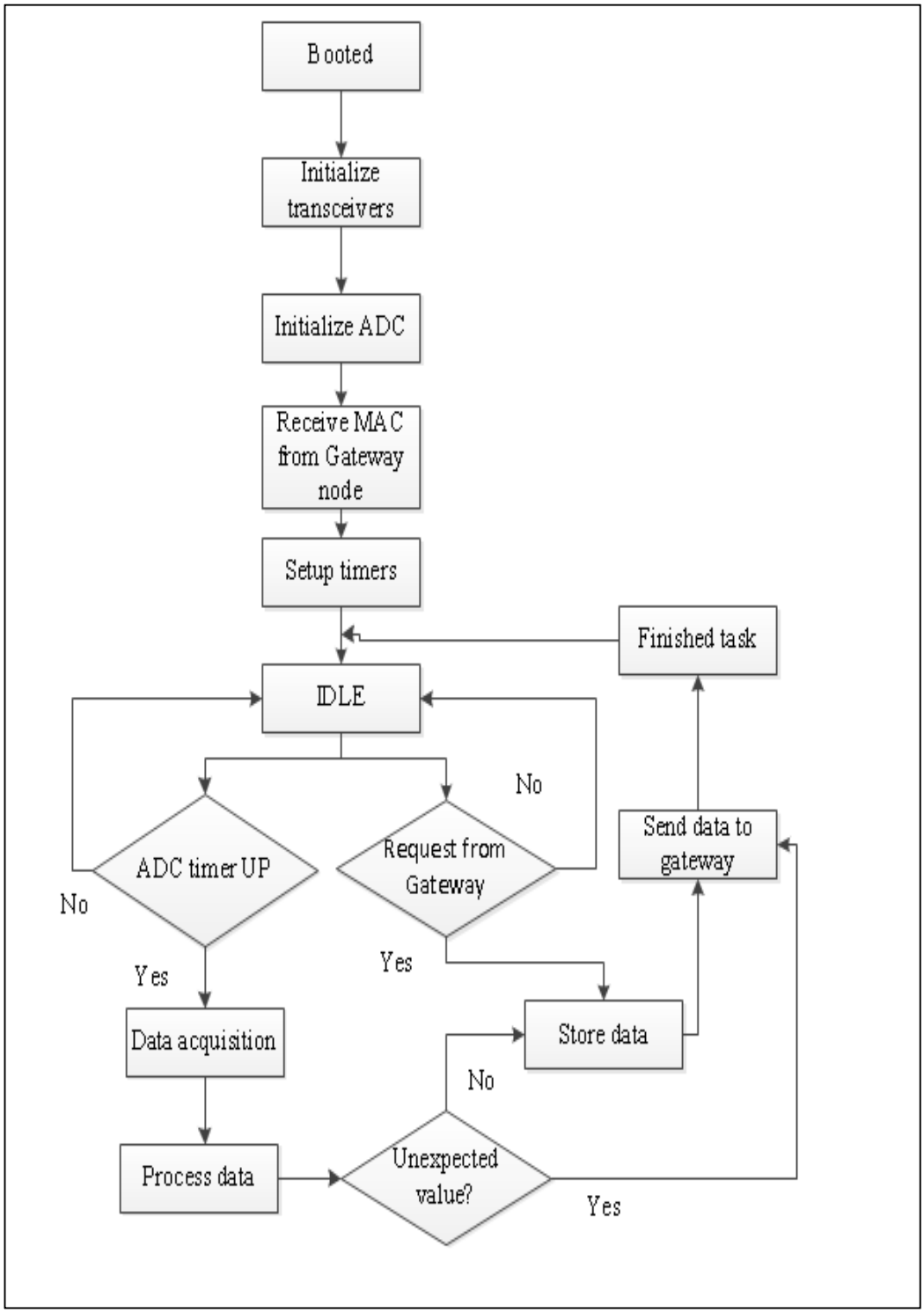

Figure 4-12 Flow chart of sensor node's main program

4.6 Gateway node design

A gateway node also has a similar architecture to the sensor nodes, with additional features, and does not contain any physical sensor connected to it. The task of the gateway node is to collect data from sensor nodes periodically, and also maintain the communication between them. It also sends the collected sensor data to the base station for further manipulation. The block diagram of the gateway node is shown in figure 4-13.

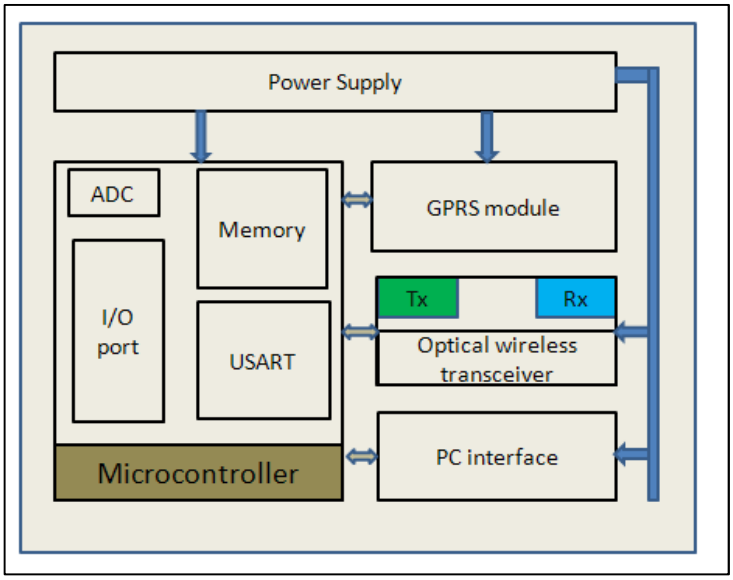

Figure 4-13 Gateway node architecture

Figure 4-13 shows the block diagram of a gateway node, which mainly consist of three modules. The first one is a microcontroller, which connects other modules; the second one is communication unit, which consist of optical wireless transceiver, GPRS module and PC serial interface unit. Finally, the power supply unit produces power to all modules in the node. The gateway node may need external memory for storing sensor data for long period of time if it does not send data to the base station periodically. It will depend on the application scenario. For example, data can be sent

periodically to the base station, which is located on land for further manipulation, or it can be collected manually, interfacing with a PC after a certain period of time. In the second case, the gateway node may need to store a substantial amount of data, which may end up needing additional memory to connect.

Three types of communication interface have designed for the gateway node to communicate with sensor nodes and the outside world. First of all, a bi-directional optical wireless transceiver was used to communicate with sensor nodes. The detail description of this transceiver was presented in chapter 3. Besides this, a GPRS module can be interfaced with the gateway node to communicate from anywhere in the world via the mobile network. Finally, to receive the data locally, a serial interface was used to connect the gateway node to a computer. Both GPRS and PC interfaces use the USART port of the microcontroller. FTDI-TTL232RG, TTL to USB serial converter cable is used to connect the gateway node to a commonly used USB port of a computer. RealTerm software is used to collect the data, and to show the received data in the monitor. The received data can be stored in a file for further manipulation using this software. The picture of the built gateway node is shown in figure 4-14.

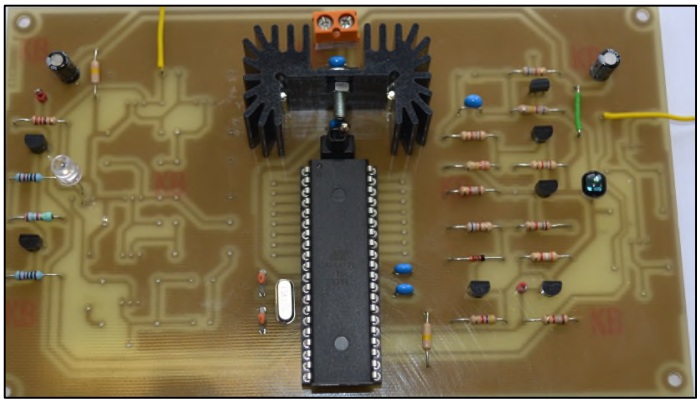

Figure 4-14 Built gateway node

As seen, a gateway node has been built using an identical board to that used for sensor nodes. Here, only one transceiver is mounted for the proposed application. The advantage of using the same board is to keep same distance between the LED and photodiode, which eventually helps in pointing nodes towards each other during experiments. If two communication branches need to be implemented, then both of the transceivers must be implemented to support communications. The maximum number of communication branches would depend on the number of USART port supported by the microcontroller. This is because, in the proposed system, the USART has been used to connect optical wireless transceivers.

4.7 Software design for Gateway node

A gateway node acts as a master node in the network, and collects sensor data from all sensor nodes. It also maintains the communication with other node and reports any failure of a node to the base station for further actions. To accomplish this, the gateway node sets two timers; one is “data request” timers, and another one is “node update” timer. A node update timer is used to send a node status request to each node periodically. Similarly, when the data request timer time is up, an interrupt is generated by the main processer, which will then send a data request signal to each sensor node sequentially. It collects data from each sensor node one by one, and, when data collection is finished, it goes into sleep mode. Figure 4-15 shows the flowchart of the gateway node task in the network.

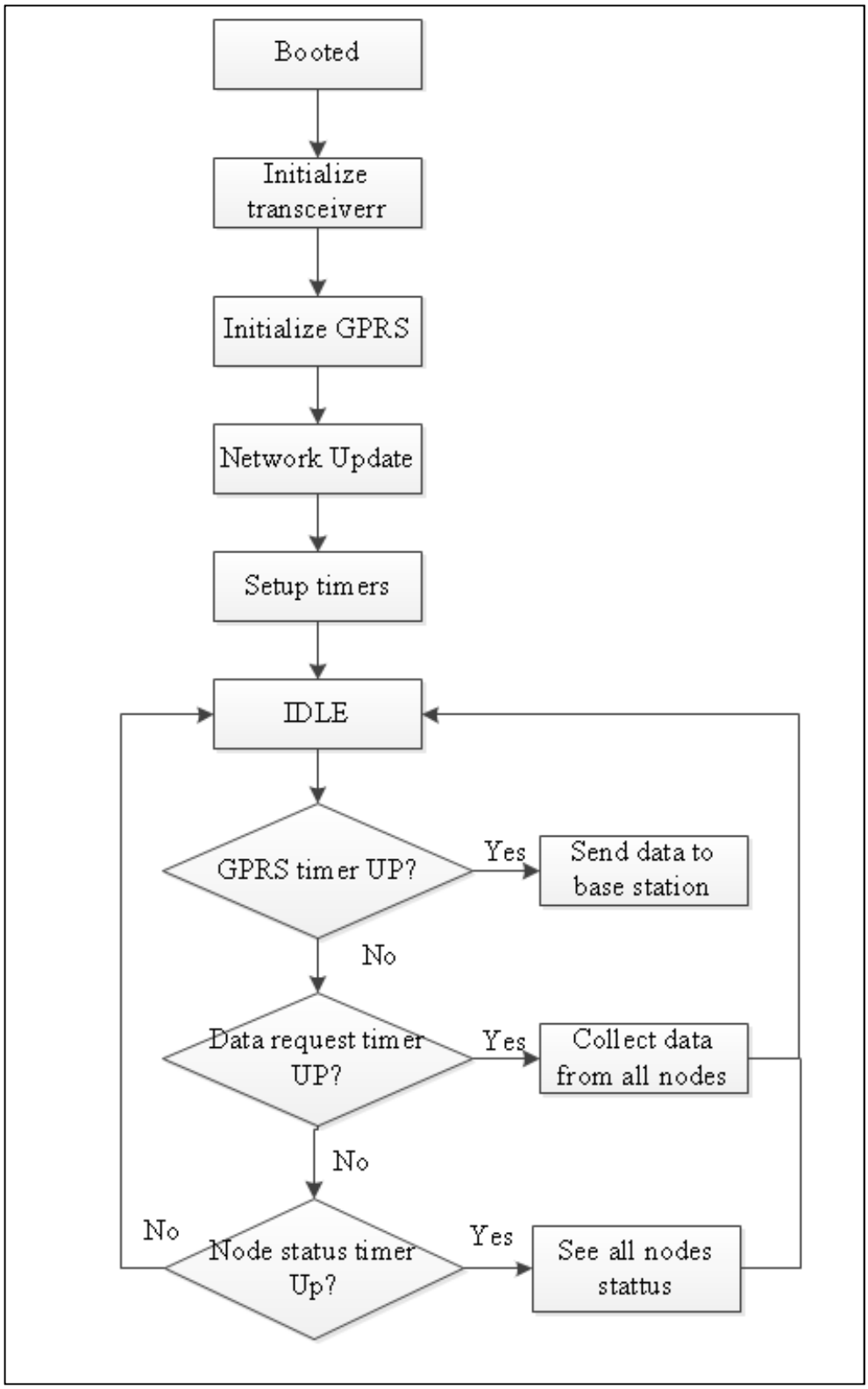

Figure 4-15 Block diagram of gateway node's main program

A detailed description of the data acquisition process is discussed in the following

chapter, which depends on the MAC layer protocol design.

4.8 Multi-hop network prototype

Figure 4-16 shows the laboratory set up of the multi-hop network prototype, which includes three nodes. To validate the received data by the gateway node, a PC interface was established with the gateway node. Here, sensor node 1 sends information to the intermediate node, which receives this information by the blue transceiver, and forwards this information to the gateway node by the green transceiver. Finally, the gateway node receives this information using a blue transceiver, and forwards this information to the computer, connected to it using the USART port. The PC receives this information, and shows it on the monitor by using Real-term software.

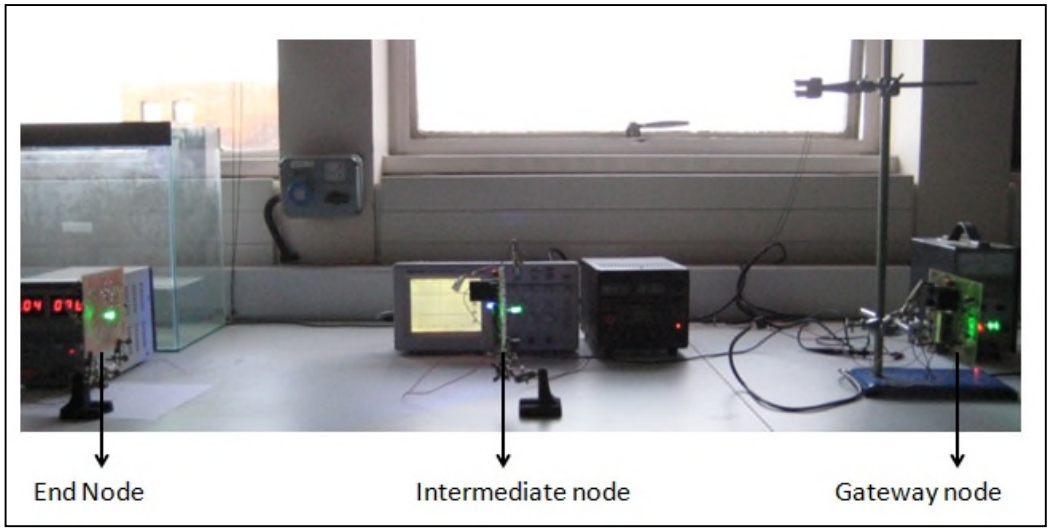

Figure 4-16 Multi-hop system setup

4.8.1 Example of an operation scenario of multi-hop system

In this section, a detailed description and waveform is shown at a different stage of a

multi-hop communication system. The microcontroller of the first node was programmed to send a fixed character for, example ‘T’, repeatedly to test the link. This was received by the intermediate node and retransmitted to the gateway node. Finally, the gateway node received the transmitted character, which was shown on the computer’s monitor. Throughout this process, one should understand how signal processing, which includes conversion from optical to electrical signal and amplification, has been done at the different stages to retrieve the original signal. Figure 4-17 shows the internal connections of the network prototype, and steps where the waveform of the transmitted signal has been observed.

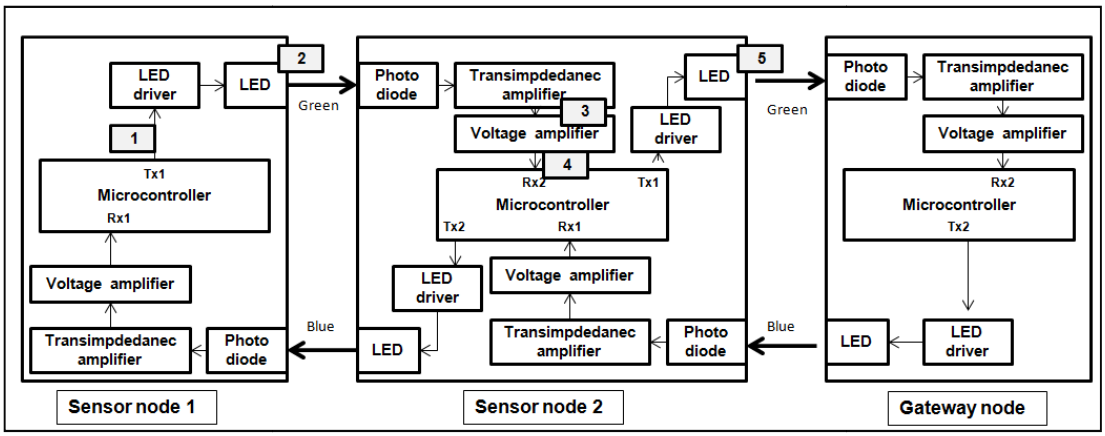

Figure 4-17 Physical layer connection of the built prototype

Figure 4-18 shows the waveform at different stages of the multi-hop communication system. As mentioned, the microcontroller of Node 1 sends “T” repeatedly which is transmitted across the TX of USART0 of microcontroller 1. TX0 pin of the microcontroller is connected to the LED driver circuit and the waveform at this stage shown in stage 1 of figure 4-18.

As the microcontroller works at TTL levels, so the Pk-Pk voltage of the transmitted signal was about 5V and the used frequency is 19.2 kHz which provided 38.4kbps

data rate in the NRZ modulation technique. This signal was modulated by the LED driver circuit, and the signal across the LED is shown in stage 2. Note that this signal was measured across the collector of transistor Q1 in figure 3-15, which is the amplified version of original signal. This signal was transmitted using visible light, and received by the photodiode of the second node. After the transimpedance amplifier, the waveform appeared as shown in stage 3 of figure 4-18.

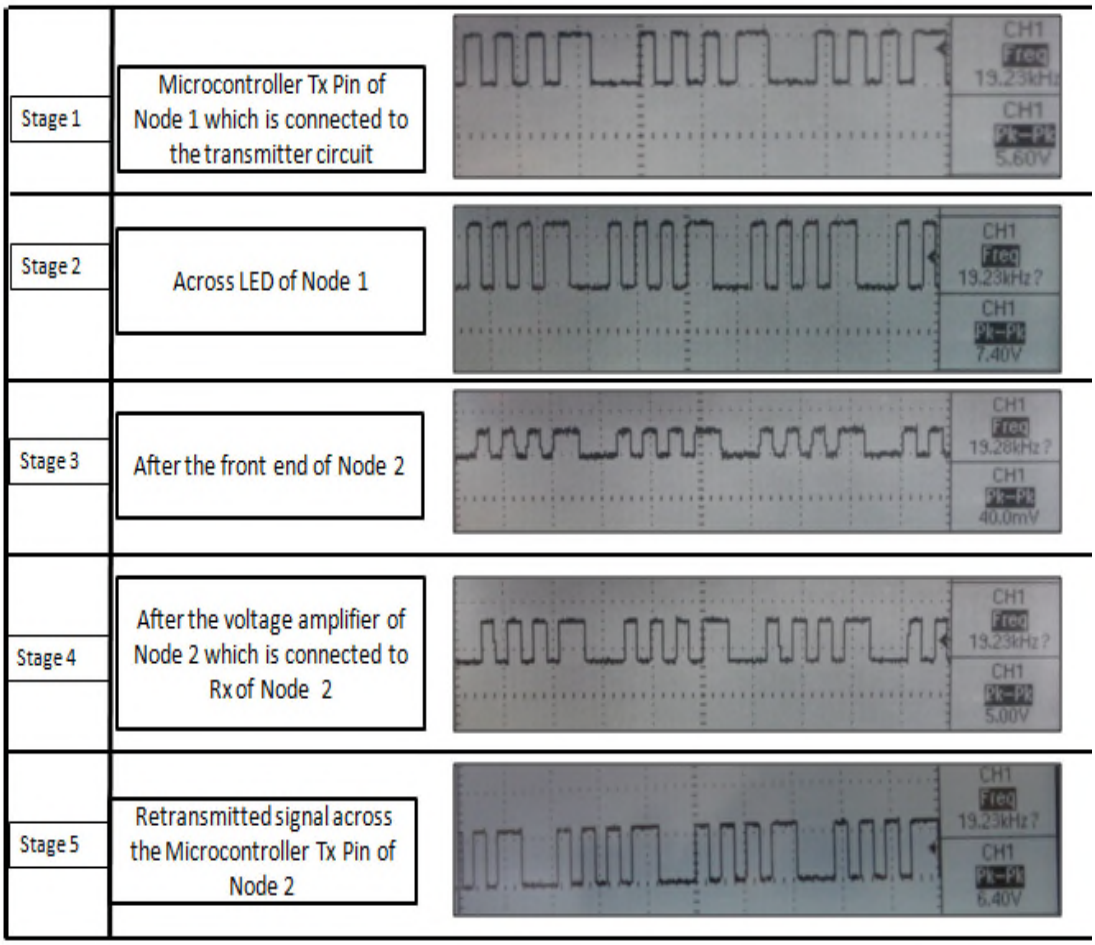

Figure 4-18 Wave form in different stages of a multi-hop network

Understandably, the strength of the received waveform was very weak. The Pk-Pk amplitude was about 40mV after 60cm, as obtained signal was attenuated by the medium and the geometry of the setup. This signal is then amplified using two stage

amplifiers, as mentioned in section 3.5. The custom-made amplifier converted the 40mV signal into 5V, as shown in stage 4. This signal was then passed to the RX0 pin of the microcontroller, which was programmed to retransmit the signal using the TX1 port. The retransmitted signal is shown in stage 5 of the figure. In the same way, node 2 retransmitted the original signal, which was then received by the gateway node. Now, to verify whether gateway node received the original character correctly or not, a serial interface using FTDI TTL-232R-5V, USB to TTL serial cable, was established. RealTerm software was used to collect the received data, and the baud rate was set up to 38400, as shown in figure 4-19.

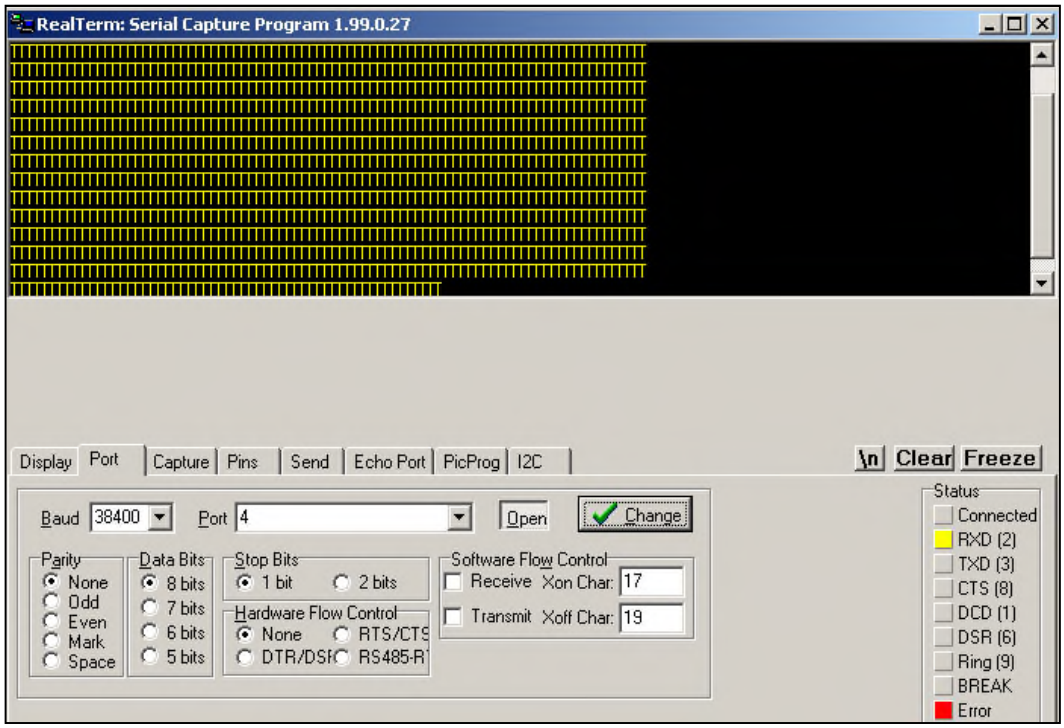

Figure 4-19 RealTerm software showing the received character in the gateway node

As seen in the figure, the transmitted signal was received by the gateway node successfully, without having any significant error at least up to 60cm distance. The gateway node also acknowledged the successful reception of the character by

sending another character, “A”, which was received by sensor node 1. This process verified the functionality of the designed, bi-directional, multi-hop, communication. Detailed performance analysis of the built system, both in air and in water, are discussed in chapter 6. This section only demonstrates the successful transmission and reception of data in a multi-hop network.

4.9 Conclusion

This chapter presented the design, built and testing of a multi-hop network for an underwater sensor application. A custom made sensor node and a gateway node were designed to support full-duplex communication underwater. Each node was equipped with two transceivers to establish uplink and downlinks. Blue and Green LEDs were used to distinguish between uplink and downlink in the network. To demonstrate the concept, a simple prototype was built and tested inside the lab, which functioned as expected. Data transmission was achieved for a two hop network, which can be increased further by adding more nodes.

Chapter5 : MAC protocol design

5.1 Introduction

A MAC protocol provides consistent connections between nodes, and also ensures error-free communication in the network by avoiding collisions. The energy and throughput efficiency of a network also depends on an efficient MAC protocol design. From the background study, it was found that most of the underwater MAC protocols currently used are based on acoustic communication, which may not be suitable for the visible light communication proposed here. The presented network is directional, whereas most of the acoustic communication networks are Omni-directional. Moreover, the wave propagation phenomena are totally different for acoustic waves and visible light in water. Acoustic waves propagates very slowly, which results multipath propagation, and also are prone to different types of noise, for example; noise from ships, noise from underwater species, man-made noise, etc. As a result, for the proposed visible light network, a TDMA-based directional MAC protocol has been proposed, which has unique features.

As a directional line type, multi-hop network, it is more justified to use a directional

MAC to avoid collisions, with each node only transmitting on its allocated time slot. The gateway node controls the communication slots, and also maintains the node information in the network. To implement the proposed communication protocol, different frames have been designed, which is not necessarily similar to the traditional MAC frame format. Detailed description of the proposed MAC protocols and different frame format are discussed in the following sections. Some of the performance analysis has also been illustrated, which includes throughput efficiency, delay measurement, and node power consumption. Firstly, the overview of the current underwater MAC protocol has been discussed in the following section.

5.2 Overview of existing underwater MAC protocols

As mentioned earlier, possible communication carriers in underwater can be acoustic, optical, or RF, which are under discussion by researchers for different applications. Among them, acoustic technology is mostly used for long distances, and low bandwidth network deployment. On the other hand, optical wireless and RF can be more suitable for short distances and high data rate applications, but are still in the development phase. As a mature technology, the acoustic system has been developed for a quite sometimes now, so there is much research on acoustic MAC protocols. During the last few years, a couple of research groups proposed a MAC protocol for underwater RF communications. When it comes to optical wireless, it is hard to find research papers related to an underwater MAC. One group proposed an underwater MAC protocol based on free space optics, and another group tried to integrate wireless MAC for an underwater optical wireless sensor network, based on IEEE 802.15.4. To understand the features and working principles of different underwater MAC protocols, some of the related literature is reviewed in this section.

5.2.1 Underwater acoustic MAC

Most of the underwater MAC protocols have been designed for acoustic technology. Underwater acoustic MAC protocols were developed either using carrier-sense multiple access (CSMA) using RTS/CTS messaging, or code-division multiple access (CDMA) techniques [72]. The network configuration which was considered is shown in figure 5-1.

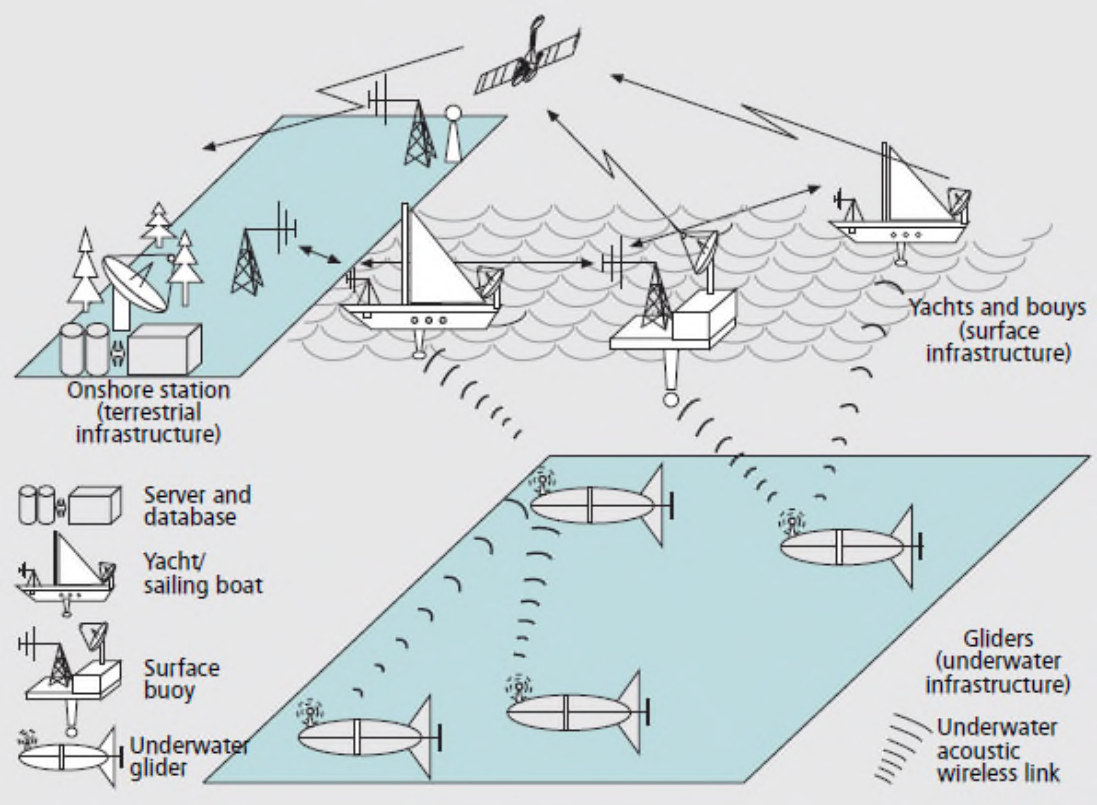

Figure 5-1 Network scenario for underwater acoustic MAC [72]

Narrow bandwidth and multi-path propagation of acoustic waves are reasons not to use frequency division multiple accesses (FDMA). The TDMA-based system is also proposed for some applications, but shows very limited channel utilization efficiency because of the long guard time requirement. Moreover, variable delay caused by the multi-path propagation makes it more complicated to implement a synchronization

protocol. Thus, it can be used locally, but for a greater geographical area, more sophisticated techniques are needed. Again, the effect of multi-path propagation varies in different depths of water. As a result, each MAC protocol has been designed for a specific network, depending on the application scenario.

In the case of deep water, a distributed single carrier CDMA technique performs better than a multiple carrier CDMA solution [73] . It is less complex but can still guarantee high network throughput, low delay and minimum power consumption. A direct-sequence spread spectrum (DSSS) based CDMA using a multicarrier technique proved to be more spectral efficient, but system complexity increases significantly for multiple carriers [74]. For each of the cases, CDMA has been as a medium access protocols, because of the use of CDMA as a physical layer technique.

Two types of Aloha-based carrier sense protocols for acoustic MAC have been proposed in [75]; one is Aloha-based carrier sense (Aloha-CS) and another one is Aloha-based advance notification (Aloha-AN). In Aloha-CS, an overhead packet is used to extract the sender-receiver information. By knowing the propagation delay of the packet, the status of the channel is calculated. Based on this calculation, nodes decide when to transmit to avoid collisions. In the Aloha-AN technique, any transmitting node sends a notification packet before transmitting any data packet by which other nodes knows about data packet arrival time. A CSMA/CA-based MAC protocol for underwater ad-hoc with prioritized message is introduced in [76]. The demonstration shows that, to make a connection between nodes, this protocol works well. A CSMA/CD-based MAC protocol has been developed in [77], which does not address the collision detection procedure.

A TDMA based MAC protocol is proposed in [78], where the time slot is divided into two parts. One slot is used by all nodes to transmit data using the same principle

of TDMA, and another one is used for unscheduled access to channels for variable traffic situations. The large data requires nodes to use unscheduled slots, which make the transmitting slot very extended, eventually building a long delay and an inefficient system.

5.2.2 Underwater MAC for radio communications

A radio frequency based, small scaled sensor network for the underwater environment, is proposed in [79]. For the medium access, a TDMA based approach has been taken which can resolve the issue of half-duplex radio communication. Each node has been allocated with a time slot and it only transmits during this period as shown in figure 5-2.

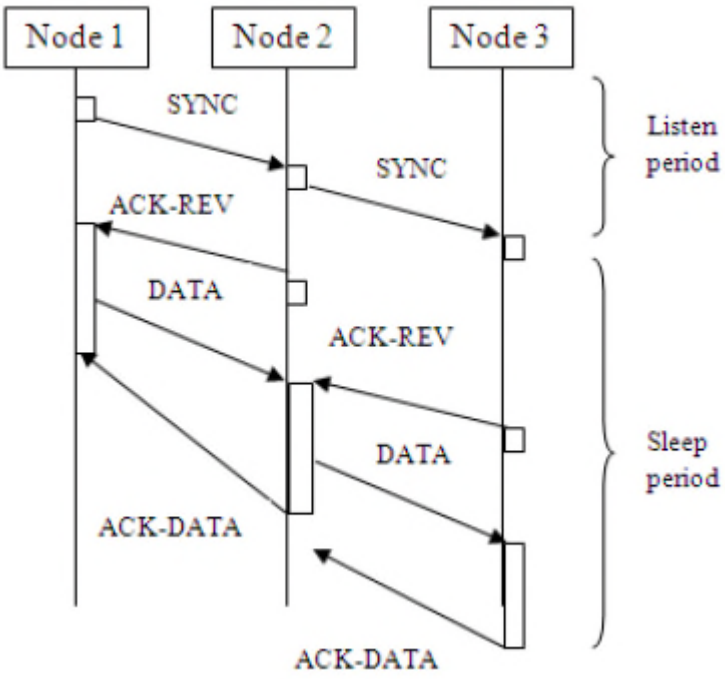

Figure 5-2 A TDMA based protocol for underwater radio communication [79]

Because of the small scale network, a static routing is proposed for the data forwarding process. The intermediate node needs to wake up for data relaying which

is defined and programmed by the administrator. The different frames format and some of the performance analysis of the proposed protocols are also mentioned in the paper.

For the shallow water environment, a MAC protocol has been proposed using RF communication, which is based on reservation MAC (R-MAC) [80]. In this process, periodic sleep and listen has been used to reduce the collision. The proposed mechanism introduced an SYNC packet instead of a REV packet, which was used in the original R-MAC protocol [81] .

5.2.3 Underwater optical wireless MAC

Traditionally, underwater optical wireless links have been designed for point-to-point communication for a long range, and do not consider the upper layer issues. As a result it was essential to design a MAC protocol for underwater optical wireless sensor network. Significant changes need to be considered when moving from a point-to-point system to a full network deployment, where multiple nodes communicate with each other. Research on a MAC protocol for an underwater optical wireless sensor networks is a relatively a new topic. Only a few research groups have proposed a MAC protocol for underwater optical wireless sensor networks. Among them, a CSMA/CA-based medium access control was proposed in [82], which is similar to that for the free space optical wireless networks. In this process, when any node wants to transmit, it first waits for a random number of back-off periods before detecting the channel. If the channel is busy, then the node increases the attempts by one until it reaches the maximum limit. The process is repeated until the node accesses the channel successfully. The used network prototype was a star type Omni-directional, which uses planar type transceivers to cover a 360 degree radius. This type of architecture produces a shared medium,

which cannot be accessed by more than a single node at a specific time. Moreover, the motivation of this research was to integrate the current free space optical wireless technologies with underwater communications.

A dynamic TDMA-based directional MAC protocol has been proposed in [70], which uses CSMA/AC to handle the randomness of simultaneous transmission by two neighbouring nodes. The Master-slave architecture, which is mainly proposed for a free space optical wireless sensor network, has been extended for underwater applications. In this architecture, a cluster head controls the communication in the network, which consists of several sensor nodes named as motes. Under each cluster head, there are multiple motes which send data to the cluster head. Also a neighbouring cluster head can communicate with each other. Each mote is assigned with a pre-programmed generic MAC address by which it can transmit a MAC request to the cluster head. The cluster head generates a unique MAC address for each mote when a MAC request is received. When a cluster head receives any packet without having a pre-programmed generic MAC, or a unique MAC assigned by the cluster head, it assumes a collision in the network. This is because either two nodes tried to communicate at the same time, or a neighbouring cluster head tried to relay a signal. In this type of scenario, the cluster head utilizes its dynamic TDMA scheme to add new nodes by assigning time slots to them. When a collision is detected by a cluster head, it broadcasts a SYNC message to the entire FOV to halt all communications in the network. After receiving the SYNC message, the node which does not have a time slot sends its unique MAC to the cluster head. Afterwards, the cluster head replies with an ACK message to the node, and also update its TDMA slot to incorporate a time slot for the node. This process is repeated until all nodes get a time slot and are acknowledged by the cluster head.

Another TDMA based MAC is proposed for an underwater optical wireless sensor network in [83]. The proposed technique uses visible light for data uploading from a sensor node to an AUV, but medium access control messages are propagated using an acoustic channel. Thus, the optical properties of the MAC were not considered for this application.

Directional MAC for underwater optical wireless sensor network has not been considered by any other groups which inspired the author to design a new MAC protocol based on directional concept.

5.3 Directional MAC concept

Most of the MAC protocols including IEEE 802.11 have been designed for Omni-directional antennas, where the signal is transmitted in all directions, and nodes in the coverage receive the signal. In this process, when one node transmits, all other nodes in the network keep silent. On the other hand, with directional communication, higher signal gain and better spatial reuse can be achieved by transmitting in a particular direction. In this method, packet reception from one direction is not affected by the interference from the other direction. With this type of communication, two pairs of nodes in a communication range can transmit simultaneously by controlling their direction. Using a directional antenna in RF communication was not common in the past, as it is bulkier and more expensive compared to the Omni-directional antennas. However, for optical wireless communication, which itself is directional, one can easily utilize the advantages of directional communication. Moreover, the Omni-directional optical transceiver requires more power and complex architecture to cover 360 degrees of geographical area. With directional transceivers, only accurate tracking between nodes has to be

ensued and an efficient MAC protocol has to be designed, which would be based on the directional network architecture. In fact, the selection of antenna would depend on the specific allocation type. The use of a directional antenna and design of a directional MAC has become popular in recent years, both in RF and the optical wireless domain.

In the RF domain, a directional antenna has been used mainly to resolve the hidden and exposed terminal problem in a sensor network. Another advantage of using a directional antenna is the spatial reuse, which significantly increases the network throughput. In [84], a directional MAC for RF sensor networks was proposed based on RTS/CTS signals as shown in figure 5-3.

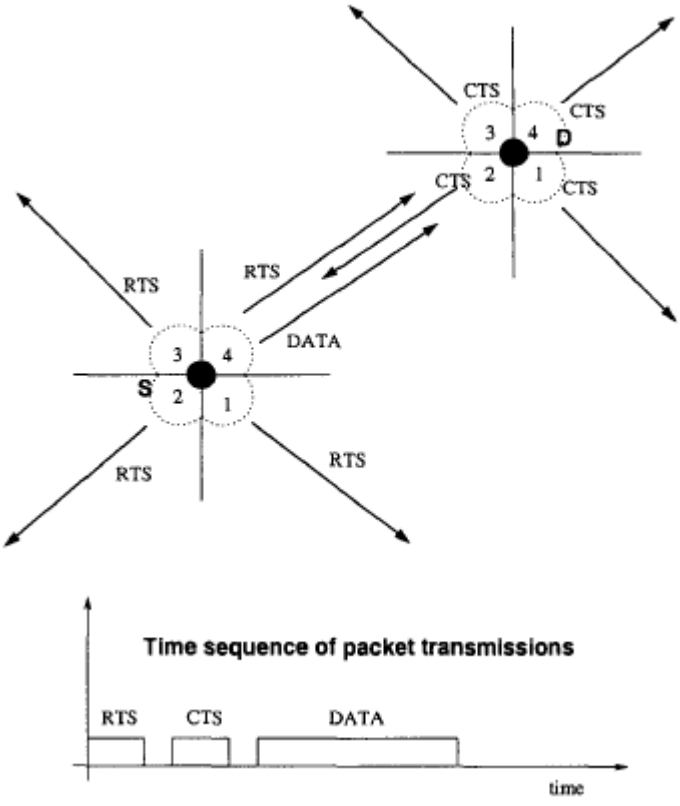

Figure 5-3 RTS/CTS based directional MAC [84]

Any mobile terminal that wishes to send data, broadcasts a RTS message using a number of directional antennas. The intended receiver replies with a CTS message by using all of its antennas. Receiving this CTS message from a specific direction, the sender automatically understands which way to transmit a data packet without knowing the specific location of the receiver. Simulation results show that this method performs two to three times better than the conventional MAC in terms of throughput analysis.

Another method, similar to the above mentioned proposal, has been illustrated in [85]. In this protocol, a directional RTS/CTS message is used instead of Omni-directional messaging. In addition, a GPS system is used to determine the location information, which is sent along with directional RTS/CTS information. This method cannot solve the hidden terminal problem, which is then modified to send an Omni-directional RTS/CTS message with location information to solve the hidden and exposed terminal problems.

A directional MAC for a multi-hop wireless network has been proposed in [86], which uses a multi-hop RTS protocol. In this method, the upper layer of source node provides the Direction-Omni (DO) neighbour route information. The source sends a multi-hop RTS packet to the Direction-Direction (DD) neighbour, using the DO neighbour route. Throughout the RTS message source requests the destination node to point its receiving beam towards the RTS sender and transmits a CTS packet. After receiving the CTS from the destination, the source node sends data using the directional link, which is acknowledged by the receiver after successful data reception.

Another directional MAC, based on CSMA/CA ,but without ACK frames, has been proposed in [87]. The proposed network architecture is line-type multi-hop network

where data traffic is mostly one-way. In this type of network, the ACK message increases the collision in the network. Therefore, ACK is removed in the proposed MAC protocols.

A directional MAC protocol has also been proposed for free space optical wireless communications [88] [89]. A dynamic TDMA-based directional MAC for a short range free space optical wireless sensor network was discussed in [88]. When collisions occur, a random access protocol was used by the master node to avoid the collision. A multi-channel directional MAC protocol was proposed for an indoor optical wireless Ad-hoc network, which uses five control handshake signals [89]. The author showed that multi-channel MAC performs better than single channel MAC to avoid any collision in the network. This can also solve the hidden and exposed terminal problems in an Ad-hoc network. An experimental demonstration was performed to demonstrate the concept of multi-channel directional MAC [90].

5.4 Proposed TDMA based Directional MAC protocol

The proposed MAC protocol is based on the TDMA concept, where features of a directional MAC protocol have been considered, as the proposed network architecture is directional. In the normal and emergency situation, a node transmits data using its directional transceivers only in a specific direction during its allocated time slots. Collisions can be avoided even in an emergency situation by following a certain message structure, which has been discussed in more detail in the following sections.

5.4.1 Some assumptions

Some assumptions have been made when designing the proposed MAC protocol, which has been described here.

- The proposed network architecture is assumed to be a static network, so the distance between two adjacent nodes has been kept fixed at 60cm, which is the length of the water tank used for the experiment. Therefore, to implement the MAC layer, it has to be ensured that the distance between the nodes is kept to the maximum possible range, so that the signal from the end node does not interfere with the gateway node, and alternatively, any signal from the gateway node does not reach the end node.
- Because of the line-of-sight communication, accurate pointing between two nodes has been maintained throughout communication.
- Pairing between up and down link transceivers has been done correctly.
- The data payload is equal for all nodes, which means the same amount of time is allocated for each node in the network.
- It is assumed that there would be two different types of sensor connected to each sensor node, and each of the sensor data values would be 16 bits long.

Also it is assumed that the accurate pointing between nodes would be maintained, but in underwater environment this would be a challenging issue; especially in the ocean environment where strong water waves could dispossess the node from its original position. As a result mobile network platform would be preferable in the underwater environment. Other than this, all other assumptions mentioned above are realistic to implement in underwater environment.

5.4.2 Basic idea

In the proposed multi-hop sensor network, the traffic follows from multiple sources to a single destination pattern. It is assumed that, for most of the time, nodes will send the same amount of information, which is mainly sensor data collected from a fixed number of sensors connected to the nodes. The basic idea of a TDMA protocol

is to allocate a fixed time slot for each node in the network to transmit information. During the TDMA time cycle, only one node transmits at a time in a specific direction, and all other nodes in the network listen. The time slot is allocated by the gateway node, and total time required for all nodes to go through a transmission phase is called the TDMA time frame. As each node sends the same amount of information, so the duration of time slots for each node would be equal. One of the nodes in the network broadcasts a time slot information named a TDMA frame, which has the timing information of all nodes when to transmit. The gateway node of the proposed application is responsible for broadcasting the TDMA frame, and also allocates a time slot for itself to transmit a SYNC message to the network to synchronize the clock of each node. For error-free communications, clock synchronization between nodes in a TDMA based protocol has to be ensured, to avoid incorrect slot assignment. There might be some drift between various nodes' clock, so a guard time has been used between each time slot to avoid simultaneous transmission.

Format of a TDMA frame for the built prototype is shown in figure 5-4.

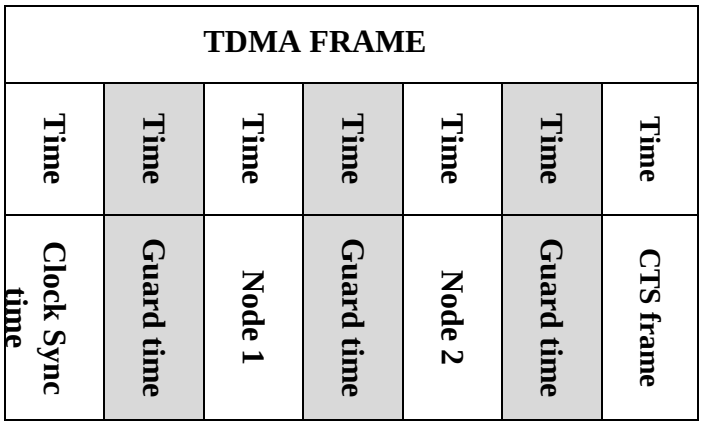

Figure 5-4 TDMA frame format

The transmission is triggered by the gateway node by sending a transmit trigger

message called an RTS frame. Here each node wakes up and transmits during its time slot only, and after transmission, the node goes back to the sleep mode. The gateway node acknowledges the successful reception of data by sending an ACK message. In this process, an intermediate node wakes up and retransmits when communication occurs between the gateway node and the end node. Since each of the communications is directional, it is assumed there would be no collisions during a normal communication scenario. But, in case of an emergency situation, several nodes may try to communicate with the gateway node, which increases the chance of collisions significantly. In this case the, gateway node will detect it, and assume an emergency situation has occurred.

The summary of the proposed MAC protocol has been illustrated here.

- After initial power up, each node will be allocated a unique MAC address by the gateway node, which will be used by the node for further communication in the network.
- Afterwards, the gateway node will broadcast a TDMA frame, as shown in figure 5-4.
- Receiving the TDMA frame, each node will be aware of its time slot information, and will act accordingly.
- The gateway node will generate a SYNC message to the network, which will have the reference clock information for each node. After receiving this message, nodes will adjust their clock following the clock synchronization protocol, as discussed in section 5-4-5. This message also informs each node in the network that the gateway node will be busy collecting data until it generates a CTS message.
- Afterwards, the gateway node will request data from each node on its

allocated time slot by sending an RTS a message.

- Receiving an RTS frame node will send sensor data, which will be acknowledged by gateway node.
- In the same way, the gateway node will collect data from all nodes in the network.
- When data collection from all nodes finishes, the gateway node will broadcast a CTS message to inform all nodes that network is idle.

Here, the presented protocol has some unique features compared to the other TDMA-based protocols. For example, the use of the RTS/CTS message is seen mostly in CSMA/CA-based MAC protocols. But here, the presented RTS/CTS message has a different meaning from the traditional RTS/CTS message. Here, the RTS message is generated only by the gateway node to inform the intended node for data transmission. In the same way, after collecting data from all nodes, the gateway node broadcasts another command message named as CTS to inform each node that gateway node is free now. By transmitting SYNC, RTS, and CTS messages, the gateway node informs the network when it is busy to collect data, and when it is free. These messages have not been used for the channel allocation process, as the channel allocation process is achieved by using a TDMA frame.

Another important feature of the proposed protocol is not to use any random access algorithm. Instead of using a random access protocol, the gateway node uses SYNC/RTS/CTS messages to avoid collision. The gateway node tells all other nodes in the network its transmission status by SYNC/RTS/CTS, which avoids collisions. Receiving a SYNC message from the gateway node means the gateway node would be busy until it generates a CTS message. Thus, in this period, only one node which receives an RTS message from the gateway node sends data. Even in the case of an

emergency, the node waits until it receives a CTS message from the gateway node to initiate any communication.

5.4.3 Data collection scenario

The ultimate objective of the built prototype is to collect sensor data from different sensor nodes in a periodic manner. The flow of data is one directional towards the gateway node, as shown in figure 5-5.

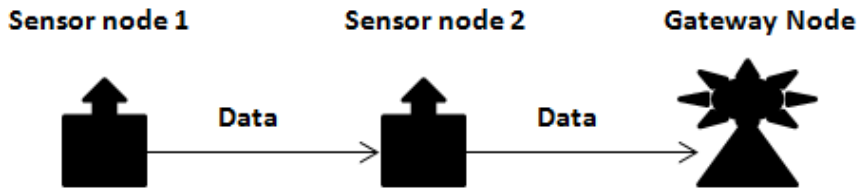

Figure 5-5 Data gathering scenario

The collection period and data payload size would depend on the data sample rate and data collection interval rate. Data sampling would be more frequent than the data collection period, as the transmission cycle consumes more power than the sensing unit in the sensor node. The occurrence of the data sampling and data collection by the gateway node would depend on the need for a specific application. The network size may be a factor in case of a large deployment. For the proposed scenario, each sensor node collects the sensor information every 15 minutes, and stores it locally unless it finds any unusual condition. For a real application scenario, it is considered that each sensor node will have two sensors, and each sensor data consists of 16 bits long, which will provide total of 16 bytes of information in every hour. All nodes send the stored sensor data to the gateway node at every 1 hour interval. The gateway node eventually sends the collected sensor information to the base station for further

manipulation, using its GPRS module in every 12 hours.

5.4.4 MAC address assignment

Initially, after powering up, each node in the network sends a unique address request to the gateway node; the gateway node receives this message, and generates a unique MAC address for that node. After receiving this address, the sensor node stops transmitting this message and uses the assigned MAC address for subsequent communication in the network. The gateway node updates its node information database for each entry, and uses this information for generating the TDMA frame. In the case of multiple branches, it is more practical to collect data from all nodes in a branch sequentially, and then move to the next branch. The gateway node maintains the database to record the branch information by seeing the received packet information. As the built prototype has only one branch, the MAC implementation scenario for a single branch has been discussed in this chapter. The MAC address assigning procedure, for a single branch consisting of two nodes, is shown in figure 5-6.

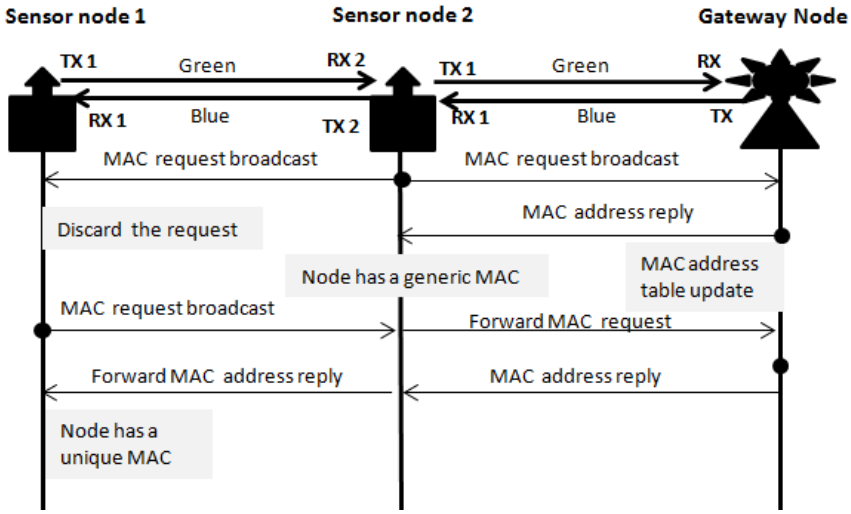

Figure 5-6 MAC assignment procedure

5.4.5 Synchronization protocol

By using synchronization frames, all nodes in the network adjust their clock references to a single clock, which is important for a TDMA-based system design. The referenced node can be either the gateway node or any other node in the network which sends the clock information. Any mismatch between two clocks may result in multiple transmissions at the same time, resulting in collision in the network. To avoid collision, it is very important to use an efficient synchronization protocol.

There are various synchronization protocols which are currently being used in wireless sensor networks. The details of the currently available synchronization protocols are illustrated in [91]. Six main protocols which were described in the paper are,

- Reference Broadcast Synchronization (RBS)
- Delay Measurement Time Synchronization for Wireless Sensor Networks (DMTS)
- Timing-Sync Protocol for Sensor Networks (TPSN)
- Probabilistic clock synchronization service in sensor networks
- Flooding Time Synchronization Protocol (FTSP)
- Time Diffusion Synchronization Protocol (TDP)

For the proposed multi-hop architecture, DMTS can be more suitable than other protocols, as it supports a multi-hop architecture, and also is easy to implement.

5.4.6 Normal operation scenario of the proposed MAC

In a normal operation scenario, it is assumed that all nodes in the network have been allocated a unique MAC address, and that a full network connection is established. Each node knows its time slot, which was previously allocated by the gateway node.

In this scenario, data collection is triggered by the gateway node, using the TDMA protocol discussed above. A step by step operation of the proposed protocol is shown in figure 5-7.

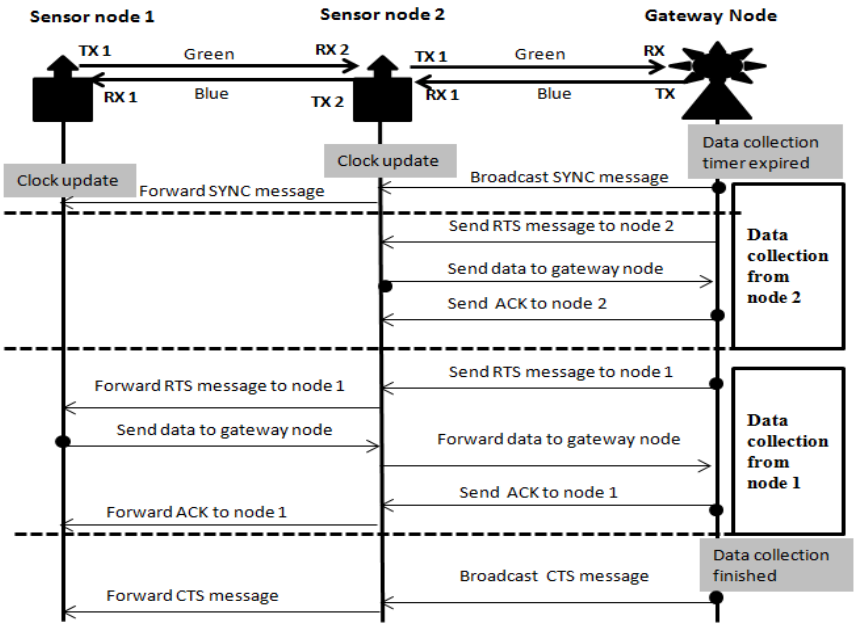

Figure 5-7 Operation scenario of the proposed MAC

As seen, when the data collection timer expires, the gateway node broadcasts a SYNC message, which has the clock timing information for all nodes to adjust their clock. For the built prototype, sensor node 2 receives this SYNC message and forwards the message to sensor node 1.

After receiving the SYNC message, each node updates their clock timing information according to the reference clock. Subsequently, the gateway node sends an RTS message to the sensor node 2 for sending data. Receiving the RTS message from the gateway node, the sensor node starts data transmission. After successfully receiving the data, the gateway node generates the ACK message to the sensor node 2. Here, it is necessary to mention that, if the sensor node does not receive ACK

message from gateway node, it will re-transmit data to the gateway node. In the same way, the gateway node collects data from sensor node 1, where sensor node 2 forwards the message both ways. Finally, the gateway node broadcasts the CTS message to the network to inform all nodes that the current data collection process is finished.

5.4.7 Emergency scenario

The emergency situation or alarm condition is reported to the gateway node by a sensor node when it detects any abnormal sensor reading. In this kind of scenario, communication is triggered by the sensor node which is opposite to the normal circumstances. After detecting an emergency situation, the node tries to determine if gateway node is free or not, by looking into the RTS /CTS message reception. If the node finds that gateway node is still at the data collection stage, it will wait until the gateway node generates CTS message. After receiving the CTS message, the node generates an emergency situation detected (ESD) frame, which is received by the gateway node. The gateway node acknowledges the reception of an ESD message by sending an ACK frame. If multiple nodes transmit at the same time, there would still not be any collision, as the gateway node uses different transceiver to communicate with a different branch. Once the gateway node receives the ESD message from a node, it triggers the data collection process immediately, as it does in a normal scenario.

5.5 Different types of frame design

To implement the designed MAC protocol, different types of frames have been designed for the proposed application, which are discussed in the following section.

5.5.1 Data frame

The sensor data is transmitted across the network, using the data frame. The format of the data frame is shown in figure 5-8. A description of each of the field is given below.

- The first field of the frame is the destination address, which consists of 8 bits, and named as “Dest Add”.
- After that, an 8 bit source address is placed, by which at best 254 sensor nodes can be connected in the network. This is the maximum possible number of address that can be assigned in the network.
- “No. of reading” field represents the total number of sensor data readings, that are ready to send. A maximum reading would depend on the number of sensors connected to each node, and also the period of data sensing.
- “No. of Hop” represents the total number of hops this frame has travelled before reaching the destination.
- “Frame type” represents the types of frame which can be either sync, data or control frame.

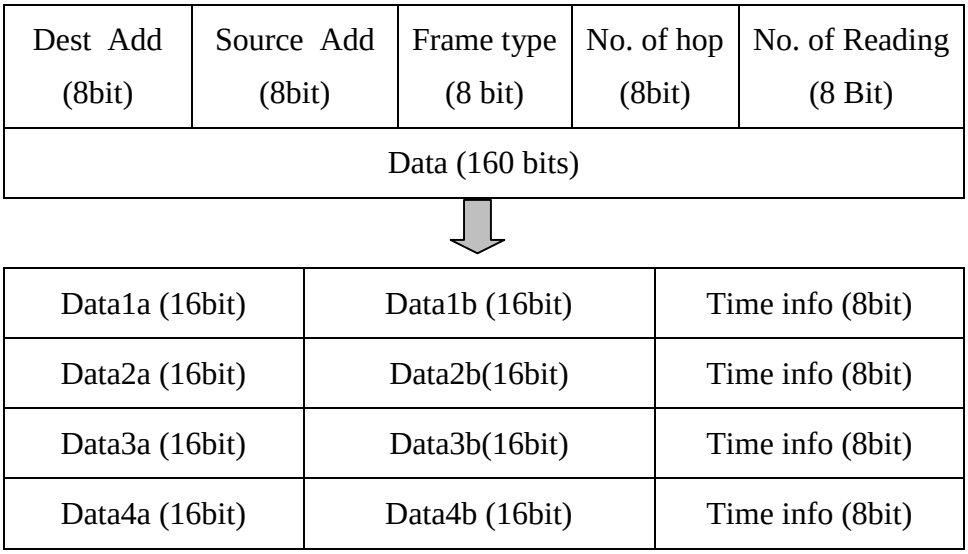

Figure 5-8 Detailed data frame format

The first 4 bits of the frame type is reserved for further use, which is defined as ‘0000’. The second 4 bits represent the types of frame, and ‘0000’ would represent the data frame.

- The final block of the frame represents data payload, where size would depend on the specific application. If it is assumed that each sensor node will have two sensors connected to it, and each of the sensor information can be 16 bit long, then there would be 32 bit data for each reading. After each sensor data, there would be an 8 bit time stamp, which would make it 40 bits. As mentioned, in every transmission period, the sensor node will have a maximum of 4 readings, which will result all together in 40 × 4 = 160 bits of information.

5.5.2 MAC request and reply frame

A MAC request and a MAC reply frame have been used to assign the unique MAC address to a node. After powering up, the sensor node sends a MAC request frame, using the format shown in figure 5-9.

Dest Add (8 bit)	Source Add (8 bit)	Frame type (8 bit)

Figure 5-9 MAC request frame

Here, “Dest Add” will be the broadcast address. “Source Add” would be a generic MAC address, and “Frame type” would be “0001”, to indicate that this is a MAC request frame. The gateway node replies with a MAC reply frame, as shown in figure 5-10. The destination address would be a generic MAC address, and “Source Add” would be the gateway node’s MAC address, and “Unique MAC” field will consists of a node’s new MAC address. “Frame type” field would be assigned with “0010”, to

indicate a MAC reply packet.

Dest Add (8 bit)	Source Add (8 bit)	Frame type (8 bit)	Unique MAC (8bit)

Figure 5-10 MAC reply frame

5.5.3 Synchronization frame

The format of the synchronization frame depends on the types of synchronization protocols being used. As DMTS has been chosen for the proposed application, only a reference timestamp need to be broadcasted through the network. In the proposed prototype, the gateway node sends the timestamp information using the synchronization frame format, as shown in figure 5-11. Here, the frame type value "0100" represents the synchronization frame.

Dest Add (8 bit)	Source Add (8 bit)	Frame type (8 bit)	Timestamp (32bit)

Figure 5-11 Time synchronization frame

5.5.4 Other control frames

There are mainly four types of control frames used in the proposed protocol. They are the RTS frame, the CTS frame, the ACK frame, and the ESD frame. The acknowledgement frame is transmitted by the gateway node when a data frame or ESD from a sensor node is received successfully. The RTS and the CTS frames are also generated by the gateway node to inform each node about the start and end of a data collection process. Finally, the EDS frame is generated by a sensor node to report any emergency situation. All of the above mentioned frame formats follow the same structure, as shown in figure 5-12. The frame contains three fields; Dest

Add, Source Add and Frame type.

Dest Add (8bit)	Source Add (8 bit)	Frame Type (8 bit)

Figure 5-12 Control frame format

Frame type field indicates the type of frame which is encoded by the following binary values.

- "0101" represents RTS message.
- "0110" represents CTS message.
- "0111" represents ESD message.

5.6 Hidden terminal problem

A hidden terminal is the one which is located outside of the source node transmission range. For the proposed application, sensor node 1 can be a hidden terminal for the gateway node, and alternatively the gateway node can be a hidden terminal for sensor node 1. When communication between sensor node 2 and the gateway node takes place, sensor node 1 may be unaware of it, and tries to establish communication with sensor node 2, as shown in figure 5-113.

In normal circumstances, a collision would occur at sensor node 2, as it is already communicating with the gateway node. In case of the proposed architecture, this problem would not happen, as signals from the sensor node 1 are received by a different transceiver which is being used to communicate with the gateway node.

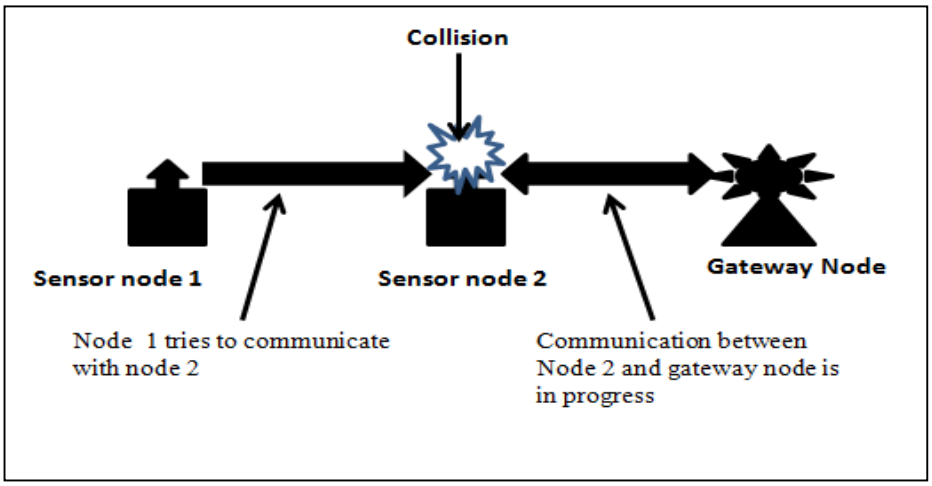

Figure 5-13 Hidden terminal problem

Because of the different directions, a sensor node is capable of receiving signals from both directions, which are then processed by the microcontroller. As the microcontroller is much faster than the intended communication speed, so the processor task will be switched between transceiver 1 and transceiver 2.

5.7 Performance analysis of the proposed MAC

Usually, the performance of a MAC protocol is accomplished in a simulation environment. In this section, the author discusses some of the performance analysis, which has been done by taking an experimental approach. The analysis presented here is accomplished for three nodes, but, in the case of a real deployment number of nodes, would be much higher. Therefore, the performance analysis could be significantly different. Node power consumption and round trip delay have been calculated using experimental observation. Here, the presented analysis is done using a simple method to understand some basic performance metrics, compared to the conventional MAC performance analysis.

5.7.1 Throughput efficiency

Network efficiency depends on the size of data payload and overhead .The overhead includes all kinds of messages used in the physical layer, and the MAC layer accepts the real data. There are basically two types of overhead in the proposed communication system. In the case of a serial communication, each 8 bits data are encoded with a start and stop bit, which makes it 10 bits. This means that, for a 1 byte of data transmission, there are 2 bits of overhead.

For a higher throughput, it is expected to have a longer data payload to increase the ratio between actual data and overhead messages. As the data flow path is static for the proposed network, the throughput would depend on the channel quality and data payload size. In the case of a reliable channel, a sensor node can successfully transmit message to the gateway node at the first attempt, whereas a poor channel can cause retransmission of data up to three times, which is the maximum possible number of re-transmissions designed for the proposed MAC protocol. Figure 5-14 shows the throughput efficiency for the different payload sizes, where throughput is the ratio between actual data and overhead. Here, it is assumed that channel quality is very good, and data has been received by the gateway node at the first attempt.

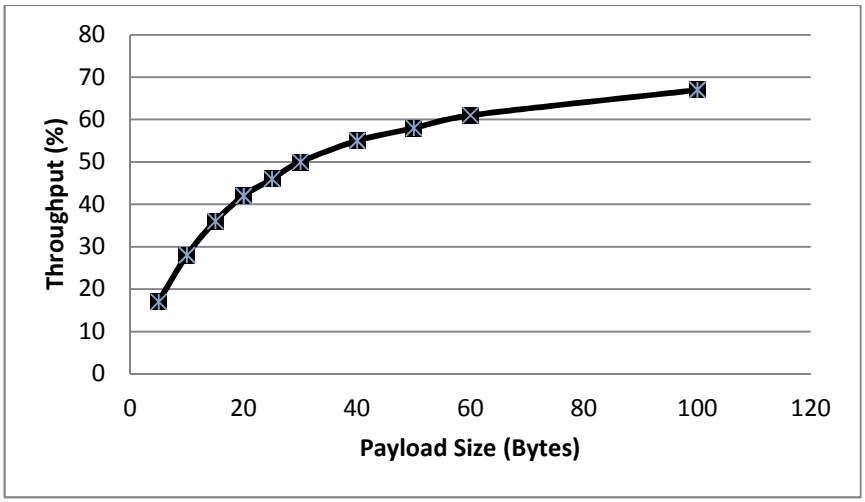

Figure 5-14 Throughput for different payload size

As seen in the figure, the throughput increases with an increase in data payload size. Initially, the throughput increases very sharply until it reaches to 60%. Afterwards, the curve becomes steady with increases in packet size. This is because the effect of overhead packet size becomes less and less significant as the payload size increases.

5.7.2 Node power consumption

Power requirement is an important performance evaluation for sensor networks, which reflects the energy efficiency of the MAC layer protocols. To estimate the performance of the proposed MAC protocol in terms of power efficiency, the power consumption of each node has been observed at various stages. As mentioned before, to minimize the system cost, different modules of the node have been built on a single PCB board, which share same power source. Meanwhile, each node in the network has different power requirements, for example, the end sensor node and gateway node were equipped with a single transceiver, whereas the intermediate node is equipped with two transceivers. Moreover, all sensor nodes are equipped with physical sensors; on the other hand, the gateway node does not have any physical sensor connected to it.

From practical observation, it is found that the power supply current of the gateway node and end sensor node in the transmission state is about 40mA, while in the receiving state it is approximately 30mA. The intermediate node power requirement is more, as it has two transceivers connected to it. Thus, the intermediate node consumes about 30mA current while in the receiving mode, and about 70mA during the transmission period. In a 1 hour period the gateway node was mostly in the receiving state, as the transmission period is very small in the 38kbps, and it

transmits only a few bytes. This means the gateway node would be in a receiving state for almost 3400 seconds, which is equivalent to 918 Joules. The energy for transmission and reception of each bit has been calculated for the gateway node. Transmission energy per bit is 9.3uJ, and consumed energy for receiving each bit is equal to 7.02uJ.

Following the same procedure, the node power consumption has been calculated for all nodes, both for the transmission state and receiving state. Figure 5-15 shows the total power consumption of the gateway node, intermediate node and the end sensor node for one hour. In this time period, the gateway node collected data from sensor nodes four times in a fifteen minute interval.

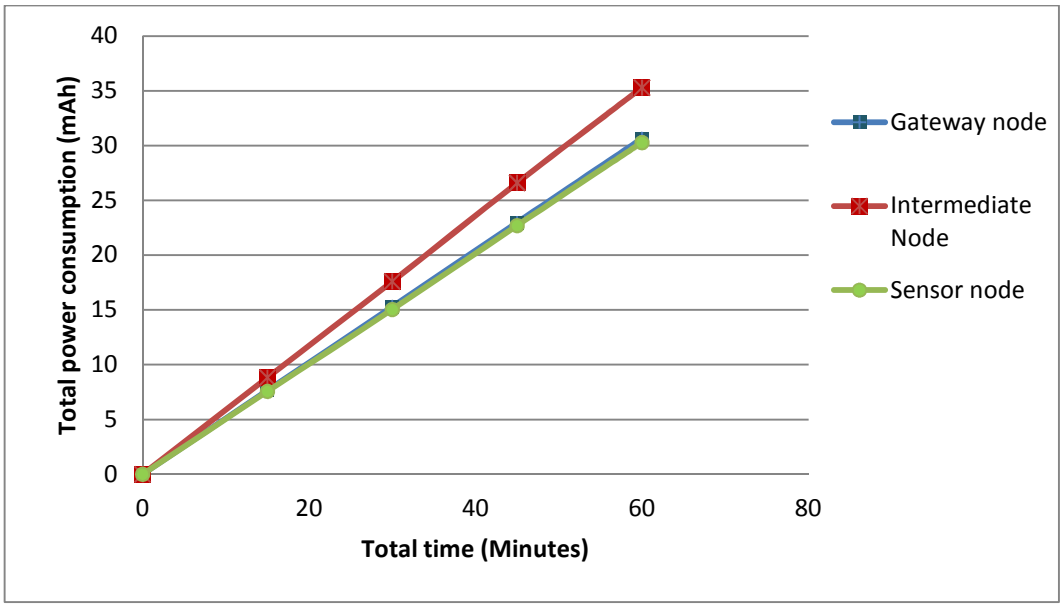

Figure 5-15 Total power consumption for one hour

As seen, an intermediate node requires more power than the gateway node and the sensor node, because, during the communication between end sensor node and gateway node, it needs to be in a transmission state, which requires more power than the receiving state. In case of a bigger payload size and large network, the node

power consumptions would increase considerably. It should be noted that the author did not consider the Idle state, when power consumption would be in the µW level. In real implementation, nodes will be in an idle state for a significant amount of time, which would eventually reduce the total power consumption considerably.

5.7.3 Delay analysis

End-to-End (ETE) delay (T_{ETE}) is the summation of transmission delay (T_{TX}), processing delay (T_{PROC}), and propagation delay (T_{PROP}). For the built network architecture, the total number of hops is two. So the maximum ETE delay would be,

$$T_{ETE} = 2\times(T_{TX} + T_{PROC} + \mathrm{T}_{PROP}) \qquad \textbf{(5-2)}$$

Again, the transmission delay and the processing delay would depend on the size of the packet, rate of the transmission, and also delay caused by the different components used in the system design. On the other hand, propagation delay is affected by the range of the transmission. The waiting time before transmission also needs to be considered when finding the ETE delay. For an optical wireless communication system, the propagation delay would be minimum compared to the transmission delay, as light travels very fast in space, as well as in water, compared to any other carriers. Experimentally the ETE delay is calculated by transmitting a signal from a source to the destination. Here, the round trip time is measured using the microcontroller's timer and counter by sending a different number of characters and averaging them to find the round trip time for a single character, as shown in figure 5-16.

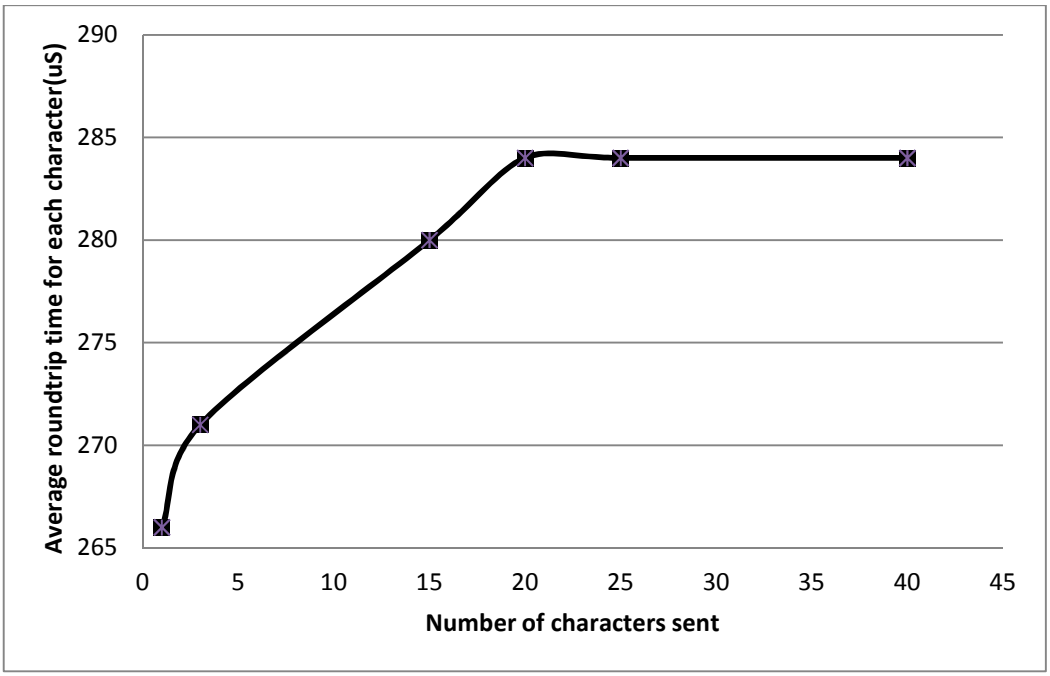

Figure 5-16 Round trip time for different packet size

From the figure it is seen that an initial round trip is about 265µS, which increases according to the increase of payload size until it reaches to 285µS. After this, it remains same with the increase of payload. The measurement was done using the 38400 baud rate which is equivalent to 38.4kbps. Here, it should be mentioned that during the round trip time measurement, the destination node receives data in one serial port and forwards the received character to another port continuously. Since data is not buffered here, round trip time for more than one node also remains the same.

The round trip time for different transmission rate was also measured which is shown in figure 5-17.

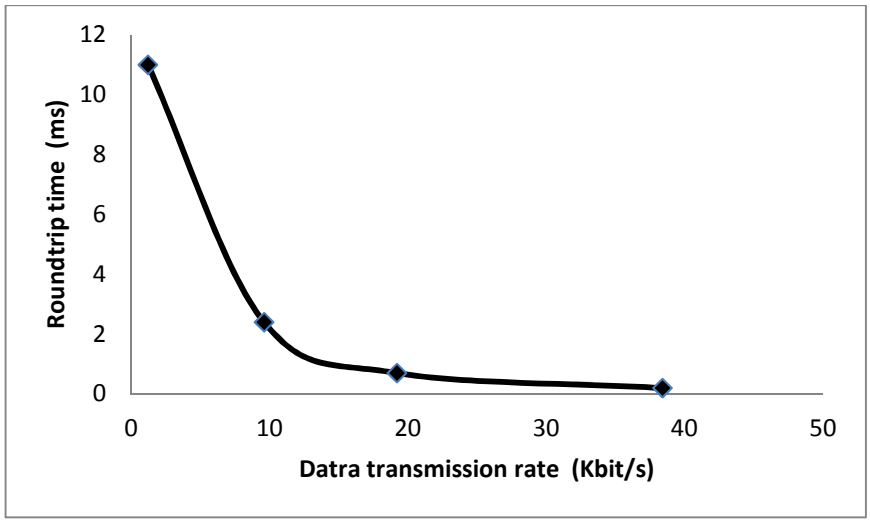

Figure 5-17 Round trip time for different transmission rate

As seen, the round trip time decreases when data transmission rate increase.

5.8 Conclusion

To implement a sensor network prototype, designing an efficient communication protocols is essential to support the error free communications. As the optical wireless communication link has been used mostly for point-to-point communications, there has not been much research on upper layer protocols including MAC. Instead, most of the optical wireless networks adopted traditional RF protocols, which have been used for many years. Moreover, being a recent technology, underwater optical wireless communication systems are still in the development phase, so there have not been many experimental results to evaluate the performance of different underwater optical wireless systems. As a result, it has been essential to design a MAC protocol and analyse performance, which would be useful for further research on underwater optical wireless MAC protocols. Here, the presented MAC protocol may not solve all the problems, but provides a guideline for further research on this topic.

Chapter6 : Experimental evaluation

6.1 Introduction

To investigate the performance of the designed network prototype, an experimental set up was implemented in the lab environment. The main objective of undertaking these experiments was to see how performance varies with different scenarios. Firstly, experiments were carried out in air both for a single hop and then for a multi-hop network. In free space communications, interference from the room light and sun light are the main factors which degrade the performance. In the case of a deep underwater deployment, these two factors may not persist, so experiments were performed in the water environment to compare the results with the air testing. Different types of water which were collected from tap, canal and ocean, were used to compare the performances. Successful transmission in various distances was measured for different environment, which has been discussed in the following sections.

6.2 Experimental setup

For experimental evaluation, one gateway node, two intermediate sensor nodes and one end sensor node were built, following the design procedure discussed in chapter four. All the experiments were first carried out for two conditions. First, the experiments were carried out in the presence of room lighting. Afterwards, measurements were at night, without the presence of any light. Figure 6-1 shows the experimental set up for the built network inside the laboratory.

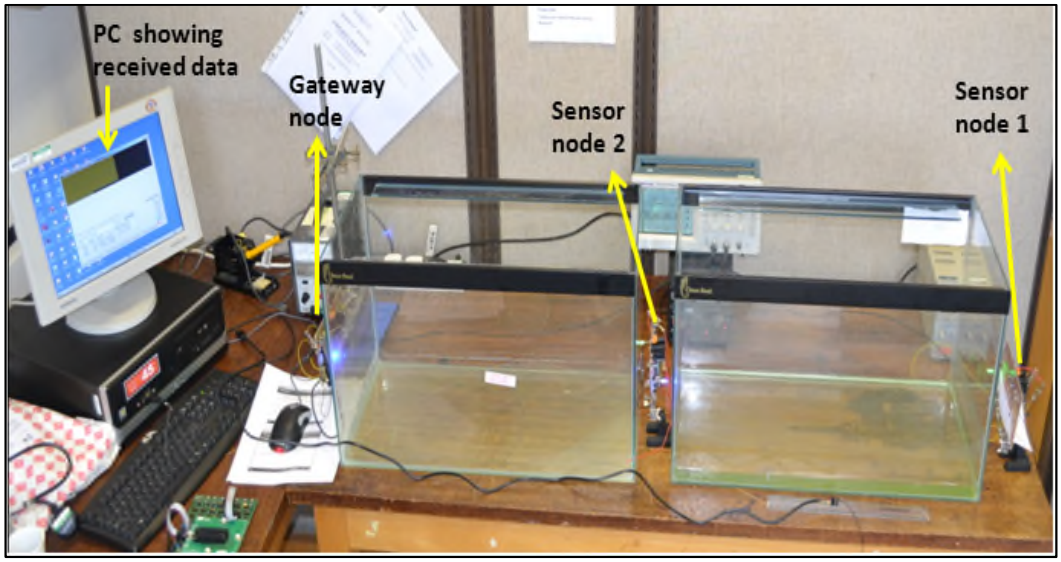

Figure 6-1 Experimental setup for performance evaluation

As seen in the figure above, three nodes have been aligned and pointed towards each other to form a line type multi-hop network. A blue channel was used to send information from the gateway node to the sensor nodes, defined as a downlink. On the other hand, to send data from a sensor node to the gateway node, a green channel was used. A computer was interfaced with the gateway node, using the serial interface to analyze the received data.

6.3 Performance analysis in air

Experiments were first conducted in free space for a single hop system, both for the blue and green channel, to find the received optical power and success rate for different communication ranges. Later, the success rate was also calculated for different transmission rates and transmission angles, to estimate the pointing requirements between nodes.

6.3.1 Received optical power at different communication range

The optical power was obtained using a photometer placing in front of the receiver at various distances, keeping the transmission data rate fixed at 9.6kbps. Figure 6-2 shows the obtained optical power for different communication distances.

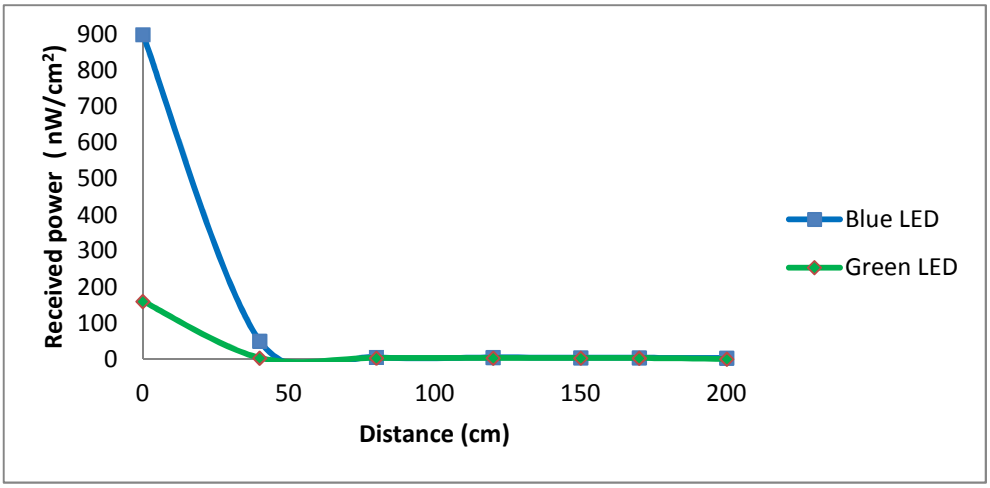

Figure 6-2 Received optical power at different distances

As seen in the figure, the blue LED illuminates at a much higher brightness compared to the green LED, for the designed system. Thus, the comparison between blue and green channel may not be justified in terms of distance, because the blue channel would always provide better results, having higher the transmitted optical power.

The received optical power for the green channel both with and without the presence of room lighting is shown in figure 6-3.

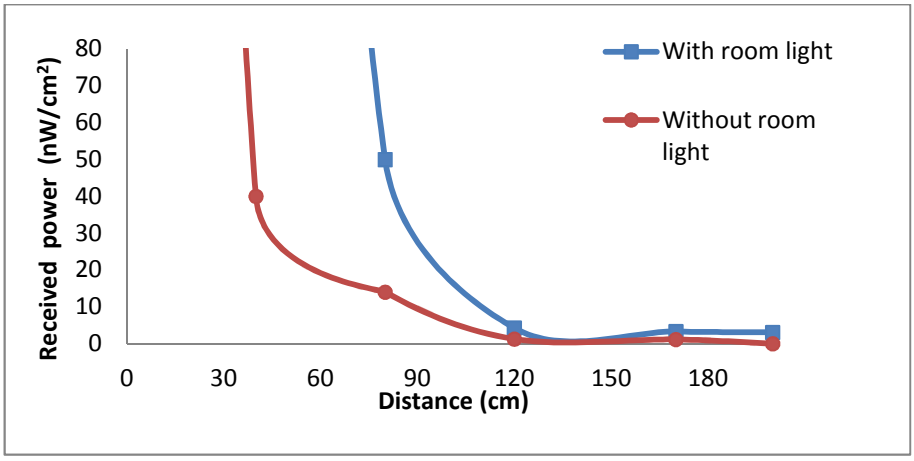

Figure 6-3 Received optical power with and without presence of room light

As seen, room lighting has a very strong effect on visible light communication. The received optical power was almost half without the presence of room lighting, compared to the presence of room light.

6.3.2 Success rate for different optical power

Now, the frame success rate for different received optical powers was found for the green channel, with and without the presence of room light, which is shown in figure 6-4.

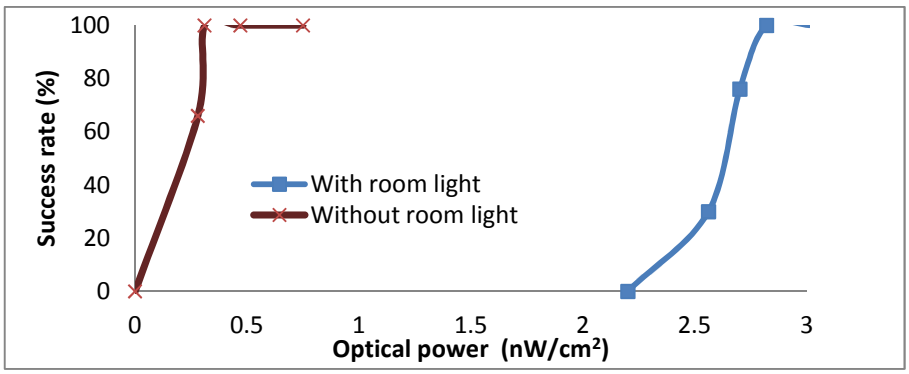

Figure 6-4 Success rate for different optical power

As seen from the figure, without the room light a higher success rate was achieved for the lower optical power. This is because, without the room lighting, most of the power received was from the transmitted power provided by the LED.

6.3.3 Single hop Success rate for different communication range

The success rate for different communication ranges was calculated with the presence of room lights, both for the blue and green channels. Afterwards, experiments were repeated to obtain the success rate without the presence of room lighting. For every set of experiments, a fixed character was transmitted for five seconds, and the received characters were saved in the PC, using the serial interface. Afterwards, the total number of sent characters and successfully received characters were compared, using MATLB program to find the success rate. Figure 6-5 shows the success rate for different communication distances.

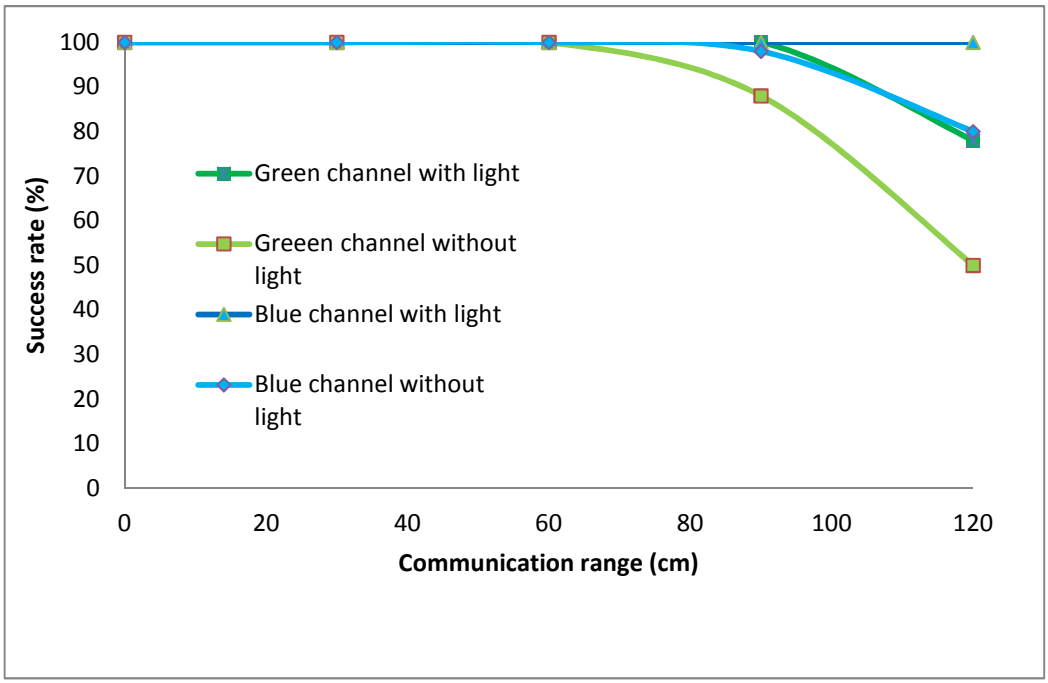

Figure 6-5 Success rate in air for a single hop system

As seen from the figure, the success rate is 100% at a communication distance of up

to 150cm for the blue channel, and in the case of a green channel, it is about 120cm, when room lighting is absent. The success rate decreases significantly for both channels afterwards. At a communication range of 200cm, successfully received characters for the green channel were about 10%, whereas for the blue channel they were about 50%. It is clearly seen that, for the built system, the blue channel performs better than the green channel.

6.3.4 Single hop test for different transmission rate

The success rate was also calculated for the different transmission rates by fixing the communication distance at 160cm as shown in figure 6-6. The measurement was conducted without the presence of room lighting.

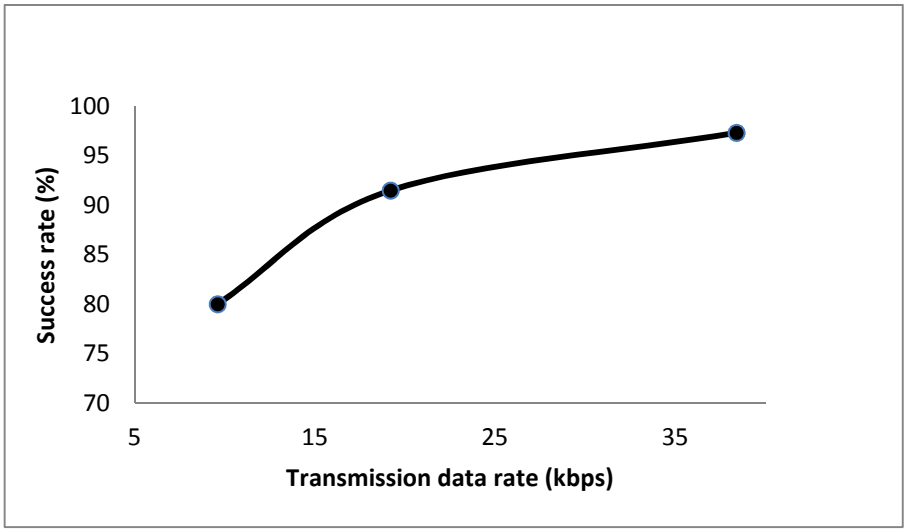

Figure 6-6 Success rate for various transmission rates

From figure 6-6 it can be observed that the packet success rate increases with an increase in transmission data rate. Although the designed optical wireless transceiver supports data rate up to 70 kHz, the author could not perform a measurement beyond 38.4kbps. As seen in the datasheet of the microcontroller, for an 8MHz external crystal, a baud rate beyond 38400 provided a very high error rate. The reason for this

is not clear from the data sheet, but this could be the reason for not receiving any data after 38.4kbps.

6.3.5 Success rate for the different angle

Because of the water current and movement, it would be hard to point out two nodes to each other underwater. There could be some displacement between nodes, and it has to be understood how much deviation is tolerated by nodes. For this reason, the success rate for different transmission angles was measured at 38.4kbps transmission data rate. Here, the receiving node was kept in a fixed position, and the transmitting node was moved slowly sidewise at a fixed communication distance of 60cm; successfully received characters were calculated for different angles, as shown in figure 6-7.

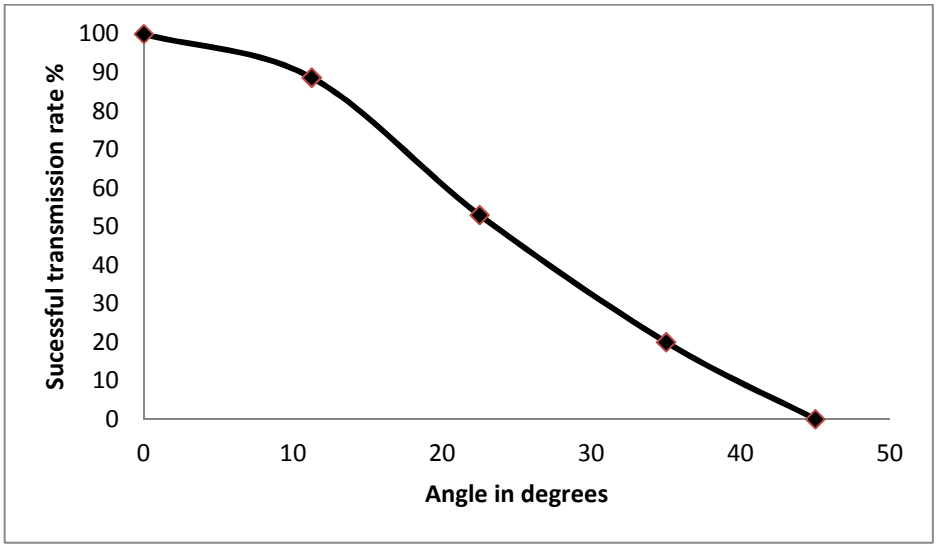

Figure 6-7 Success rate for different transmission angles

As seen from the figure, the initial success rate is 100% when the transmitter and receiver were pointed out to each other accurately. Afterwards, packet losses increase when the transmission angle increases. When the transmitter was moved to around 22.5 degrees, the successfully received packets were 50%, and nothing was received

at a 45 degree angle. As a result, it has to be ensured that the node does not deviate more than 15 degrees, which would guarantee successful communication between nodes.

6.3.6 Success rate for a multi-hop system in air

The success rate for a two hop system using the green channel was obtained in the presence of room lighting. End to end success rate was calculated, as shown in figure 6-8.

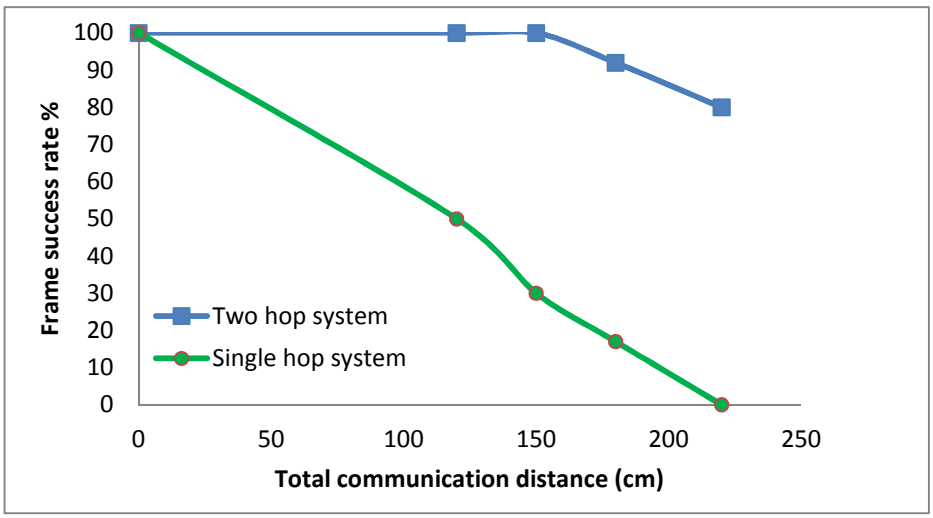

Figure 6-8 Success rate for multi-hop communication range

As seen, the multi-hop technique increases the communication range significantly compared to the single hop system. The author could not perform a test beyond 220cm because of space constraints in the laboratory.

6.3.7 Number of hops vs. Success rate

For a multi-hop communication system, the success rate may decrease with increase of number of hops. The author tested the system using four nodes at a communication distance of 60cm, and received 100% frames successfully. Thus, it can be said that at least communication of up to three hops was achieved, which

increases the communication range almost three times compared to a single hop system.

6.4 Performance analysis for a single hop system through water

Here, the presented network prototype was designed for an underwater communication system, so the results in free space do not reflect the capability of the designed system underwater. As a consequence, the author made an underwater environment inside the laboratory, using two glass-made fish tanks. The size of each water tank was (60cm x 30cm x 45cm), filled up to half of their height with water. Nodes were placed on each side of the tank, and a signal was passed through the water. Three types of water were used to compare the performance, as described in the followings sub-sections. Merging the system into real water would have been more justified, but considering the complexity, time and money, the author did not take this approach.

6.4.1 Water tank setup

During the initial transceiver testing, the author found that the signal losses were apparently smaller for water than in air. Since water is denser medium than air for the blue and green part of the visible light spectrum, this result was not acceptable. One of the reasons for this could be that, some of the transmitted light reflected back from the side and bottom of the glass made tank, which causes better performance in water than in air. Because of this phenomenon, the author covered the side and bottom of the glass tank with black paint to absorb the light, as seen in figure 6-9. After taking this action, the loss of the transmission in water was decreased to the expected level. The peak-to-peak value of the received signal was measured for different conditions at a fixed distance. Through the air, the received voltage was

36mV at the output of the transimpedance amplifier, whereas through water received signal at same point was about 50mV. But after covering the side and bottom of the tank with black paint, the received signal strength was about 40mV. The strength of the received signal was still higher than in the air, because some light was reflected back to the receiver from the water surface. Afterwards, the surface of the water was covered with black paint, and thus, the strength of the received signal dropped to 28mV, which is the expected result. Thus, from now on, all the experiments through water were carried out using this set up. It is believed that with this action, the nature of light propagation in the laboratory set up was much closer to the real environment.

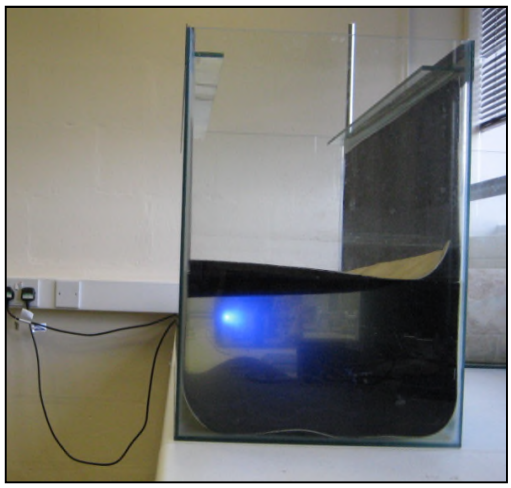

Figure 6-9 Side, bottom and top of the water surface is covered with black paint

Another important factor should be noted that, because of the fixed sized water tank, the author could not perform experiments at random distances. Rather, the success rate was calculated at a fixed distances of 30, 60, 90 and 120cm by combining the length and width of the tanks.

6.4.2 Tap water testing

For initial tests, the water tanks were filled with tap water. The success rate for

different scenarios was calculated by varying the communication distance. Figure 6-10 shows the success rate for green channel, both with and without the presence of room lighting by inserting a surface painted black just below the water surface as shown in figure 6-9.

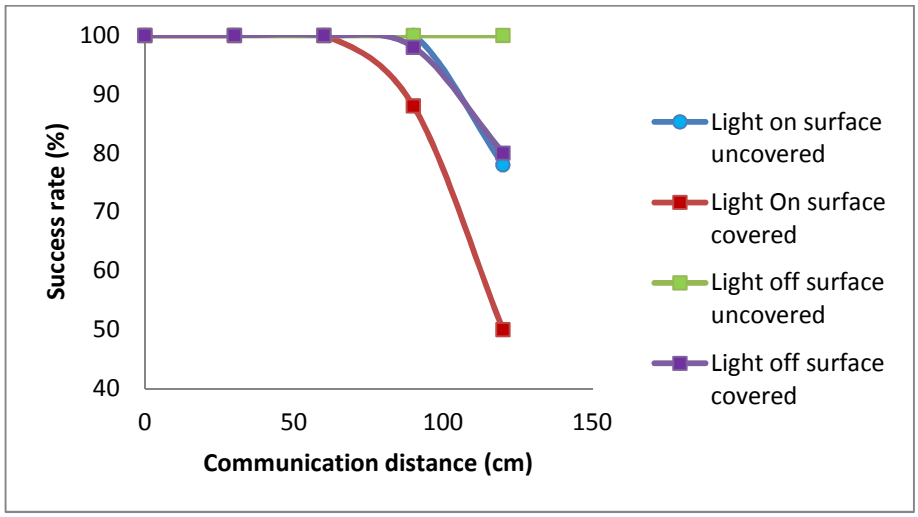

Figure 6-10 Success rate for tap water

As seen, the best results were achieved when the top of the tank was uncovered and room lighting was turned OFF. In contrast, the worst result was achieved when the water surface was covered and the room lighting was turned ON. The success rate was almost similar for the rest of the two scenarios; when room lighting was ON with water surface uncovered and room lighting OFF surface covered.

Similarly, the success rate for the blue channel was measured. It was found that the success rate was 100% in all cases, except for when the surface was covered by turning the lighting ON.

6.4.3 Canal water testing

To analyze the performance using canal water, the author collected 50 litres of water from Coventry canal, using 5 plastic made water carriers, as shown in figure 6-11.

The success rates for different transmission ranges and transmission rates were found, both for the blue and green channel. The received optical power was also measured for different distances. The visibility of canal water is less than that of tap water; thus the performance was expected to be degraded compared to tap water.

Figure 6-11 Canal water collection from Coventry canal

Figure 6-12 shows the rate of successfully received frames for different communication ranges, at a fixed transmission rate of 38.4kbps. In this case the top of the tank was covered by black paint, and the room light was turned ON.

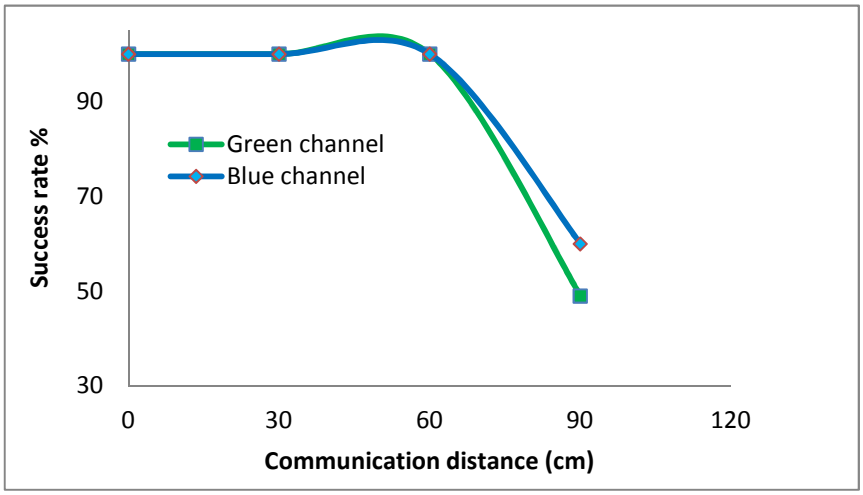

Figure 6-12 Success rate for different communication ranges

As seen from the figure, the success rate was 49% for the green channel and 60% for the blue channel at a communication distance of 90 cm.

The same set of experiments was repeated by taking out the black paint layer from the top of the water surface to see how much light reflects from the water surface and its effect on visible light communication underwater. Figure 6-13 shows the success rate for different communication distances, when the surface of the water is not covered by black paint and room light is turned OFF.

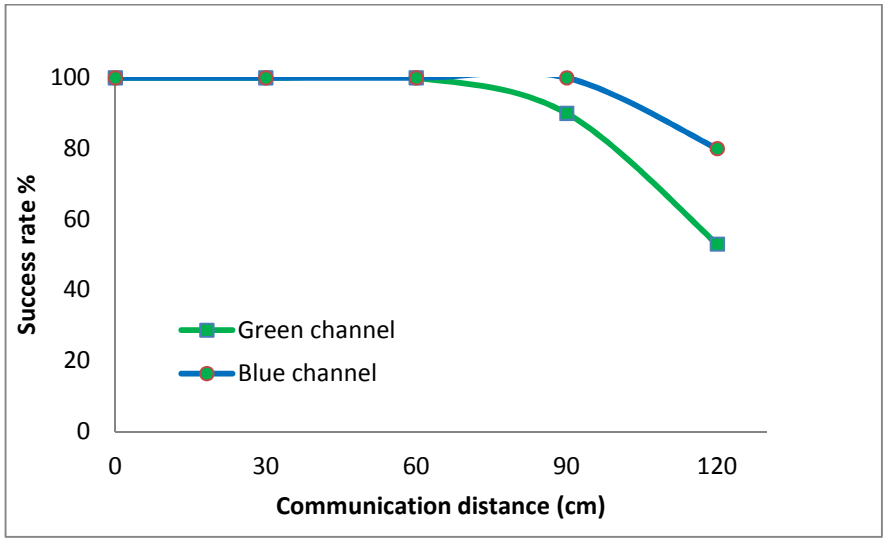

Figure 6-13 Success rate for different range without covering the surface

As seen in figure 6-13, the success rate increases significantly when the surface is not covered. From figure 6-12 and 6-13, it is understood that, when surface is not covered, the success rate increases from 60% to 100 % for the blue channel at distance of 90cm. This confirmed that a very large amount of light reflects from the water surface, which needs to be accounted when designing an underwater communication system. Thus, the depth of the system below the surface is an important factor, and has a significant effect on the performance of such a visible light communication system.

6.4.4 Sea water testing

The objective of sea water testing was to estimate the performance in this environment in contrast to the tap and canal water. For this reason, the author travelled to Blackpool pleasure beach, which is about 150 miles north of the University of Warwick, to collect some sea water from the Irish Sea. From visual observation it was seen that the water clarity was very poor. Around 50 litres of water were collected, as shown in figure 6-14.

Figure 6-14 Water collection from Irish Sea at Blackpool

With the collected sea water, the performance of the system was tested, and it was found that only a 30cm range was achievable both for the blue and green channels. No signal could be retrieved at 60cm. It was not possible to measure the performance between 30cm and 60cm, because of the fixed size water tank. At up to 30cm, the success rate was found 100% for all scenarios. However, in the case of 60cm, the success rate was 0% for every operation scenario.

6.5 Comparison between different water testing

In this section, the performance analysis for different water types mentioned above is compared in terms of success rate and the obtained optical powers. In both cases, the top of the surface was covered by black painted layer, and the room light was turned OFF.

6.5.1 Received power vs. Communication range

The received power at different communication distances for the three types of water is plotted in figure 6-15.

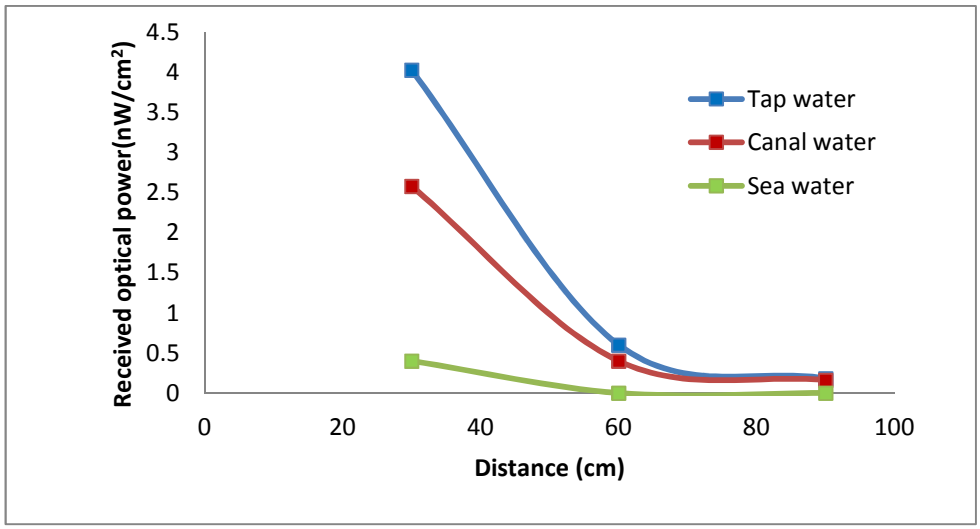

Figure 6-15 Received power for different water

As seen, the received power through tap water is much higher compared to the canal and sea water. This is because the visible light attenuates much less in clean tap water compared to when in sea water. The received power through clean water was almost 12 times higher than that of sea water collected from the Irish Sea.

6.5.2 Success rate vs. Communication distance

The frame success rate for a different communication distance using three types of

water can be compared, as shown in figure 6-16.

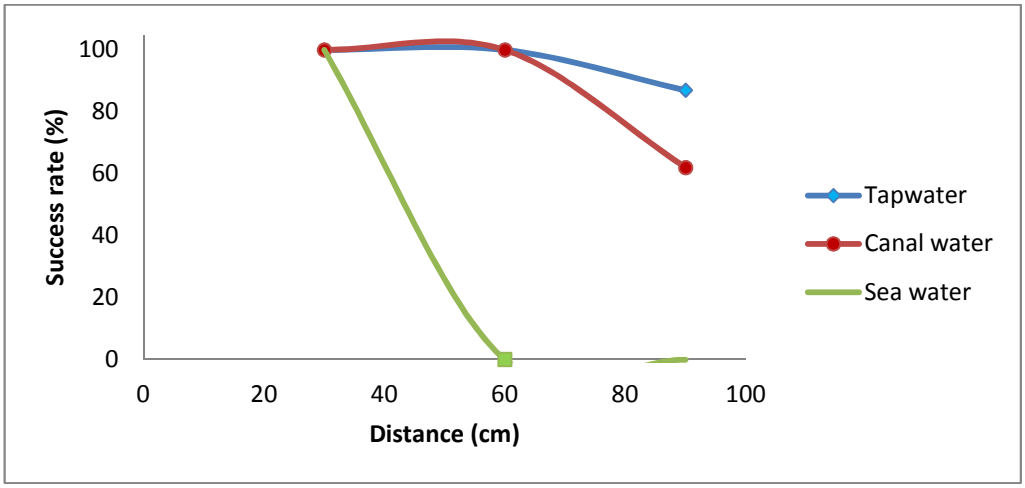

Figure 6-16 Frame success rate for different communication distance

As expected, the sea water performs the worst in terms of frame success rate. Only a communication distance of 30cm was achieved using sea water, whereas through the canal water, communication up to 90cm was achieved for a 40% error rate. The best result was obtained using the tap water, where communication over 100cm was achieved.

6.6 Multi-hop water testing

A multi-hop water test cannot be performed for most of the cases because of the limitation of the fixed size water tank. In most of the scenarios, successful communication was achieved at 60cm distance, so the author tested two hop systems by putting an intermediate node in between the water tanks. This way, successful communication was achieved for 120cm, for most of the cases. In the case of sea water testing, the author achieved 60cm by using two water tanks using a multi-hop technique. Thus, it can be said that, using the multi-hop technique, communication can be increased, which cannot be achieved by a single hop transmission.

6.6.1 Performance analysis using lenses

As discussed before, a communication range up to 1m may not be a realistic distance, but could easily be extend using external lenses or by increasing the transmitted power. Thus, the author tried to investigate the performance of the system by placing two convex lenses in front of the transmitter and receiver. The diameter of the lenses was 100mm with a focal length of 150mm. The experimental set up is shown in figure 6-17.

As shown, the transmitter is placed at one corner of the laboratory and the receiver is placed on the other corner. The distance between the transmitter and receiver were over 10 metres, which was the possible maximum distance the author was able to get inside the laboratory. It was found that 100% frames were received successfully, even in the presence of room lighting.

Figure 6-17 Experimental set up using lenses

In the same way, lenses were used for the sea water communication testing. It was found that a communication distance at least up to 120cm was achieved using the lenses. This proves that a realistic range in the few metres could potentially be

achieved using lenses. Moreover, a multi-hop network can increase this range many depending on the number of hops being used.

6.7 Conclusion

In this chapter, some performance evaluation of the built system was accomplished. The main objective of doing these experiments was to understand the different underwater communication criteria, and to see how a visible light communication system behaves in different water types. It was understood that accurate pointing between two nodes, is very important for LOS type communication. This would be very challenging for the underwater environment in deploying a static type of network. Even in a laboratory test it was not easy to align two nodes to each other to obtain the optimum performance. Some of the results obtained here were influenced by the pointing errors, which were not expected, although highest attention was associated with accurate alignment of the nodes.

Another very important aspect of visible light communication, which should always be considered, is the use of external optics. Improving the transmitter and receiver circuitry may not be sufficient for most applications. Thus, external optics such as lenses, concentrators and filters, have to be considered for obtaining the best performance.

As expected, the performance of the built prototype worked at a 1m distance quite well, but worked only at a 30cm distance in sea water, which was increased using the multi-hop network approach.

Chapter7 : Conclusion and future work

7.1 Conclusions

In previous chapters, a multi-hop underwater optical wireless sensor network prototype was designed, built, and implemented in the lab environment. To support the built network architecture, a directional MAC protocol, based on the TDMA technique was considered, and some of the performance analysis was accomplished. The focus of the present work was to demonstrate the concept of multi-hop underwater communication experimentally. For this purpose, a network prototype, consisting of three nodes, was established. The built prototype supports bi-directional communication, which was implemented using green and blue LEDs. Moreover, all nodes, transceivers, and protocols in the prototype were designed and built for the proposed application only.

Chapter 1 presented the motivation and necessity of the development of a multi-hop optical wireless communication for an underwater sensor application. The existing

problems of current underwater communication technologies were highlighted, and a solution based on optical wireless technology was proposed. Some of the limitations of the built network were also mentioned in chapter 1.

In chapter 2, the literature review and related works were mentioned. From the background study it was found that underwater optical wireless has significant potential to support high speed applications compared to other carriers, such as acoustic and electromagnetic waves. However, the limitation of an underwater optical wireless system is its short communication range. High transmission power and costly external optics can increase the communication range up to a certain level, but cannot be pushed further. Moreover, for a densely-deployed sensor application it is expected to keep the nodes cost as low as possible. As a result, a multi-hop approach was taken to increase the communication distance, and the more the number of nodes, the less the cost per node

Chapter 3 presents the detailed design procedure of the custom made transceiver. It provides the selection criteria for LED and photodiodes, which are two main components of an optical wireless communication system. It should be noted here that visible light LEDs are mostly used for illumination purpose. Most of the data sheets do not mention switching information. Before using a LED, its switching performance has to be measured, to make sure that it supports enough bandwidth for the intended application. After selecting the optoelectronic components, transmitter and receivers design were investigated. Different configurations were built and tested, mostly based on common configurations used for traditional optical wireless communication. Eventually, transimpedance based receiver configuration using a single transistor was chosen. Experimental results showed that transimpedance based configuration performs better than a bootstrap configuration in terms of link gain. It

is worth noting here that the author also investigated some complex receiver configurations based on a bootstrap amplifier with double peaking coil [58], but finally decided to use transimpedance based configuration, which supports a moderate range for the required bandwidth. Afterwards, a transistor based voltage amplifier was built to boost the signal in to 5V level. The performance analysis of the built transceiver was done both in air and in water. Finally, the built transceiver was tested for an underwater audio transmission system.

Chapter 4 discussed the development of the multi-hop communication prototype. Network architecture for the proposed application was proposed, which has two types of node. Sensor nodes are equipped with physical sensors, which measure water temperature and send this information to the gateway node periodically, using the optical wireless transceivers designed in chapter 3. Each sensor node uses two optical wireless transceivers to communicate with an up and a down node. The main task of the sensor node was to sense, process and forward data to the gateway node. An emergency alarm is also generated in case of any abnormal condition is detected. The gateway node collects data from all senor nodes, and forwards it to the base station for further manipulation. Both the sensor node and the gateway node were built around an ATmega 1284P microcontroller, which converts analogue data into a digital format, providing interface to connect external modules, such as a serial interface, to connect the gateway node to a computer, and also controls the communication in the network. A network prototype using three nodes was built and tested in the lab, both for air and through water transmission. The obtained results confirmed the successful implementation of both hardware and software of the built network for at least up to three hops.

A MAC protocol for the proposed network was developed in chapter 5. To gain the

knowledge, existing underwater MAC protocols were studied for different carriers. Underwater visible light communication is relatively a new technology and there has not been much research on a fully deployed optical wireless communication in underwater. So, free space optical wireless MAC protocols were investigated. Because of the directional nature of the network architecture, the author found directional MAC to be more suitable for this kind of scenario, which follows the TDMA-based approach to collect data from each node. The proposed technique does not use any random access protocol, which can be a very complicated process to implement. Rather, by exchanging a traditional MAC messages, collision in the network could be avoided. Moreover, because of the static and full duplex deployment, the hidden terminal problem can be resolved. Some of the performance analysis of the proposed MAC protocol was done experimentally. For example, the round trip delay of the message was measured using a microcontroller's timer/counter unit, which was also verifies by the waveform of the received signal. Power consumption by different nodes in the network was also determined.

Finally, in chapter six, an experimental set up and performance analysis of the built prototype was presented. The results presented were just for illustration purposes, and not compared to any other systems. The designed optical wireless communication system was tested in air and also using three different types of water. It was observed that the performance through air and clean water was almost similar but degrades considerably for canal and sea water. The Irish Sea water test showed that communication range decreased at least one third compared to the clean water test. It was also observed that the light reflection phenomena from the water surface have a good impact on the performance of a visible light communication system. Thus the system designed for deep water wouldn't work same way near or at the sea

surface.

7.2 Future work

There are still many opportunities to extend this research in various directions. Here, the presented work was a demonstration of an all-optical wireless underwater sensor network using the multi-hop technique. Improvements can be achieved at every stage for commercial deployment. Here, the presented network architecture is considered to be a static type, which is not a realistic solution for an actual application. Thus, further research is needed to investigate a mobile platform, where nodes can move in any direction, but are still capable of maintaining communication between neighbouring nodes. This will increase the flexibility of deployment scenarios, but will increase the deployment cost, as complex protocols will be required for maintaining communication between nodes. A sophisticated routing protocol needs to be designed, which would be able to support the mobile platform architecture.

The experimental test was done in the lab environment, where the optical signal was passed through the water tank. However, in real environment, this could be different, depending on the location, depth and type of water. To obtain a realistic result, the designed prototype needs to be submerged into different types of water.

Generic system design would be another challenge for underwater visible light communications. The turbidity of water varies according to the location, depth and even season of the year. Thus, a generic system, which can ensures a similar signal-to-noise performance, needs to be ensured for different environment. The design can be upgraded by changing the transmission window. A generic solution using different coloured LEDs could be undertaken. The optimum transmission window may shift across blue, green and red spectrum, depending on the turbidity of water.

This type of network would require more intelligence within the physical layer. A more complex transmitter and receiver design needs to be considered to support multiple transmission windows. Moreover, visible light does not cross the water/air boundary easily. Thus, more research is needed to establish the requirements for this kind of communication.

The proposed MAC layer protocol was partly deployed for the targeted system, which consists of just three nodes. Had time permitted it, the full implementation of the MAC protocols for a large scale network would have been investigated, and also the results of this would have been compared with existing MAC protocol performance.

References

[1] http://www.naka-lab.jp/product/uvlc_compare_e.html.

[2] L. Lanbo, Z. Shengli, and C. Jun-Hong, "Prospects and problems of wireless communication for underwater sensor networks," *Wirel. Commun. Mob. Comput.*, vol. 8, pp. 977-994, 2008.

[3] I. Vasilescu, K. Kotay, D. Rus, and P. Corke, "Data collection, storage and retrieval with an underwater sensor network," presented at the *International Conference on Embedded Networked Sensor Systems*, 2005.

[4] A. I. Al-Shamma'a, A. Shaw, and S. Saman, "Propagation of electromagnetic waves at MHz frequencies through seawater," *IEEE Transactions on Antennas and Propagation, ,* vol. 52, pp. 2843-2849, 2004.

[5] A. M. Chancey, "Short Range Underwater Opticlal Communciaiton Links," M.S. thesis, North Carolina State University, Raleigh, NC, 2005.

[6] N. Farr, A. D. Chave, L. Freitag, J. Preisig, S.N.White, D. Yoerger, and F.Sonnichsen, "Optical modem technology for seafloor observatories," in *Proceedings of IEEE OCEANS*, 2006.

[7] S. Arnon and D. Kedar, "Non-line-of-sight underwater optical wireless communcaiiton nework," *J. Opt. Soc,* vol. 26, pp. 530-539, 2009.

[8] M. Doniec and D. Rus, "BiDirectional optical communication with AquaOptical II," in *IEEE International Conference on Communication Systems (ICCS)*, 2010, pp. 390-394.

[9] F. Hanson and S. Radic, "High bandwidth underwater optical communication," *Appl. Opt.*, vol. 47, pp. 277-283, 2008.

[10] J. H. Smart, "Underwater optical communications systems part 1: variability of water optical parameters," in *IEEE Military Communications Conference*, 2005, pp. 1140-1146 Vol. 2.

[11] M. Doniec, I. Vasilescu, M. Chitre, C. Detweiler, M. Hoffmann-Kuhnt, and D. Rus, "AquaOptical: A lightweight device for high-rate long-range

underwater point-to-point communication," in *MTS/IEEE OCEANS 2009*, pp. 1-6.

[12] J. A. Simpson, W. C. Cox, J. R. Krier, B. Cochenour, B. L. Hughes, and J. F. Muth, "5 Mbps optical wireless communication with error correction coding for underwater sensor nodes," in *IEEE OCEANS 2010*, pp. 1-4.

[13] S. Jaruwatanadilok, "Underwater Wireless Optical Communication Channel Modeling and Performance Evaluation using Vector Radiative Transfer Theory," *IEEE Journal on Selected Areas in Communications*, vol. 26, pp. 1620-1627, 2008.

[14] J. W. Giles and I. N. Bankman, "Underwater optical communications systems. Part 2: basic design considerations," in *IEEE Military Communications Conference, 2005*, Vol. 3, pp. 1700-1705.

[15] D. Anguita, D. Brizzolara, and G. Parodi, "Optical wireless communication for underwater Wireless Sensor Networks: Hardware modules and circuits design and implementation," in *IEEE OCEANS 2010*, pp. 1-8.

[16] A. Palmeiro, M. Martin, I. Crowther, and M. Rhodes, "Underwater radio frequency communications," in *IEEE OCEANS, 2011*.

[17] C. Uribe and W. Grote, "Radio Communication Model for Underwater WSN," in *3rd International Conference on New Technologies, Mobility and Security (NTMS)*, 2009, pp. 1-5.

[18] A. Shaw, A. I. Al-Shamma'a, S. R. Wylie, and D. Toal, "Experimental Investigations of Electromagnetic Wave Propagation in Seawater," in *36th European Microwave Conference*,2006, pp. 572-575.

[19] J. Lucas and C. K. Yip, "A determination of the propagation of electromagnetic waves through seawater," *Underwater Technology: The International Journal of the Society for Underwater*, vol. 27, pp. 1-9, 2007.

[20] R. Somaraju and J. Trumpf, "Frequency, Temperature and Salinity Variation of the Permittivity of Seawater,"*IEEE Transactions on Antennas and Propagation, ,* vol. 54, pp. 3441-3448, 2006.

[21] J. Lloret, S. Sendra, M. Ardid, and J. J. P. C. Rodrigues, "Underwater Wireless Sensor Communications in the 2.4 GHz ISM Frequency Band," *Sensors*, vol. 12, pp. 4237-4264, 2012.

[22] C. Xianhui, I. Wells, P. Kear, G. Dickers, G. Xiaochun, and M. Rhodes, "A Static Multi-hop Underwater Wireless Sensor Network Using RF Electromagnetic Communications," in *29th IEEE International Conference on Distributed Computing Systems Workshops, 2009.* pp. 460-463.

[23] W. F. systems. *http://www.wirelessfibre.co.uk/*.

[24] A. F.Ian, P. Dario, and M. Tommaso, "Underwater Acoustic Sensor Networks: Research Challenges," *Ad Hoc Networks (Elsevier),* vol. 3, pp. 257-279, March 2005.

[25] B. Cochenour, L. Mullen, A. Laux, and T. Curran, "Effects of Multiple Scattering on the Implementation of an Underwater Wireless Optical Communications Link," in *OCEANS 2006*, pp. 1-6.

[26] D. Anguita, D. Brizzolara, and G. Parodi, "VHDL modules and circuits for underwater optical wireless communication systems," *WTOC*, vol. 9, pp. 525-552, 2010.

[27] N. Miller, "An Underwater Communication System," *IRE Transactions on Communications Systems*, vol. 7, pp. 249-251, 1959.

[28] A. Kaya and S. Yauchi, "An Acoustic Communication System for Subsea Robot," in *OCEANS '89. Proceedings*, pp. 765-770.

[29] P. Costas, S. Milica, and F. Lee, "High rate acoustic link for underwater video transmission," in *IEEE OCEANS*, 2003, pp. 1091-1097.

[30] H. Yan, S. Zhou, Z. J. Shi, and B. Li, "A DSP implementation of OFDM acoustic modem," presented at the Proceedings of the second workshop on Underwater networks, Montreal, Quebec, Canada, 2007.

[31] W. C. Cox, "A 1 Mbps underwater communication system using a 405nm laser diode and photomultiplier tube," M.S thesis, Dept. of Elec. and Comp. Eng, North carolina state university, Raleigh,NC, 2007.

[32] J. Simpson, "A 1Mbps underwater communication system using LEDs and Photodiodes with signal processing capability," M.S. thesis, Dept. of Elec. and Comp. Eng, North carolina state university, Raleigh, NC, 2007.

[33] S. J. Everett, "Forward-error correction coding for underwater free-space optical communication," M.S. thesis, Dept. of Elec. and Comp. Eng, North carolina state university, Raleigh, NC, 2009.

[34] W.C. Cox, J. Simpson, C. P. Domizioli, J. Muth, and B. Hughes, "An underwater optical communication system implementing Reed-Solomon channel coding," in *OCEANS 2008*, pp. 1-6.

[35] J. A. Simpson, B. L. Hughes, and J. F. Muth, "A spatial diversity system to measure optical fading in an underwater communications channel," in *OCEANS 2009*, pp. 1-6.

[36] C. Pontbriand, N. Farr, J. Ware, J. Preisig, and H. Popenoe, "Diffuse high-bandwidth optical communications," in *OCEANS 2008*, pp. 1-4.

[37] N. Farr, A. Bowen, J. Ware, C. Pontbriand, and M. Tivey, "An integrated, underwater optical /acoustic communications system," in *OCEANS 2010*, pp. 1-6.

[38] N. Farr, J. Ware, C. Pontbriand, T. Hammar, and M. Tivey, "Optical communication system expands CORK seafloor observatory's bandwidth," in *OCEANS 2010*, pp. 1-6.

[39] S. Felix, Z. U. R., and T. Jochen, "Visible Spectrum Optical Communication and Distance Sensing for Underwater Applications," presented at the ACRA, Australia, 2004.

[40] F. Lu, S. Lee, J. Mounzer, and C. Schurgers, "Low-cost medium-range optical underwater modem: short paper," presented at the Proceedings of the Fourth ACM International Workshop on UnderWater Networks, Berkeley, California, 2009.

[41] S. Arnon, "Underwater optical wireless communication network," *Optical*

Engineering, January,2010.

[42] M. Stojanovic, "Underwater Acoustic Communications: Design Considerations on the Physical Layer," in *Fifth Annual Conference on Wireless on Demand Network Systems and Services, 2008* , pp. 1-10.

[43] E. Y. S. Young and A. M. Bullock, "Underwater-airborne laser communication system: characterization of the channel," pp. 146-157, 2003.

[44] A. M. A. El–Naser, R. A. N. Zaki, and E.-N. A. E. M., "Under Water Optical Wireless Communications Technology for Short and Very Short Ranges," *IJITCS,* vol. 4, pp. 46-57, 2012.

[45] V. I. Haltrin, "Chlorophyll-Based Model of Seawater Optical Properties," *Appl. Opt.,* vol. 38, pp. 6826-6832, 11/20 1999.

[46] B. Greg, B. Yassiah, and M. Andrew, "Paving the way for a future underwater omni-directional wireless optical communication systems," *Ocean Engineering,* vol. 36, pp. 633-640, 2009.

[47] B. Heather, "Designing a wireless underwater optical communication system," MS thesis, MIT, Feb 2010.

[48] R.-I. Roberto, I. M. Sevia, and S. Ziran, *Optical Wireless Communications: IR for Wireless connectivity* New York: Auerbach Publications, Taylor and Francis Books Inc, 2007.

[49] K. M. Joseph and B. R. John, "Wireless infrared communications," in *IEEE Proc.,* 1997, pp. 265-298.

[50] R. J. Green, H. Joshi, M. D. Higgins, and M. S. Leeson, "Recent developments in indoor optical wireless " *IET Communications,* vol. 2, pp. 3-10, 2008.

[51] T. Luftner, C. Kropl, R. Hagelauer, M. Huemer, R. Weigel, and J. Hausner, "Wireless infrared communications with edge position modulation for mobile devices," *IEEE Wireless Communications,* vol. 10, pp. 15-21, 2003.

[52] B. R. John, *Wireless Infrared Communications*: Kluwer Academic Publishers, 1994.

[53] Z. Yu, "Adaptive modulation scheme for optical wireless communication systems," PhD thesis, School of Engineering, University of warwick, 2009.

[54] M. Sui, X. Yu, and Z. Zhou, "The Modified PPM Modulation for Underwater Wireless Optical Communication," in *ICCSN '09* , pp. 173-177.

[55] S. Meihong, Y. Xinsheng, and Z. Fengli, "The Evaluation of Modulation Techniques for Underwater Wireless Optical Communications," in *International Conference on Communication Software and Networks, 2009*, pp. 138-142.

[56] H. Joshi, "Modulation for optical wireless communications," PhD thesis, School of engineering, University of Warwick, Coventry, 2012.

[57] D. Kedar and S. Arnon, "Non-line-of-sight optical wireless sensor network operating in multiscattering channel," *Applied Optics,* vol. 45, pp. 8454-8461, 2006.

[58] A. Ramli, S. M. Idrus, and A. S. M. Supa'at, "Optical wireless front-end

receiver design," in *IEEE International RF and Microwave Conference*, 2008, pp. 331-334.

[59] R. J. Green and M. G. McNeill, "Bootstrap transimpedance amplifier: a new configuration," *IEE Proceedings of Circuits, Devices and Systems*, vol. 136, pp. 57-61, 1989.

[60] R. Green, M. Higgins, H. Joshi, and M. Leeson, "Bandwidth extension for optical wireless receiver-amplifiers," in *Transparent Optical Networks, 2008. ICTON 2008. 10th Anniversary International Conference on*, 2008, pp. 201-204.

[61] C. Hoyle and A. Peyton, "Shunt bootstrapping technique to improve bandwidth of transimpedance amplifiers," *Electronics Letters*, vol. 35, pp. 369-370, 1999.

[62] S. M. Idrus, N. Ngajikin, N. N. N. A. Malik, and S. I. A. Aziz, "Performance Analysis of Bootstrap Transimpedance Amplifier For Large Windows Optical Wireless Receiver," in *International RF and Microwave Conference*, 2006, pp. 416-420.

[63] A. F. L. Mohammad, "Techniques for signal to noise ratioadaption in infrared optical wireless for optimisation of receiver performance," PhD thesis, School of Engineering, University of warwick, Coventry, 2006.

[64] H. A Alhagagi, "Theory and Optimisation of Double Conversion Heterodyne Photoparametric Amplifier," PhD, School of Engineering, University of Warwick, Coventry, 2012.

[65] J. C. H. Edgar, *Wireless Sensor Networks Architectures and Protocols*: Auerbach Publications, 2004.

[66] J. Heidemann, Y. Wei, J. Wills, A. Syed, and L. Yuan, "Research challenges and applications for underwater sensor networking," in *IEEE Wireless Communications and Networking Conference*, pp. 228-235,2006.

[67] Z. Junjie, Z. Shudao, L. Zhihua, Y. Song, L. Lilong, and Y. Lu, "A new underwater sensor networks architecture," in *IEEE International Conference on Information Theory and Information Security*, pp. 845-848,2010.

[68] L. Wenli, L. Deshi, T. Ying, C. Jian, and S. Tao, "Architecture of Underwater Acoustic Sensor Networks: A Survey," in, *First International Conference on Intelligent Networks and Intelligent Systems*, pp. 155-159,2008.

[69] A. Gkikopouli, G. Nikolakopoulos, and S. Manesis, "A survey on Underwater Wireless Sensor Networks and applications," in *20th Mediterranean Conference on Control & Automation (MED)*, pp. 1147-1154,2012.

[70] N. Agrawal, C. C. Davis, and S. D. Milner, "Free Space Optical Sensor Networking for Underwater Sensing Application," presented at the ISSNIP, 2009.

[71] A. Davide, B. Davide, and P. Giancarlo, "VHDL moduled and circuits for underwater optical wireless communication system," *WSEAS Transactions on Communications*, vol. 9, pp. 525-552, 2010.

[72] D. Pompili and I. F. Akyildiz, "Overview of networking protocols for underwater wireless communications," *IEEE Communications Magazine*, vol.

47, pp. 97-102, 2009.

[73] D. Pompili, T. Melodia, and I. F. Akyildiz, "A CDMA-based Medium Access Control for UnderWater Acoustic Sensor Networks," *IEEE Transactions on Wireless Communications, ,* vol. 8, pp. 1899-1909, 2009.

[74] L. Freitag, M. Stojanovic, S. Singh, and M. Johnson, "Analysis of channel effects on direct-sequence and frequency-hopped spread-spectrum acoustic communication," *IEEE Journal of Oceanic Engineering, ,* vol. 26, pp. 586-593, 2001.

[75] N. Chirdchoo, S. Wee-Seng, and C. Kee Chaing, "Aloha-Based MAC Protocols with Collision Avoidance for Underwater Acoustic Networks," *26th IEEE International Conference on Computer Communications*, 2007, pp. 2271-2275.

[76] S. M. Smith, J. C. Park, and A. Neel, "A peer-to-peer communication protocol for underwater acoustic communication," in *OCEANS '97*, pp. 268-272 .

[77] G. Lapierre, L. Chevallier, F. Gallaud, and G. Ayela, "Design of a communication protocol for underwater acoustic modems and networks," in *OCEANS, 2001*, pp. 2220-2226.

[78] I. Kurtis B. Kredo and P. Mohapatra, "A hybrid medium access control protocol for underwater wireless networks," presented at the Proceedings of the second workshop on Underwater networks, Montreal, Quebec, Canada, 2007.

[79] X. Che, I. Wells, G. Dickers, P. Kear, and X. Gong, "Re-evaluation of RF electromagnetic communication in underwater sensor networks," *IEEE Communications Magazine,* vol. 48, pp. 143-151, 2010.

[80] F. Yunus, S. H. S. Ariffin, and Y. Zahedi, "A Survey of Existing Medium Access Control (MAC) for Underwater Wireless Sensor Network (UWSN)," in *Fourth Asia International Conference on Mathematical/Analytical Modelling and Computer Simulation*, 2010, pp. 544-549.

[81] X. Peng and C. Jun-Hong, "R-MAC: An Energy-Efficient MAC Protocol for Underwater Sensor Networks," in *International Conference on Wireless Algorithms, Systems and Applications*, 2007, pp. 187-198.

[82] D. Anguita, D. Brizzolara, and G. Parodi, "VHDL modeling of PHY and MAC Layer modules for underwater optical wireless communication," in *European Conference on Circuits and Systems for Communications (ECCSC),*2010, pp. 185-188.

[83] I. Vasilescue, "Using light underwater: devices,algorithms and systems for maritime persistent surveillance," PhD, MIT, 2009.

[84] A. Nasipuri, S. Ye, J. You, and R. E. Hiromoto, "A MAC protocol for mobile ad hoc networks using directional antennas," in *IEEE Wireless Communications and Networking Confernce, 2000,* pp. 1214-1219 vol.3.

[85] K. Young-Bae, V. Shankarkumar, and N. F. Vaidya, "Medium access control protocols using directional antennas in ad hoc networks," in *INFOCOM 2000*, pp. 13-21 vol.1.

[86] R. R. Choudhury, Y. Xue, R. Ramanathan, and N. F. Vaidya, "On designing MAC protocols for wireless networks using directional antennas," *IEEE Transactions on Mobile Computing*, vol. 5, pp. 477-491, 2006.

[87] K. Miura and M. Bandai, "Node architecture and MAC protocol for full duplex wireless and directional antennas," in *IEEE 23rd International Symposium on Personal Indoor and Mobile Radio Communications (PIMRC), 2012*, pp. 369-374.

[88] N. Agrawal, C. C. Davis, and S. D. Milner, "Design and performance of a directional media access control protocol for optical wireless sensor networks," in *Seventh International Conference on Intelligent Sensors, Sensor Networks and Information Processing (ISSNIP),* 2011, pp. 568-573.

[89] Z. A. Bakar and R. J. Green, "Medium Access Control (MAC) algorithm for Directional Optical Wireless Transceivers for Indoor Ad-Hoc Networking," in *London Communication Symposium*, University College London, Sept 2004, pp. 233-236.

[90] Z. A. Bakar, "Infrared Ad Hoc Networking," PhD Thesis, University of Warwick, 2007.

[91] I.-K. Rhee, J. Lee, J. Kim, E. Serpedin, and Y.-C. Wu, "Clock Synchronization in Wireless Sensor Networks: An Overview," *Sensors*, vol. 9, pp. 56-85, 2009.

Appendixes

Appendix 1: Data sheets

Kingbright LED data sheet

Kingbright

7.6mmx7.6mm SUPER FLUX LED LAMP

ATTENTION

OBSERVE PRECAUTIONS FOR HANDLING ELECTROSTATIC DISCHARGE SENSITIVE DEVICES

L-7676CVGC-H GREEN

Features

- SUPER FLUX OUTPUT.
- DESIGN FOR HIGH CURRENT OPERATION.
- OUTSTANDING MATERIAL EFFICIENCY.
- RELIABLE AND RUGGED.

Description

The Green source color devices are made with InGaN on SiC Light Emitting Diode.
Static electricity and surge damage the LEDS.
It is recommended to use a wrist band or anti-electrostatic glove when handling the LEDs.
All devices, equipment and machinery must be electrically grounded.

Package Dimensions

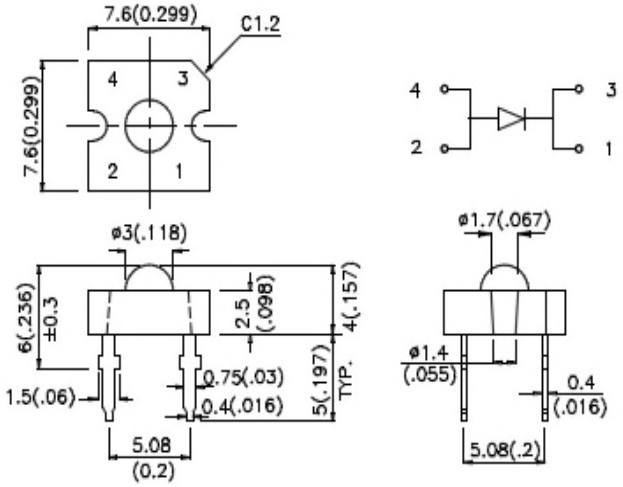

Notes:
1. All dimensions are in millimeters (inches).
2. Tolerance is ±0.25(0.01") unless otherwise noted.
3. Lead spacing is measured where the lead emerge package.
4. Specifications are subject to change without notice.

SPEC NO: DSAB3625 REV NO: V.4 DATE: MAY/28/2003 PAGE: 1 OF 3
APPROVED: J. Lu CHECKED: Allen Liu DRAWN: Z.Y.YANG

Kingbright

Selection Guide

Part No.	Dice	Lens Type	Iv (mcd) @ 20 mA *70mA		Viewing Angle
			Min.	Typ.	2θ1/2
L-7676CVGC-H	GREEN (InGaN)	WATER CLEAR	2500	4300	70°
			*5700	*9500	70°

Notes:
1. θ1/2 is the angle from optical centerline where the luminous intensity is 1/2 the optical centerline value.
2. * Luminous intensity with asterisk is measured at 70mA.
3. Drive current between 10mA and 30mA are recommended for long term performance.
4. Operation at current below 10mA is not recommended.

Electrical / Optical Characteristics at T_A=25°C

Symbol	Parameter	Device	Typ.	Max.	Units	Test Conditions
λpeak	Peak Wavelength	Green	520		nm	I_F=20mA
λD	Dominate Wavelength	Green	525		nm	I_F=20mA
Δλ1/2	Spectral Line Half-width	Green	35		nm	I_F=20mA
C	Capacitance	Green	45		pF	V_F=0V;f=1MHz
V_F	Forward Voltage	Green	3.7	4.1	V	I_F=20mA
I_R	Reverse Current	Green		10	uA	V_R = 5V

Absolute Maximum Ratings at T_A=25°C

Parameter	Green	Units
Power dissipation	120	mW
DC Forward Current	30	mA
Peak Forward Current [1]	150	mA
Reverse Voltage	5	V
Operating/Storage Temperature	-40°C To +85°C	
Lead Solder Temperature [2]	260°C For 5 Seconds	

Notes:
1. 1/10 Duty Cycle, 0.1ms Pulse Width.
2. 2mm below package base.

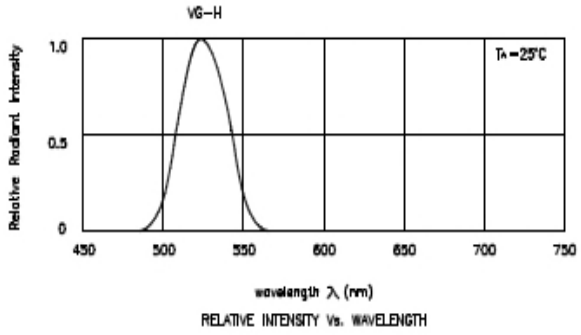

RELATIVE INTENSITY Vs. WAVELENGTH

Green **L-7676CVGC-H**

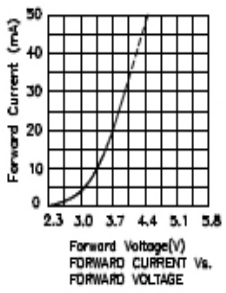

FORWARD CURRENT Vs.
FORWARD VOLTAGE

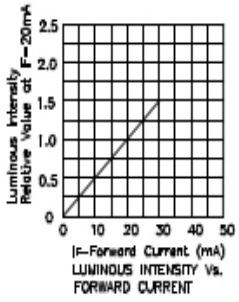

LUMINOUS INTENSITY Vs.
FORWARD CURRENT

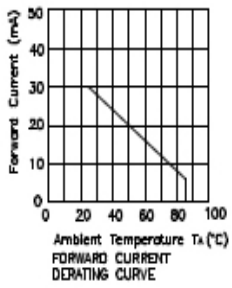

FORWARD CURRENT
DERATING CURVE

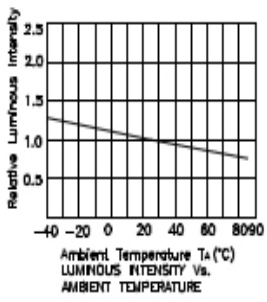

LUMINOUS INTENSITY Vs.
AMBIENT TEMPERATURE

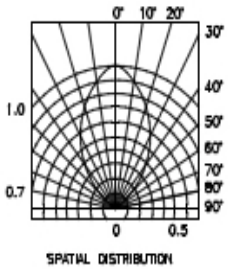

SPATIAL DISTRIBUTION

Avago LED data sheet

HLMP-CBxx, HLMP-CMxx

Precision Optical Performance Blue and Green

AVAGO TECHNOLOGIES

Data Sheet

Lead (Pb) Free
RoHS 6 fully compliant

Description

This high intensity blue and green LEDs are based on the most efficient and cost effective InGaN material technology. This LED lamps is untinted and non-diffused, T-1 ¾ packages incorporating second-generation optics producing well defined spatial radiation patterns at specific viewing cone angles.

These lamps are made with an advanced optical grade epoxy, offering superior temperature and moisture resistance in outdoor signal and sign applications. The package epoxy contains both UV-A and UV-B inhibitors to reduce the effects of long term exposure to direct sunlight.

Features

- Well defined spatial radiation pattern
- High luminous output
- Untinted, Non-diffused
- Viewing angle: 15º, 23º and 30º
- Standoff or non-standoff leads
- Superior resistance to moisture

Applications

- Traffic signals
- Commercial outdoor advertising
- Front panel backlighting
- Front panel indicator

Package Dimensions

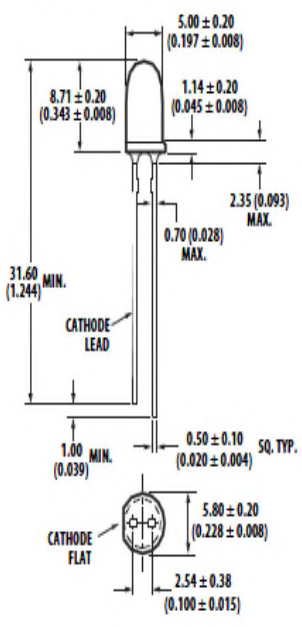

PACKAGE DIMENSION A

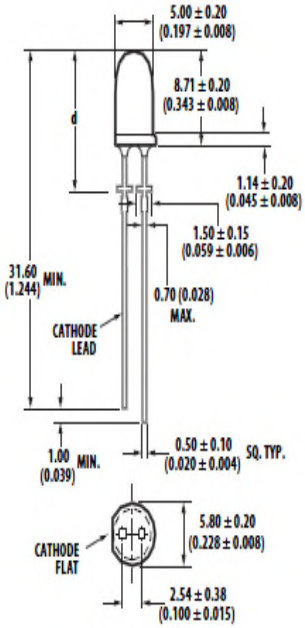

PACKAGE DIMENSION B

HLMP-Cx14	HLMP-Cx25	HLMP-Cx35
d = 12.6 ± 0.25 (0.496 ± 0.010)	d = 12.52 ± 0.25 (0.493 ± 0.010)	d = 11.96 ± 0.25 (0.471 ± 0.010)

Notes:
1. Measured just above flange.
2. All dimensions are in millimeters (inches).
3. Epoxy meniscus may extend about 1mm (0.040") down the leads.

Device Selection Guide

Part Number	Color	Typical Viewing Angle, 2θ½ (Degree)	Intensity (mcd) at 20 mA		Leads with Stand-Offs
			Min.	Max.	
HLMP-CB13-UX0xx	Blue	15°	3200	9300	No
HLMP-CB14-UX0xx	Blue	15°	3200	9300	Yes
HLMP-CB22-SV0xx	Blue	23°	1900	5500	No
HLMP-CB25-SV0xx	Blue	23°	1900	5500	Yes
HLMP-CB34-RU0xx	Blue	30°	1500	4200	No
HLMP-CB35-RU0xx	Blue	30°	1500	4200	Yes
HLMP-CM13-Z30xx	Green	15°	12000	35000	No
HLMP-CM14-Z30xx	Green	15°	12000	35000	Yes
HLMP-CM22-X10xx	Green	23°	7200	21000	No
HLMP-CM25-X10xx	Green	23°	7200	21000	Yes
HLMP-CM34-X10xx	Green	30°	7200	21000	No
HLMP-CM35-X10xx	Green	30°	7200	21000	Yes

Notes:
1. Tolerance for luminous intensity measurement is ±15%
2. The optical axis is closely aligned with the package mechanical axis.
3. LED light output is bright enough to cause injuries to the eyes. Precautions must be taken to prevent looking directly at the LED without proper safety equipment.
4. 2θ1/2 is the off-axis angle where the luminous intensity is ½ the on axis intensity.

Part Numbering System

HLMP - x x xx - x x x xx

Packaging Option
DD: Ammopacks

Color Bin Selection
0 : Full Distribution

Maximum Intensity Bin
Refer to Device Selection Guide

Minimum Intensity Bin
Refer to Device Selection Guide

Viewing Angle
13: 15° without standoff
14: 15° with standoff
22: 23° without standoff
25: 23° with standoff
34: 30° without standoff
35: 30° with standoff

Color
B: Blue 470nm
M: Green 525nm

Package
C: 5mm round Lamps

Note: Please refer to AB 5337 for complete information on part numbering system.

Absolute Maximum Rating ($T_A = 25°C$)

Parameters	Value	Unit
DC forward current [1]	30	mA
Peak pulsed forward current [2]	100	mA
Power dissipation	116	mW
LED junction temperature	110	°C
Operating temperature range	-40 to +85	°C
Storage temperature range	-40 to +100	°C

Notes:
1. Derate linearly as shown in figure 2.
2. Duty factor 10%, frequency 1KHz.

Electrical/Optical Characteristics ($T_A = 25°C$)

		Blue and Green				
Parameters	**Symbol**	**Min**	**Typ**	**Max**	**Units**	**Test Condition**
Forward Voltage	V_F	2.8	3.2	3.8	V	$I_F = 20$ mA
Reverse Voltage[1]	V_R	5.0			V	$I_R = 10$ µA
Thermal resistance	$R\theta_{J\text{-}PIN}$		240		°C/W	LED Junction to cathode lead
Dominant wavelength [2]	λ_d				nm	$I_F = 20$ mA
Blue		460	470	480		
Green		520	525	540		
Peak wavelength	λ_{PEAK}				nm	Peak of wavelength of spectral distribution at $I_F = 20$ mA
Blue			464			
Green			516			
Spectral half width	$\Delta\lambda_{1/2}$					Wavelength width at spectral distribution 1/2 power point at $I_F = 20$ mA
Blue			22			
Green			35			
Luminous Efficacy [3]	η_v				lm/W	Emitted luminous power/Emitted radiant power
Blue			78			
Green			545			
Luminous Flux	φv				mlm	If = 20mA
Blue			830			
Green			3500			
Luminous Efficiency[4]	η_e				lm/W	Luminous Flux/Electrical Power at I_F = 20mA
Blue			13			
Green			56			

Notes:
1. The reverse voltage of the product is equivalent to the forward voltage of the protective chip at $I_R = 10$ µA
2. The dominant wavelength λd is derived from the Chromaticy Diagram and represents the color pf the lamp.
3. The radiant intensity, Ie in watts/steradian, may be found from the equation $Ie = Iv/\eta_v$, where Iv is the luminous intensity in candelas and η_v is the luminous efficacy in lumens/watt.
4. $\eta_e = \varphi v / I_F \times V_F$ where φv is the emitted luminous flux, I_F is electrical forward current and V_F is the forward voltage.

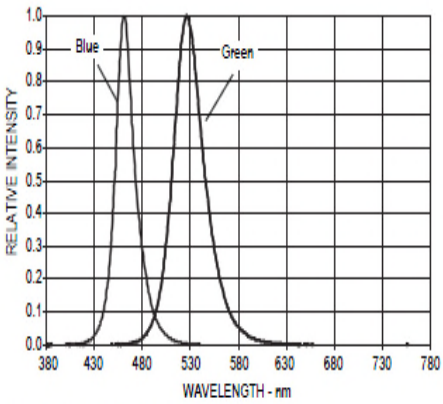

Figure 1. Relative Intensity vs. Wavelength

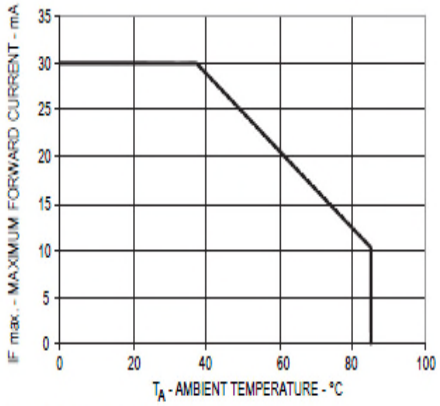

Figure 2. Forward Current vs. Ambient Temperature

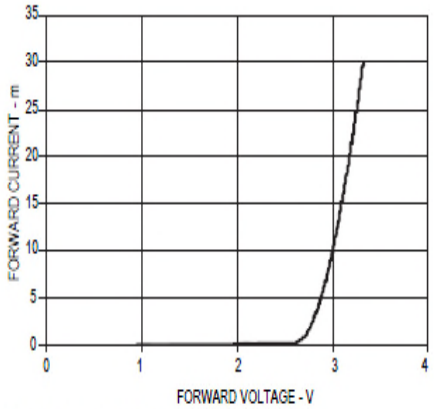

Figure 3. Forward Current vs. Forward Voltage

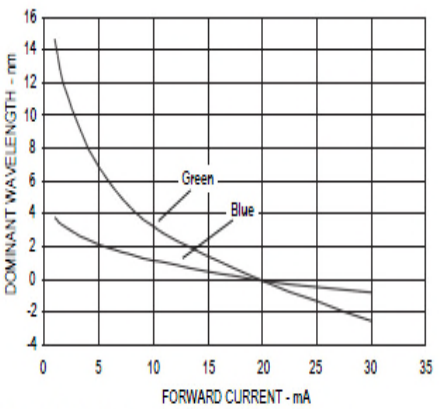

Figure 4. Relative Dominant Wavelength vs. DC Forward Current

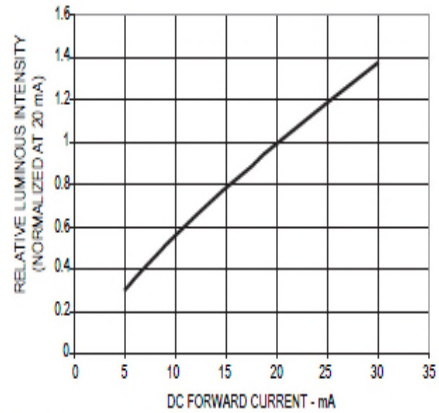

Figure 5. Relative Intensity vs. DC Forward Current

SILONEX photodiode data sheet

SILONEX inc

SLD-70IR1

Visible Light Rejection Filter Planar Photodiode

Features

- Low capacitance
- Low leakage current
- Linear response vs irradiance
- IR pass filter
- Multiple dark current ranges available

Description

This planar photodiode is designed to maximize response in the infrared spectrum of received energy. It is supplied on a ceramic base with an IR transmissive epoxy dome package that rejects visible light wavelengths. Photodiodes may operate in either photovoltaic or reverse bias mode to provide low capacitance with fast switching speed. High sensitivity and low dark current allow use in even low irradiance applications.

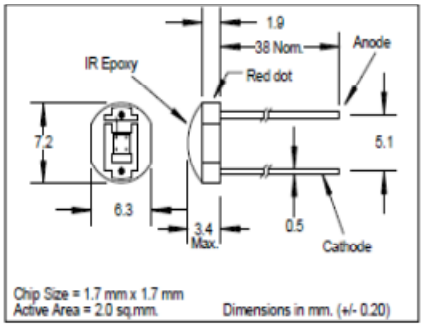

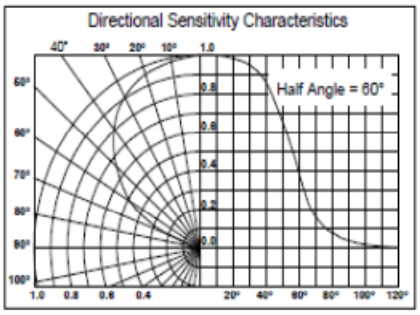

Absolute Maximum Ratings

Storage Temperature	-20°C to +85°C
Operating Temperature	-20°C to +85°C
Soldering Temperature (1)	260°C

Notes: (1) >2 mm from case for < 5 sec.
(2) Ee = source @ 2854°K.
(3) Ee = source @ λ = 880 nm

Electrical Characteristics (T_A=25°C unless otherwise noted)

Symbol	Parameter	Min	Typ	Max	Units	Test Conditions
I_{SC}	Short Circuit Current	60	100		µA	V_R=0V, Ee=25mW/cm^2 (2)
V_{OC}	Open Circuit Voltage		0.40		V	Ee=25mw/cm^2 (2)
I_D	Reverse Dark Current:					
	SLD-70IR1A			100	nA	V_R=100mV, Ee=0
	SLD-70IR1B			100	nA	V_R=5V, Ee=0
	SLD-70IR1C			10	nA	V_R=5V, Ee=0
	SLD-70IR1D			1	nA	V_R=5V, Ee=0
	SLD-70IR1E			250	pA	V_R=5V, Ee=0
C_J	Junction Capacitance		50		pF	V_R=0, Ee=0, f=1MHz
t_R	Rise Time		1.0		µs	V_R=5V, R_L=1kΩ (3)
t_F	Fall Time		1.5		µs	V_R=5V, R_L=1kΩ (3)
TC_I	Temp. Coef., I_{SC}		+0.2		%/°C	(2)
V_{BR}	Reverse Breakdown Voltage	50			V	I_R=100µA
λ_P	Maximum Sensitivity Wavelength		990		nm	
λ_R	Sensitivity Spectral Range	700		1100	nm	
$\theta_{1/2}$	Acceptance Half Angle		60		deg	(off center-line)

Specifications subject to change without notice. 101737 REV 3

5200 St. Patrick St., Montreal
Que., H4E 4N9, Canada
Tel: 514-768-8000
Fax: 514-768-8889

The Old Railway, Princes Street
Ulverston, Cumbria, LA12 7NQ, UK
Tel: 01 229 581 551
Fax: 01 229 581 554

QF-84

OSRAM Photodiode data sheet

Silizium-Fotodiode für den sichtbaren Spektralbereich
Silicon Photodiode for the Visible Spectral Range

BPW 21

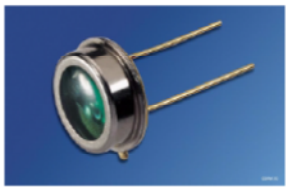

Wesentliche Merkmale

- Speziell geeignet für Anwendungen im Bereich von 350 nm bis 820 nm
- Angepaßt an die Augenempfindlichkeit (V_λ)
- Hermetisch dichte Metallbauform (ähnlich TO-5)

Features

- Especially suitable for applications from 350 nm to 820 nm
- Adapted to human eye sensitivity (V_λ)
- Hermetically sealed metal package (similar to TO-5)

Anwendungen

- Belichtungsmesser für Tageslicht
- Für Kunstlicht mit hoher Farbtemperatur in der Fotografie und Farbanalyse

Applications

- Exposure meter for daylight
- For artificial light of high color temperature in photographic fields and color analysis

Typ Type	Bestellnummer Ordering Code
BPW 21	Q62702-P885

Grenzwerte
Maximum Ratings

Bezeichnung Parameter	Symbol Symbol	Wert Value	Einheit Unit
Betriebs- und Lagertemperatur Operating and storage temperature range	T_{op}; T_{stg}	– 40 … + 80	°C
Löttemperatur (Lötstelle 2 mm vom Gehäuse entfernt bei Lötzeit $t \leq 3$ s) Soldering temperature in 2 mm distance from case bottom ($t \leq 3$ s)	T_S	235	°C
Sperrspannung Reverse voltage	V_R	10	V
Verlustleistung, T_A = 25 °C Total power dissipation	P_{tot}	250	mW

Kennwerte (T_A = 25 °C, Normlicht A, T = 2856 K)
Characteristics (T_A = 25 °C, standard light A, T = 2856 K)

Bezeichnung Parameter	Symbol Symbol	Wert Value	Einheit Unit
Fotoempfindlichkeit, V_R = 5 V Spectral sensitivity	S	10 (≥ 5.5)	nA/lx
Wellenlänge der max. Fotoempfindlichkeit Wavelength of max. sensitivity	$\lambda_{S\,max}$	550	nm
Spektraler Bereich der Fotoempfindlichkeit S = 10% von S_{max} Spectral range of sensitivity S = 10% of S_{max}	λ	350 … 820	nm
Bestrahlungsempfindliche Fläche Radiant sensitive area	A	7.34	mm^2
Abmessung der bestrahlungsempfindlichen Fläche Dimensions of radiant sensitive area	$L \times B$ $L \times W$	2.73 × 2.73	mm × mm
Abstand Chipoberfläche zu Gehäuseoberfläche Distance chip front to case surface	H	1.9 … 2.3	mm
Halbwinkel Half angle	φ	± 55	Grad deg.

Kennwerte (T_A = 25 °C, Normlicht A, T = 2856 K)
Characteristics (T_A = 25 °C, standard light A, T = 2856 K) (cont'd)

Bezeichnung **Parameter**	**Symbol** **Symbol**	**Wert** **Value**	**Einheit** **Unit**
Dunkelstrom Dark current V_R = 5 V V_R = 10 mV	 I_R I_R	 2 (≤ 30) 8 (≤ 200)	 nA pA
Spektrale Fotoempfindlichkeit, λ = 550 nm Spectral sensitivity	S_λ	0.34	A/W
Quantenausbeute, λ = 550 nm Quantum yield	η	0.80	Electrons Photon
Leerlaufspannung, E_v = 1000 lx Open-circuit voltage	V_O	400 (≥ 320)	mV
Kurzschlußstrom, E_v = 1000 lx Short-circuit current	I_{SC}	10	µA
Anstiegs- und Abfallzeit des Fotostromes Rise and fall time of the photocurrent R_L = 1 kΩ; V_R = 5 V; λ = 550 nm; I_p = 10 µA	t_r, t_f	1.5	µs
Durchlaßspannung, I_F = 100 mA, E = 0 Forward voltage	V_F	1.2	V
Kapazität, V_R = 0 V, f = 1 MHz, E = 0 Capacitance	C_0	580	pF
Temperaturkoeffizient von V_O Temperature coefficient of V_O	TC_V	– 2.6	mV/K
Temperaturkoeffizient von I_{SC} Temperature coefficient of I_{SC}	TC_I	– 0.05	%/K
Rauschäquivalente Strahlungsleistung Noise equivalent power V_R = 5 V, λ = 550 nm	NEP	7.2×10^{-14}	$\frac{W}{\sqrt{Hz}}$
Nachweisgrenze, V_R = 5 V, λ = 550 nm Detection limit	D*	1×10^{12}	$\frac{cm \times \sqrt{Hz}}{W}$

Relative Spectral Sensitivity
$S_{rel} = f(\lambda)$

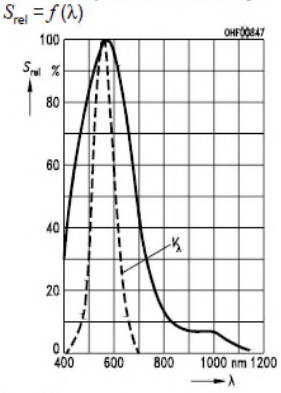

Photocurrent $I_P = f(E_v), V_R = 5$ V
Open-Circuit Voltage $V_O = f(E_v)$

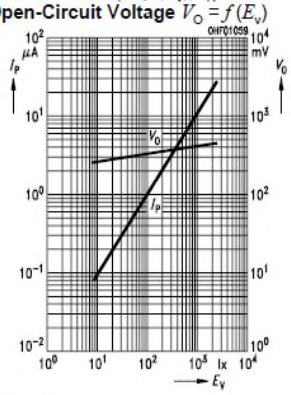

Total Power Dissipation
$P_{tot} = f(T_A)$

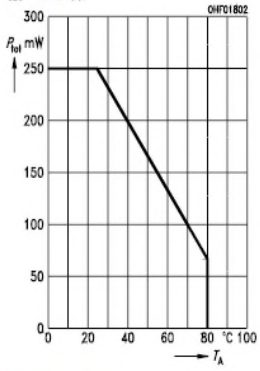

Dark Current
$I_R = f(V_R)$

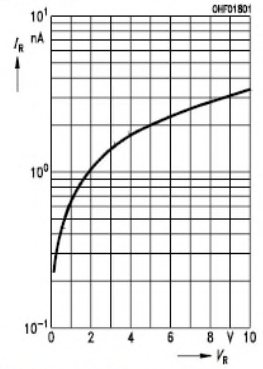

Capacitance
$C = f(V_R), f = 1$ MHz, $E = 0$

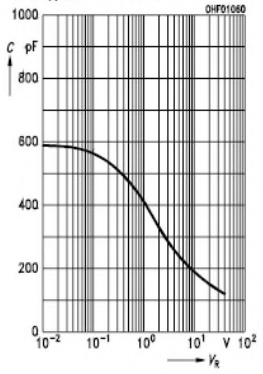

Dark Current
$I_R = f(T_A), V_R = 5$ V

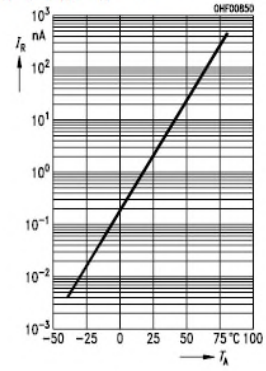

Directional Characteristics
$S_{rel} = f(\varphi)$

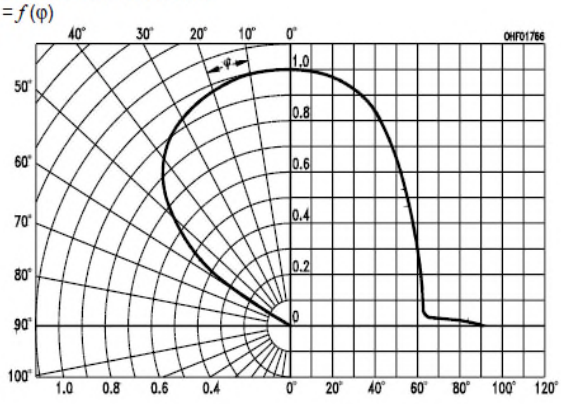

Appendix 2 :PCB layouts of the sensor nodes

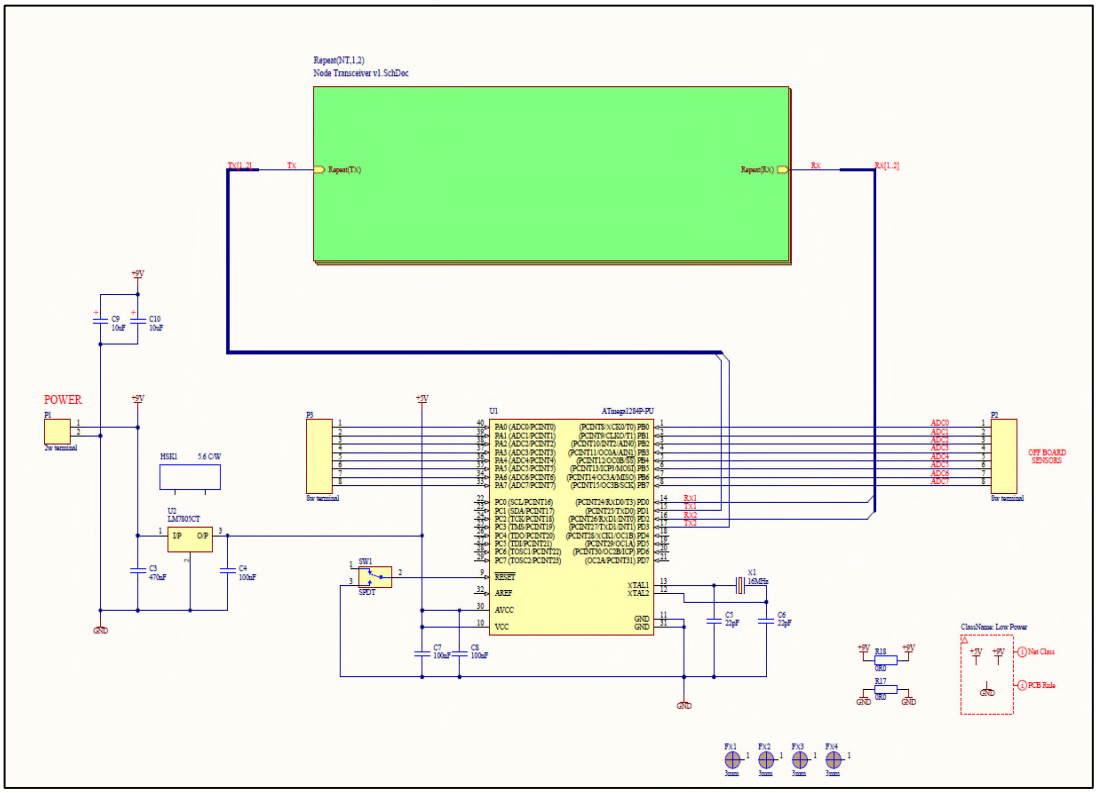

Figure: Schematic of the Sensor node

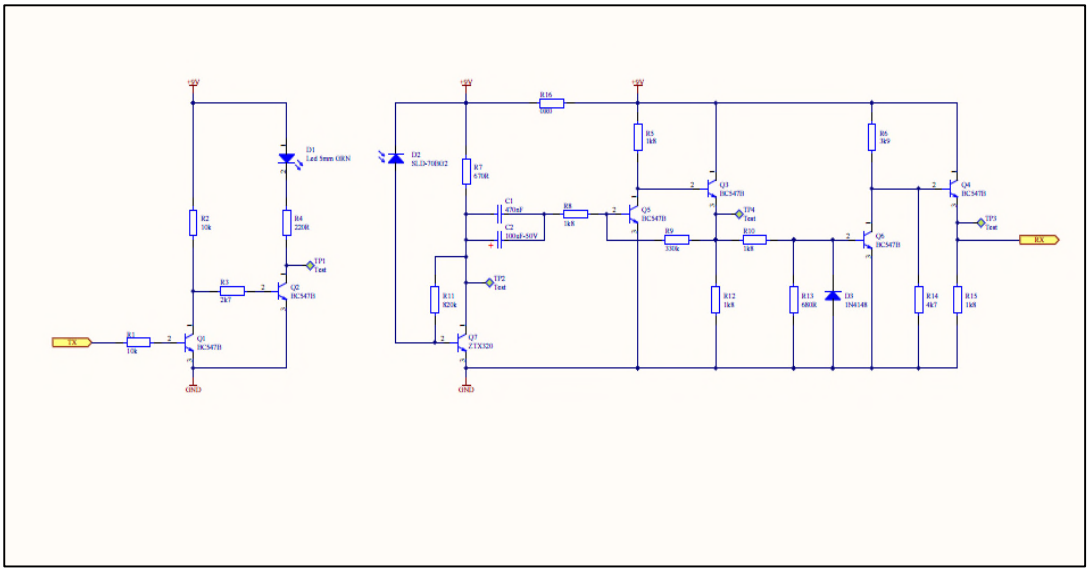

Figure: Scematic of the designed transceiver

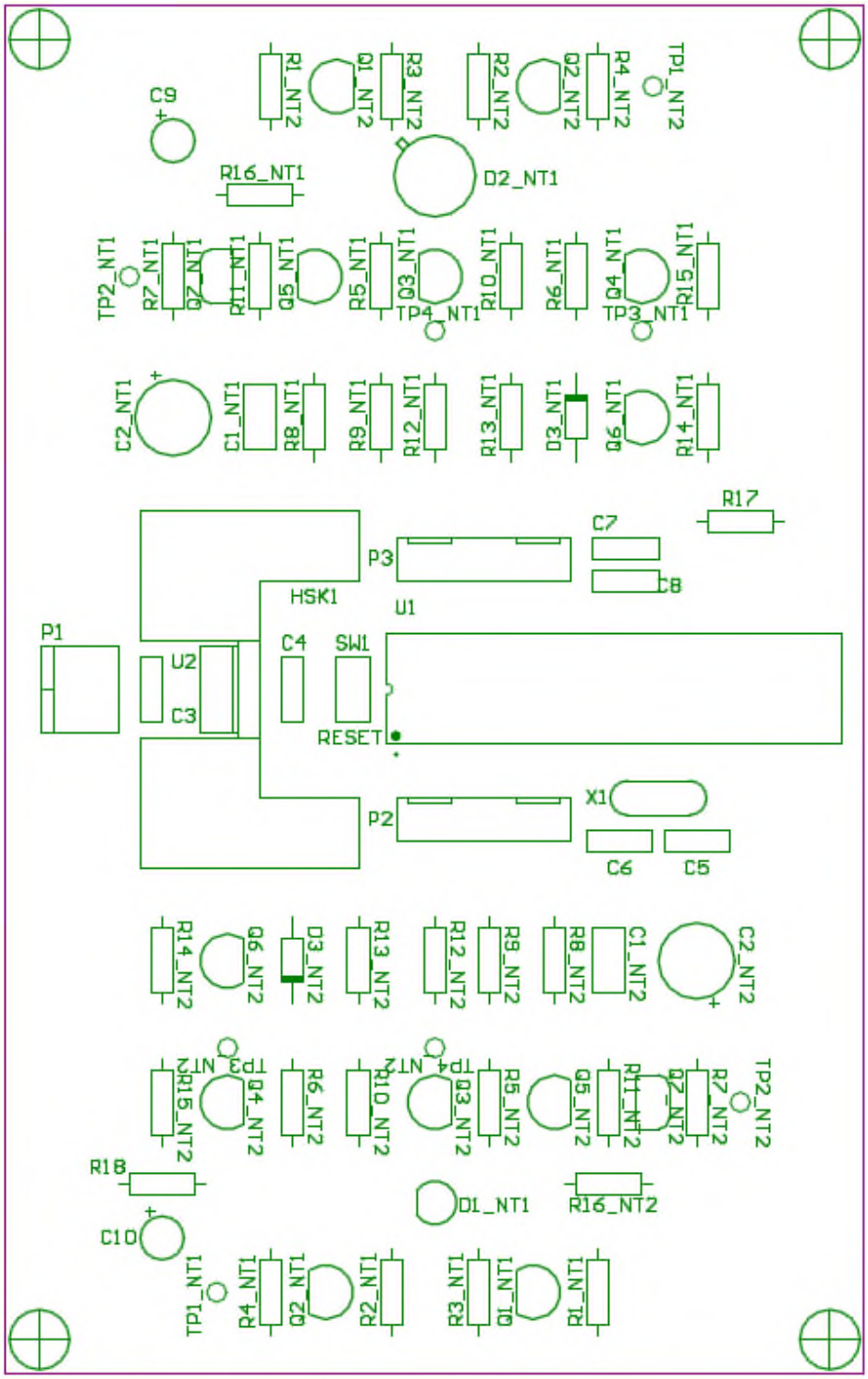

Figure: PCB layout (Top silkscreen overlay)

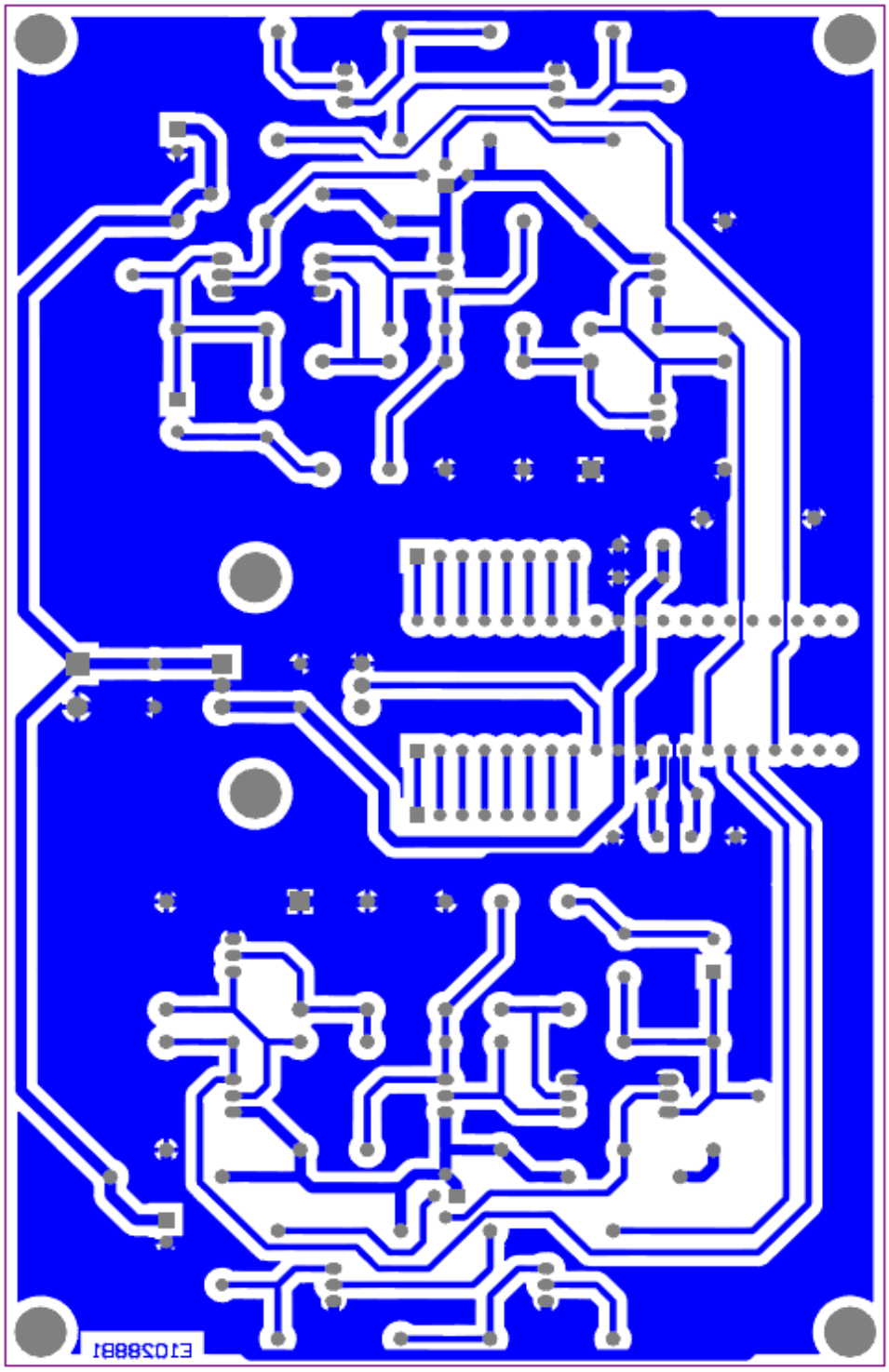

Figure: PCB layout (Bottom layer)

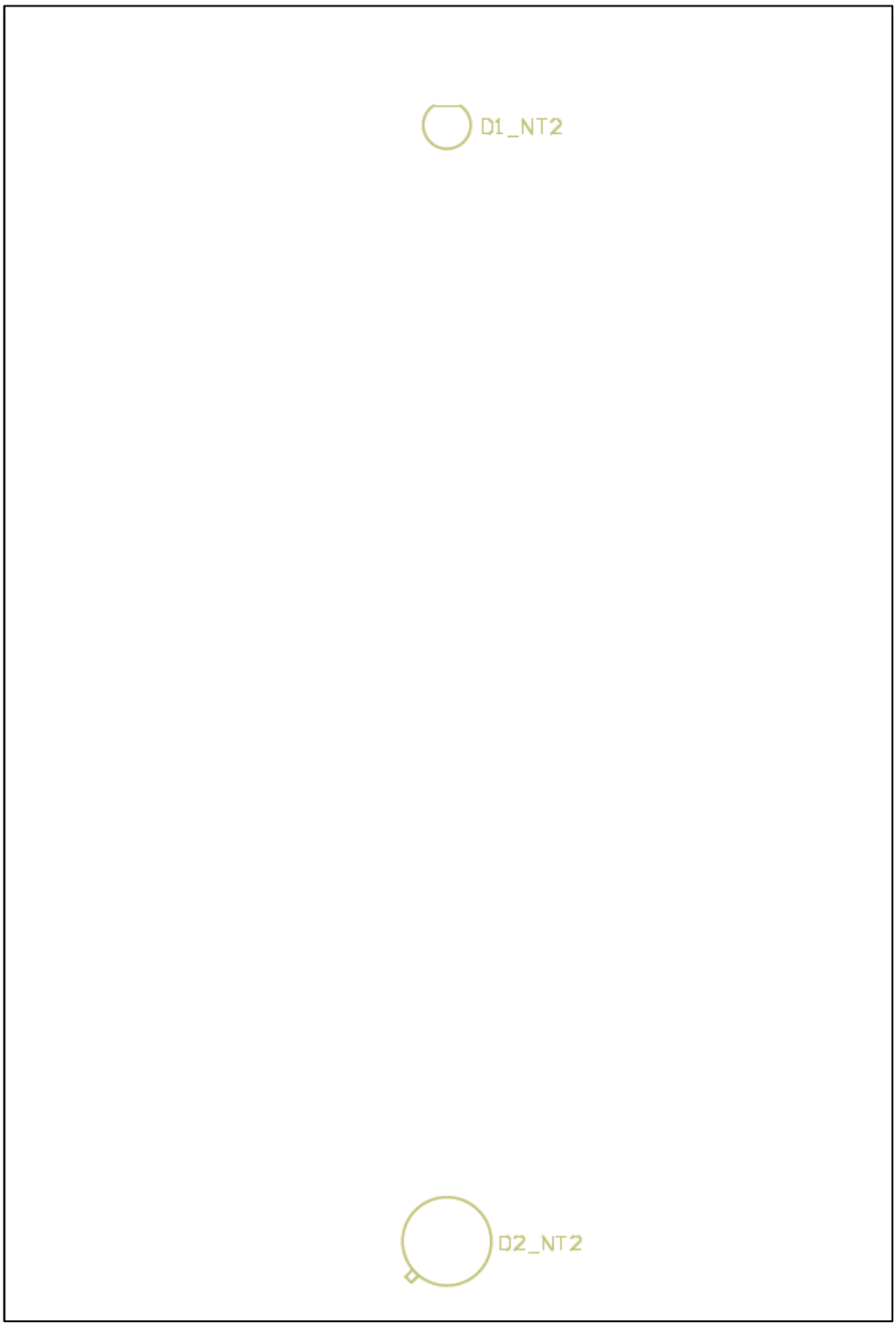

Figure: PCB layout (Bottom overlay)